NASA TECHNICAL MEMORANDUM

NASA TM X-2355

NASA TM X-2355

AERODYNAMIC HEATING AT MACH 8 OF ATTACHED INFLATABLE DECELERATOR CONFIGURATIONS

by Theodore R. Creel, Jr., and Robert Miserentino

Langley Research Center

Hampton, Va. 23365

NATIONAL AERONAUTICS AND SPACE ADMINISTRATION • WASHINGTON, D. C. • OCTOBER 1971

1. Report No.	2. Government Accession No.	3. Recipient's Catalog No.
NASA TM X-2355		

4. Title and Subtitle	5. Report Date
AERODYNAMIC HEATING AT MACH 8 OF ATTACHED INFLATABLE DECELERATOR CONFIGURATIONS	October 1971
	6. Performing Organization Code
7. Author(s)	8. Performing Organization Report No.
Theodore R. Creel, Jr., and Robert Miserentino	L-7864
	10. Work Unit No.
9. Performing Organization Name and Address	117-07-04-08
NASA Langley Research Center Hampton, Va. 23365	11. Contract or Grant No.
	13. Type of Report and Period Covered
12. Sponsoring Agency Name and Address	Technical Memorandum
National Aeronautics and Space Administration Washington, D.C. 20546	14. Sponsoring Agency Code

15. Supplementary Notes

16. Abstract

Heat-transfer coefficients on four attached inflatable decelerator (AID) configurations were obtained in the Langley Mach 8 variable-density tunnel at angles of attack of 0°, 5°, and 10° for a Reynolds number range of 0.22×10^6 to 1.23×10^6 in air. A fusible-temperature-indicator technique which employs a temperature-sensitive material that changes from an opaque solid to a clear liquid at a known temperature was used to obtain these coefficients. The results of this investigation indicate that the heat-transfer coefficients on the ram-air inlets and the burble fence are up to five times larger than the coefficients at identical locations on a smooth AID body. Moving the ram-air inlets rearward reduces the heating rates immediately behind the aft row of inlets. This placement of the inlets also increases the heating rate on the burble fence. Increasing Reynolds number resulted in an increase in heat-transfer coefficient primarily on the burble fence.

17. Key Words (Suggested by Author(s))	18. Distribution Statement
Attached inflatable decelerators Aerodynamic heating Fusible temperature indicators	Unclassified – Unlimited

19. Security Classif. (of this report)	20. Security Classif. (of this page)	21. No. of Pages	22. Price*
Unclassified	Unclassified	78	$3.00

*For sale by the National Technical Information Service, Springfield, Virginia 22151

AERODYNAMIC HEATING AT MACH 8 OF ATTACHED INFLATABLE DECELERATOR CONFIGURATIONS

By Theodore R. Creel, Jr., and Robert Miserentino
Langley Research Center

SUMMARY

Heat-transfer coefficients on four attached inflatable decelerator (AID) configurations were obtained in the Langley Mach 8 variable-density tunnel at angles of attack of 0°, 5°, and 10° for a Reynolds number range of 0.22×10^6 to 1.23×10^6 in air. A fusible-temperature-indicator technique which employs a temperature-sensitive material that changes from an opaque solid to a clear liquid at a known temperature was used to obtain these coefficients. The results of this investigation indicate that the heat-transfer coefficients on the ram-air inlets and the burble fence are approximately five times larger than the coefficients at identical locations on a smooth AID body. Moving the ram-air inlets rearward also changes the bow-shock shape and reduces the heating rates immediately behind the aft row of inlets. This movement of the inlets also increases the heating rate on the burble fence. Increasing Reynolds number effected an increase in heat-transfer rate primarily on the burble fence.

INTRODUCTION

Planetary-mission studies of entry into low-density atmospheres such as that of Mars have demonstrated the need for a low-mass deployable device for deceleration at supersonic speeds. (See refs. 1 to 3.) This need prompted a research program to develop and evaluate an attached inflatable decelerator (AID) which is essentially a low-mass inflatable canopy attached directly to a payload as described in reference 4. The AID canopy is aerodynamically shaped to provide high drag at high supersonic speeds. The concept is illustrated in figure 1, in which the canopy is shown attached to a conical planetary entry body. Ram-air inlets at the aeroshell periphery initiate canopy deployment and additional inlets near the burble fence maintain the inflated shape.

The analytical development of AID configurations is presented in reference 4 and the design and fabrication of wind-tunnel models 1.5 meters in diameter is presented in reference 5. Deployment and aerodynamic performance data from wind-tunnel tests (refs. 3 and 6) demonstrate good stability characteristics and a high drag coefficient over a wide supersonic speed range. The application of the AID in a simulated Mars mission

has been studied analytically in reference 7 to determine the thermal and structural response of the inflated canopy in the hostile environment. The present investigation was initiated to provide experimental heating rates on the AID configuration for correlation with analytical results and to provide data on changes in heat-transfer rates due to the protuberances such as ram-air inlets and burble fence, which were not amenable to calculation.

Tests were made in the Langley Mach 8 variable-density tunnel on solid 0.0154-scale AID models 11.2 cm in diameter. The models were coated with fusible temperature indicators to measure heat-transfer rates. Four model configurations were tested at angles of attack of 0°, 5°, and 10° and four Reynolds numbers varying from 0.22×10^6 to 1.23×10^6.

SYMBOLS

H	local heat-transfer coefficient
HS	reference stagnation-point heat-transfer coefficient
$\bar{h}$	interference heating factor, ratio of heat-transfer coefficients on models 2, 3, and 4 to that on model 1
MINF	free-stream Mach number
$N_{Re,\infty}$	free-stream Reynolds number
R	maximum model radius
R/M	free-stream Reynolds number per meter
r	model radial coordinate
s	surface model length at $\alpha = 0$ (see fig. 2)
T	time
z	axial coordinate (positive toward nose)
α	angle of attack

FACILITY

The Langley Mach 8 variable-density tunnel, described in reference 8, was used for all tests. To obtain in air a Reynolds number range of 0.22×10^6 to 1.23×10^6 based on maximum model diameter, the stagnation pressure was varied from 0.69 to 4.8 MN/m^2 with stagnation temperature ranging from 710 to 830 K. The tunnel has a contoured axisymmetric nozzle with a test-section diameter of 45.7 cm and a model injection mechanism located directly beneath the test section.

MODELS

The models were made of high-temperature plastic so that data could be obtained by using fusible temperature indicators. (See ref. 9.) Four different model configurations were used in this investigation. Model 1 consists of the AID configuration with the burble fence only. The coordinates of model 1 are given in table I and the profile is shown in figure 2; a photograph of model 1 is shown in figure 3. Model 2 has the same profile as model 1 with the addition of a nose protuberance; dimensions for the nose protuberance are given in figure 4. Models 3 and 4 were the same as model 2 with the

TABLE I.- COORDINATES OF MODEL 1 PROFILE

[R = 5.6 cm (2.2 in.)]

r/R	z/R	r/R	z/R
0.418	0.578	0.955	0.024
.442	.567	.975	.008
.488	.544	.988	-.010
.535	.520	.995	-.029
.581	.493	1.000	-.060
.628	.465	.991	-.088
.675	.434	.973	-.110
.721	.399	.936	-.121
.768	.358	.907	-.108
.814	.310	.884	-.149
.862	.248	.861	-.178
.884	.207	.814	-.219
.907	.151	.768	-.245
.920	.036	.721	-.261
.938	.031	.675	-.270
		.623	-.272

addition of two rows of eight equally spaced inlet protuberances at longitudinal stations shown in figure 5 for model 3 and figure 6 for model 4. The geometry of these inlet protuberances is shown in figure 7. A photograph shows them clearly on model 4 in figure 8.

TEST TECHNIQUE

The fusible-temperature-indicator technique described in reference 9 was used to determine heat-transfer coefficients. Briefly, a thin layer of a contrasting color pigment of known melting temperature is sprayed on the model outside the wind tunnel. When the tunnel flow has been established, the model is injected into the flow, and a motion-picture camera photographs the model at known time intervals. The assumption of one-dimensional heat flow inside the model permits the calculation of a relationship of the time to reach the melting temperature, the model thermal properties, and the aerodynamic heat input rate, from which a heat-transfer coefficient can be determined by specifying a driving temperature potential. For the present tests, on a very blunt configuration, an adequate approximation was obtained by neglecting the variation in local adiabatic wall temperature around the model, and by using the stagnation temperature instead of local adiabatic wall temperature to determine the temperature difference driving the aerodynamic heat flow. These computed heat-transfer coefficients were then normalized by the value calculated (by using ref. 10) for the stagnation point of a sphere of radius 1.356 cm (equal to the aeroshell nose radius).

RESULTS AND DISCUSSION

Heat-transfer coefficients on four attached inflatable decelerator configurations were obtained in the Langley Mach 8 variable-density tunnel at angles of attack of 0°, 5°, and 10° over a Reynolds number range of 0.22×10^6 to 1.23×10^6 based on maximum model diameter.

Figure 9 is a series of sketches representing a typical phase-change pattern sequence during one tunnel run. In figures 9(a) and 9(b) is shown a simple growth of the melted area. In figure 9(c), however, although the nose melted area has grown larger, there is a detached region of melted paint bounded by contours 3. The heating rate in the unmelted area is lower than that in the downstream melted area. Such a reduction could be due to separation of the boundary layer in the vicinity of the aeroshell—inflatable-structure junction where there is, in fact, a change in surface inclination.

In figure 9(d), the probably separated area has been heated above the melting temperature, and the melt boundary proceeds monotonically downstream in figures 9(e)

and 9(f). In figure 9(g) an isolated area of melted paint on the burble fence again indicates an area of increased heating rate on the fence, and a minimum heating rate region in the corner; this condition can be interpreted as separation and reattachment.

For convenience, the successive contour lines from a test can be drawn on a single figure. This procedure has been followed in presenting the results of the present study in figures 10 to 33. The legend with each figure gives the time at which the contour occurs, the calculated heat-transfer coefficient for each contour, and the relative heating rate referenced to the calculated value for the stagnation point of a sphere with a radius of 1.356 cm.

Figure 10 is a graphic representation of model 1, the basic configuration, showing the isotherms or contour lines for tests at four Reynolds numbers. The contours of figure 10 indicate two areas of low heating, possibly caused by separated flow. The first area of low heating occurs at the aeroshell and AID junction and is bracketed by the two upstream contours marked 3. After approximately 10 seconds of tunnel run time, all the phase-change paint has been heated to the melting point except in an area between contours 8 and 7,8. Again, flow separation is the most likely explanation.

This description of the time history of the isotherms is typical of that for all tests on model 1 at all Reynolds numbers. The results can be summarized by plotting the calculated local heat-transfer coefficients, when expressed as a ratio to the stagnation-point heat-transfer coefficient, against surface distance s/R, as shown in figure 11. The curve drawn in figure 11 is intended only to indicate the trend and should not be considered an accurate estimate of local values between points. It is apparent that the shape of the distribution of H/HS is not greatly affected by Reynolds number except on the burble fence, where peak relative heating values increase with increasing Reynolds number.

Isotherms on the windward side of model 1 are shown in figures 12 and 13 at angles of attack of 5° and 10°, respectively, again at four Reynolds numbers.

Figures 14 to 16 present all the data recorded on the windward side of model 2 in the present tests. The primary difference between these data and those of figures 10 to 13 is due to the nose protuberance of model 2, which now causes an additional region of low heating between the nose and aeroshell as indicated by the unmelted paint on the model surface between the nose protuberance and contour 1. (See fig. 14(a).) The pattern indicates a small area of flow separation at the base of the nose protuberance. The separation-reattachment pattern shown by model 1 at the aeroshell-AID junction can be seen in figure 14(c) downstream at contour 1. Figure 17 is a plot of the heat-transfer data of model 2 expressed as a ratio to the reference-stagnation-point heat-transfer rate against s/R at an angle of attack of 0° and Reynolds numbers from 2.2×10^5 to 1.12×10^6. Heat-transfer coefficients were obtained on the nose of model 2 for the

lowest Reynolds number and indicated that the nose protuberance will have extremely high heating rates. The effect of varying Reynolds number is not apparent on the nose but the burble fence area has an increasing relative heat-transfer coefficient with increasing Reynolds number.

Figures 18 to 25 contain the heat-transfer data obtained on models 3 and 4. In figure 18 data taken along a meridian which passes between inlets in the first row and bisects an inlet in the second row are presented. This meridian is indicated in figures 19 to 24. The ram-air inlets are located closer to the nose of model 3 than to that of model 4. This difference in ram-air inlet location produces a noticeable difference in flow patterns around the most downstream ram-air inlet and on the burble fence. In general, the air stagnates at the upstream surface of the inlet and then expands around the inlet. Note that contour 1 reoccurs behind each inlet and represents an interference heating factor $\bar{h}$ of approximately 3.5. There is a high heating region on the burble fence, model 3 (fig. 19), which is probably associated with the wake flow behind the protuberance. Contours 1, 2, and 3 are shown on the AID body and burble fence.

Model 4 (figs. 22 to 24) is different from model 3 in that the high heating on the body immediately behind the inlet protuberance can be seen only for the forward row of inlets on the AID body. There is an increased heating on the burble fence downstream of both rows of ram-air inlets.

In order to measure accurate heating rates on the ram-air inlets of model 4, a high-melting-point phase-change paint was used to obtain the data of figure 25. These data indicate heat-transfer rates almost twice the reference-stagnation-point heat-transfer rates and a maximum $\bar{h}$ of approximately 5.

Figures 26 to 33 present the results of this investigation on the model side 90° from the most windward ray. The results of angle-of-attack variation are a reduction of heat-transfer coefficient and an enlargement of the separated-flow region on the leeward side of models 1 and 2. (See figs. 26 to 29.) The enlarged separated region is not observed on models 3 and 4. (See figs. 30 to 33.)

A comparison of the heat-transfer coefficients on the AID configuration is presented in figure 34 for a Reynolds number of 2.24×10^5 at $\alpha = 0^{\circ}$. For this Reynolds number the heating rates on models 3 and 4 are approximately equal, as are the heating rates on models 1 and 2. Figure 34 illustrates the fact that the ram-air inlets cause a large increase in local heating on the inlets and on the burble fence immediately behind the inlets. Heating rates representing an $\bar{h}$ approximately five times greater than those on models 1 and 2 were observed on models 3 and 4 for the ram-air inlets and burble-fence locations. Shown in figure 35 are typical schlieren pictures of the four test models at $\alpha = 0^{\circ}$.

CONCLUDING REMARKS

Heat-transfer coefficients have been obtained on four attached inflatable decelerator (AID) configurations in the Langley Mach 8 variable-density tunnel at angles of attack of 0°, 5°, and 10° for a Reynolds number range of 0.22×10^6 to 1.23×10^6 in air. The results of this investigation indicate that the maximum heat-transfer coefficients on the ram-air inlets and the burble fence are approximately five times larger than the coefficients at identical locations on a smooth AID body. Moving the ram-air inlets rearward reduces the heating rates immediately behind the aft row of inlets. This movement of the inlets also increases the heat-transfer coefficients on the burble fence. Increasing Reynolds number effected an increase in relative heat-transfer coefficients primarily on the burble fence.

Langley Research Center,
National Aeronautics and Space Administration,
Hampton, Va., September 13, 1971.

REFERENCES

1. Gillis, Clarence L.: Aerodynamic Deceleration Systems for Space Mission. AIAA Paper No. 68-1081, Oct. 1968.

2. Guy, L. D.: Structural and Decelerator Design Options for Mars Entry. J. Spacecraft Rockets, vol. 6, no. 1, Jan. 1969, pp. 44-49.

3. Bohon, Herman L.; and Miserentino, Robert: Attached Inflatable Decelerator Performance Evaluation and Mission Application Study. AIAA Paper No. 70-1163, Sept. 1970.

4. Mikulas, Martin M., Jr.; and Bohon, Herman L.: Development Status of Attached Inflatable Decelerators. J. Spacecraft Rockets, vol. 6, no. 6, June 1969, pp. 654-660.

5. Barton, R. Reed: Development of Attached Inflatable Decelerators for Supersonic Application. NASA CR-66613, 1968.

6. Bohon, Herman L.; and Miserentino, R.: Deployment and Performance Characteristics of 5-Foot-Diameter (1.5 m) Attached Inflatable Decelerators From Mach Number 2.2 to 4.4. NASA TN D-5840, 1970.

7. Faurote, G. L.; and Burgess, J. L.: Thermal and Stress Analysis of an Attached Inflatable Decelerator (AID) Deployed in the Mars and Earth Atmospheres. Rep. No. GER-14939 (Contract NAS1-9726), Goodyear Aerosp. Corp., Aug. 12, 1971. (Available as NASA CR 111920.)

8. Stainback, P. Calvin: Heat-Transfer Measurements at a Mach Number of 8 in the Vicinity of a 90° Interior Corner Alined With the Free-Stream Velocity. NASA TN D-2417, 1964.

9. Jones, Robert A.; and Hunt, James L.: Use of Fusible Temperature Indicators for Obtaining Quantitative Aerodynamic Heat-Transfer Data. NASA TR R-230, 1966.

10. Reshotko, Eli; and Cohen, Clarence B.: Heat Transfer at the Forward Stagnation Point of Blunt Bodies. NACA TN 3513, 1955.

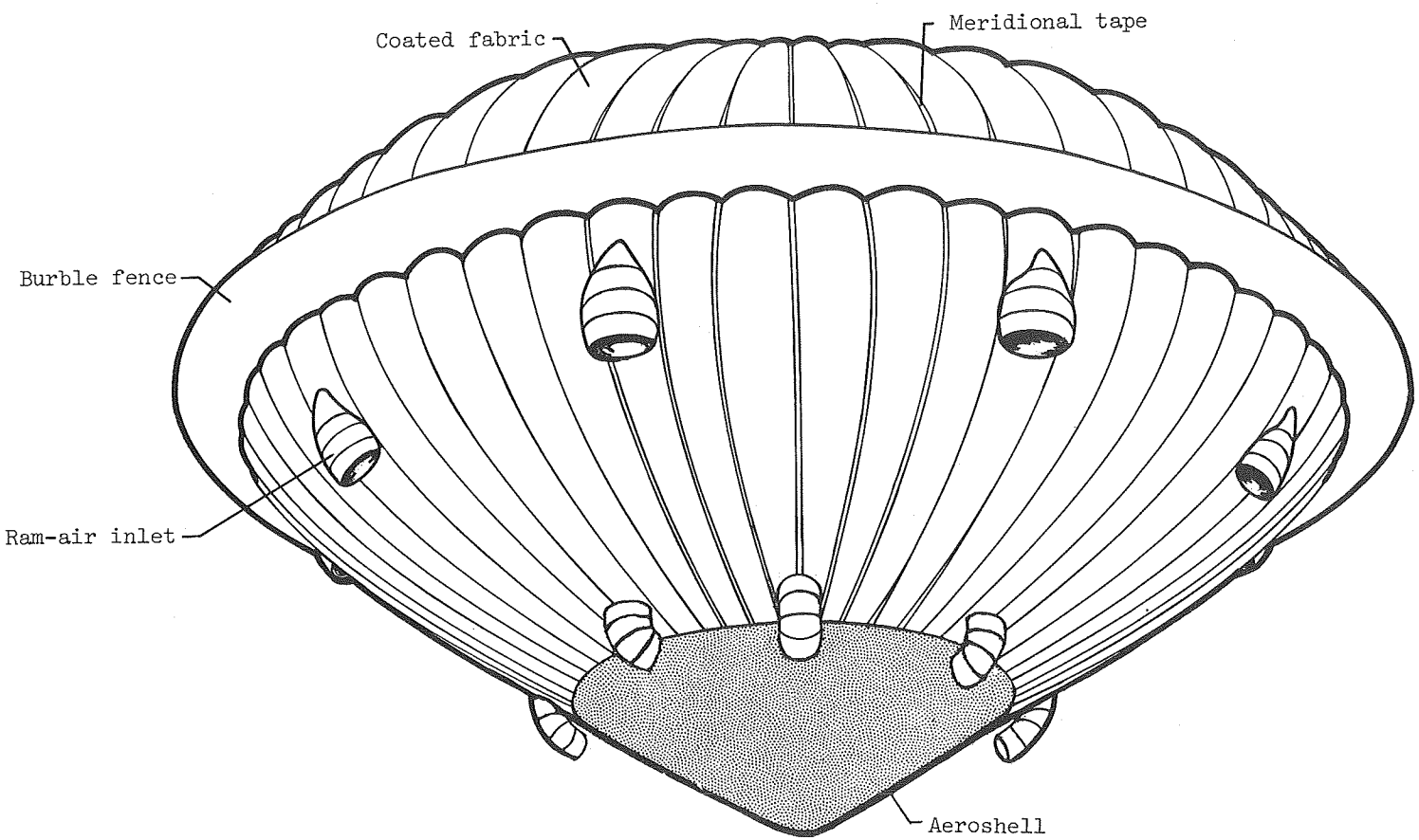

Figure 1.- Attached inflatable decelerator (AID).

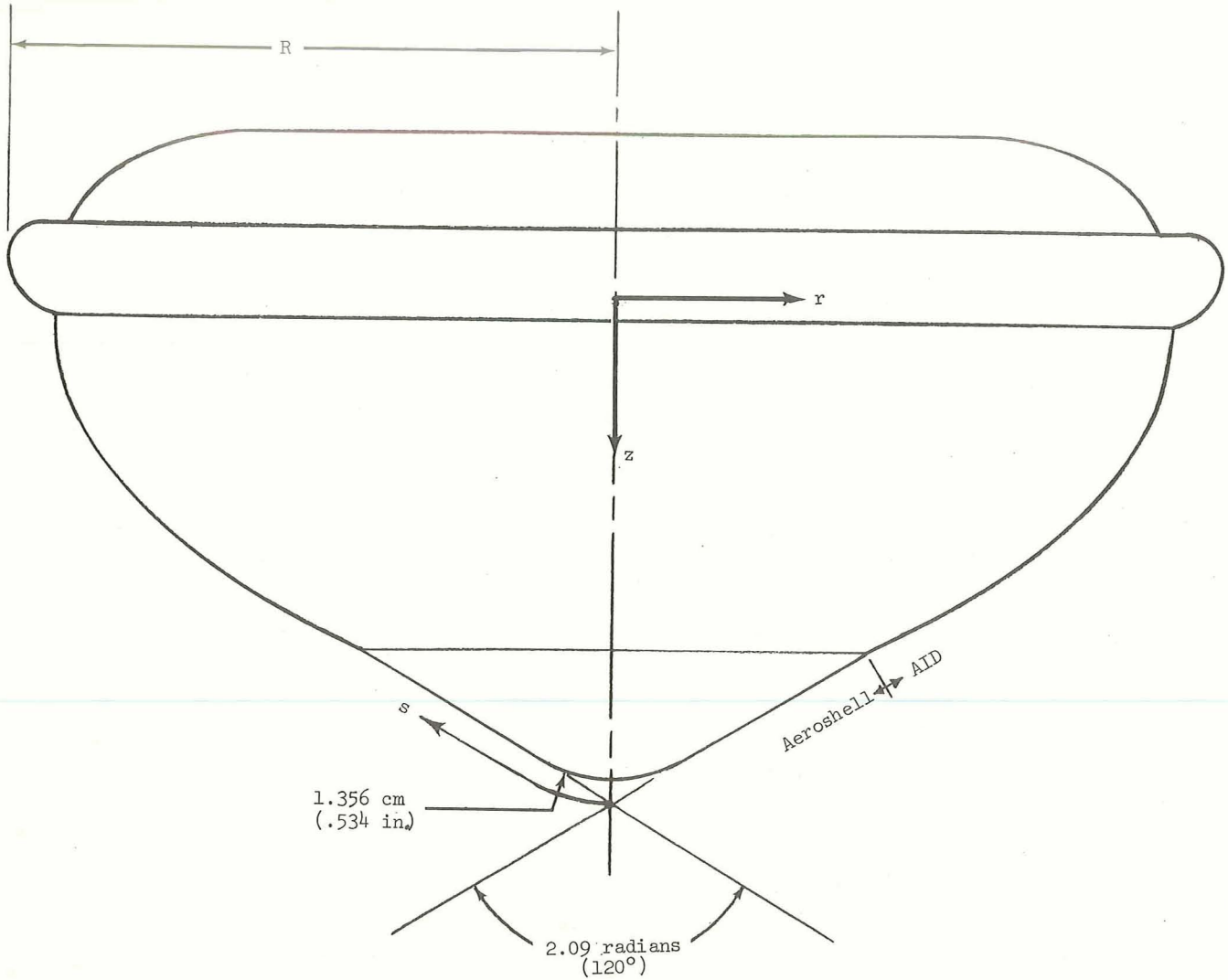

Figure 2.- Configuration of model 1 and primary AID profile for all models.

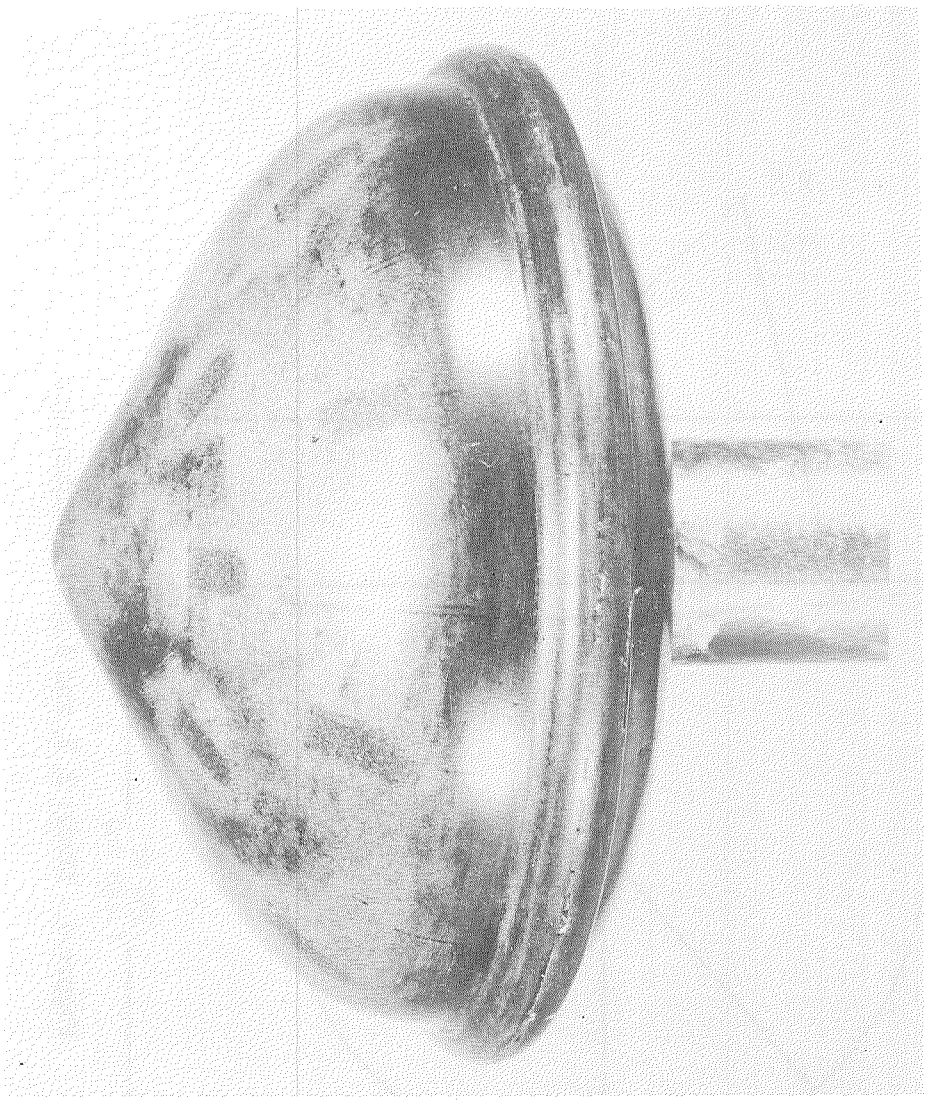

L-70-8909

Figure 3.- Model 1.

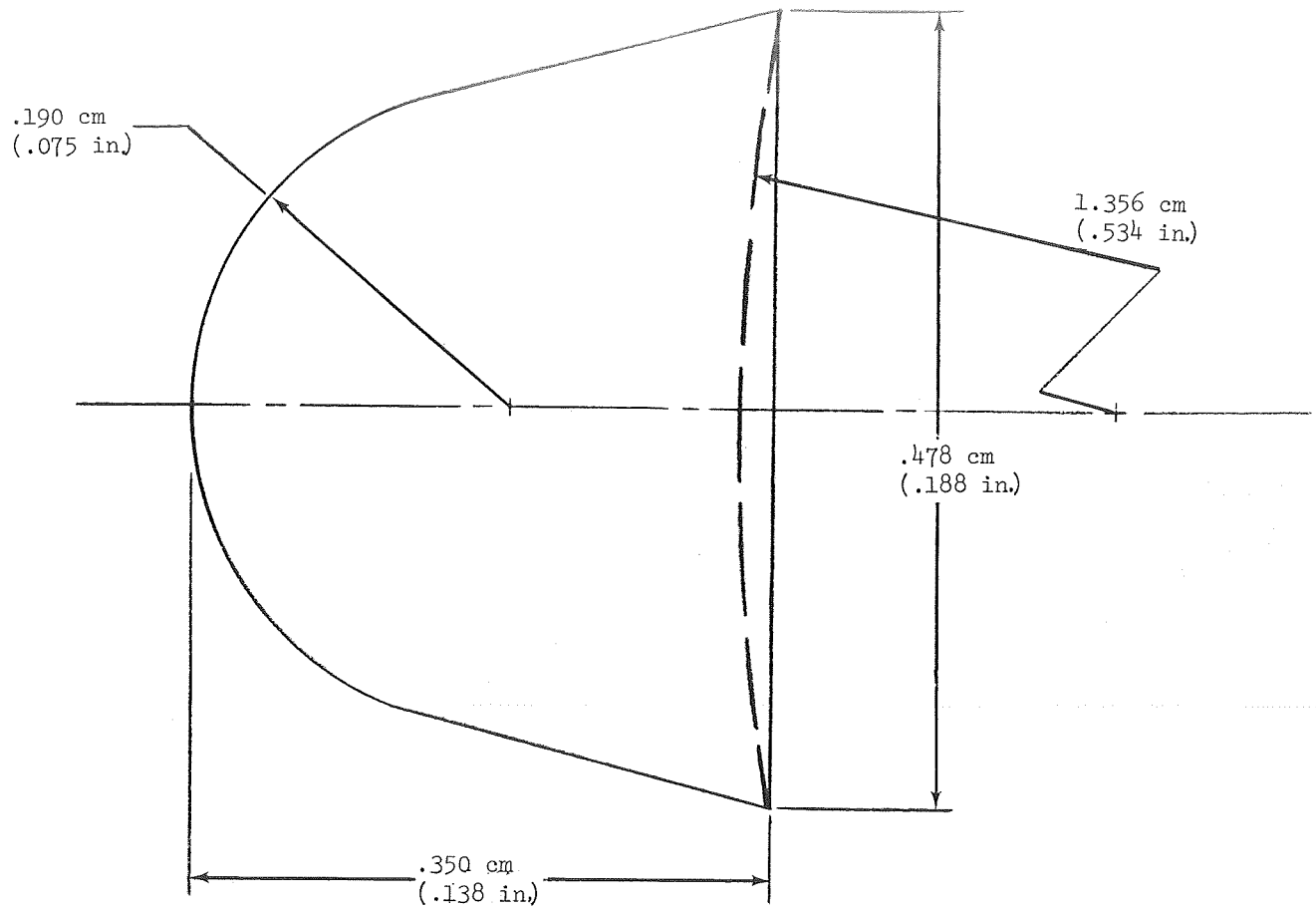

Figure 4.- Model 2, 3, and 4 nose protuberance.

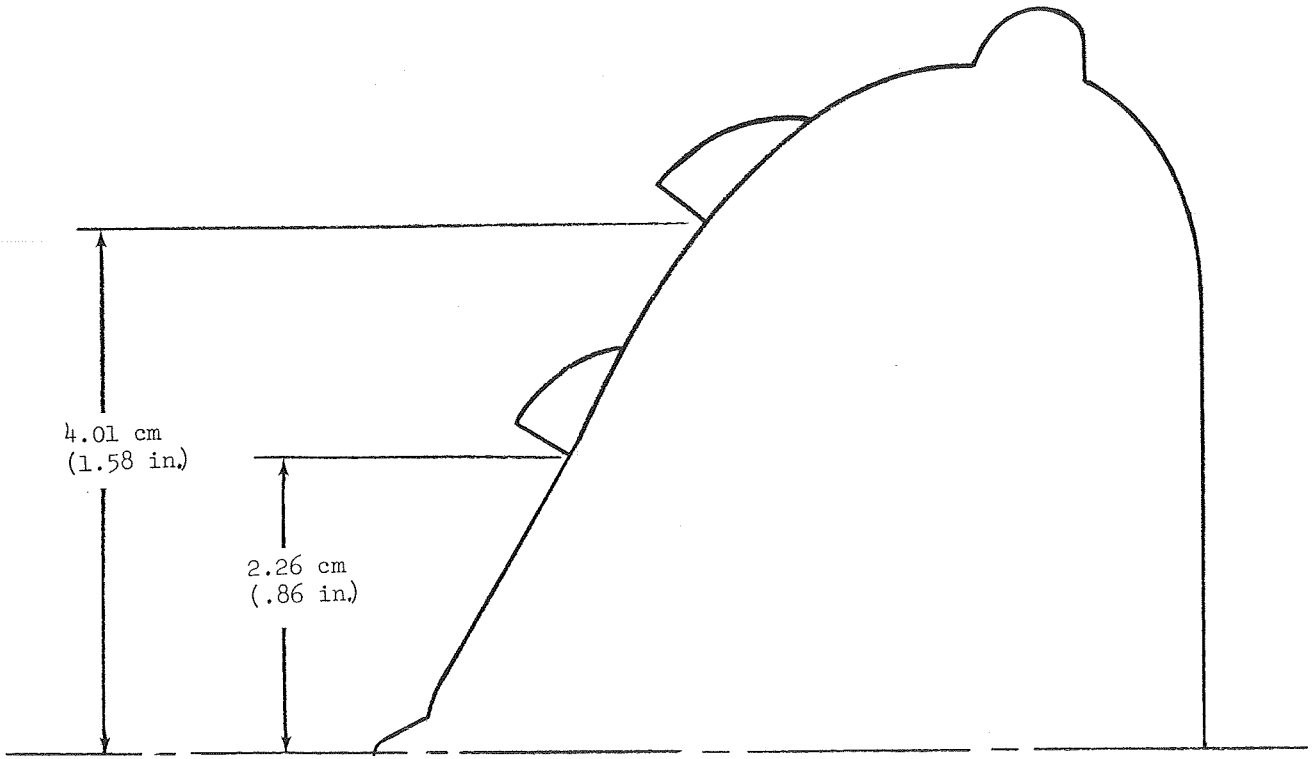

Figure 5.- Model 3 inlet protuberance longitudinal location.

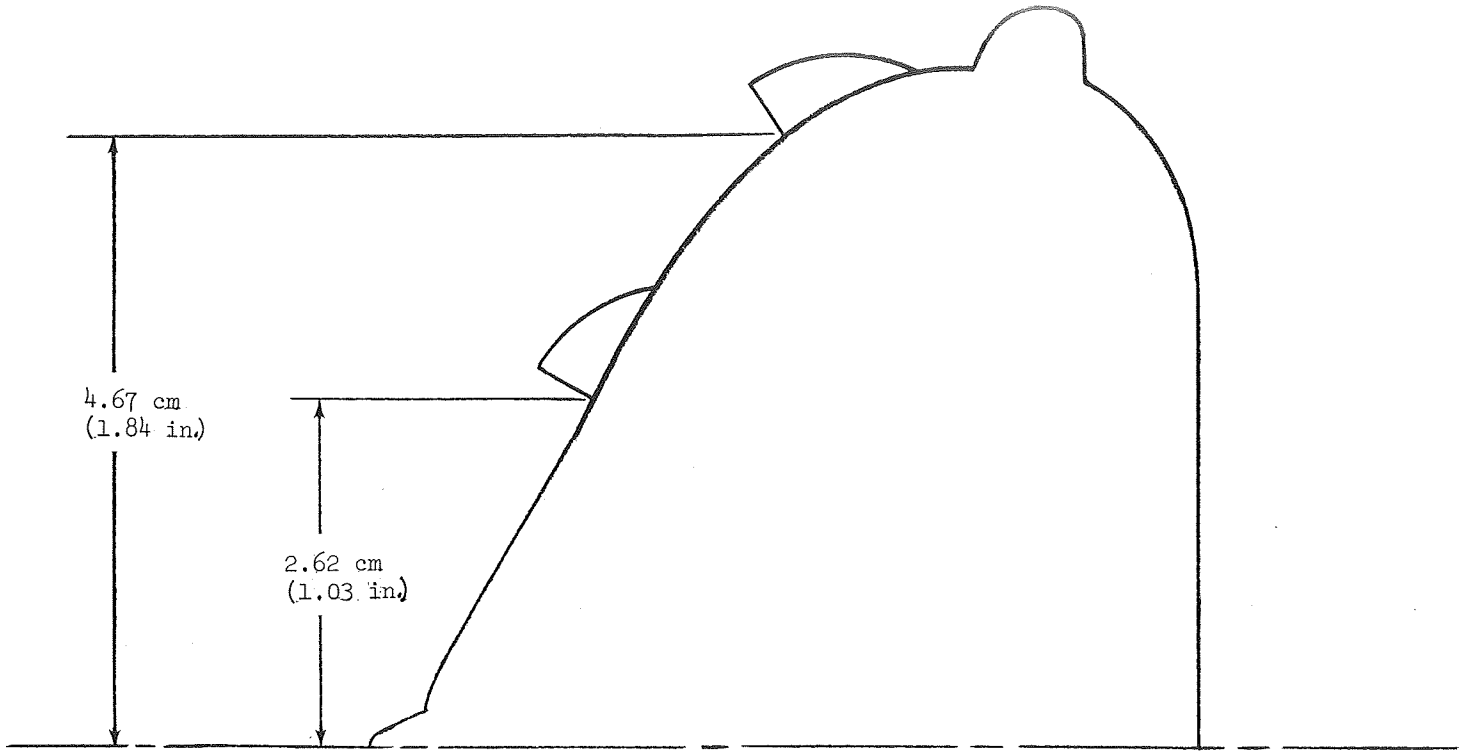

Figure 6.- Model 4 inlet protuberance longitudinal location.

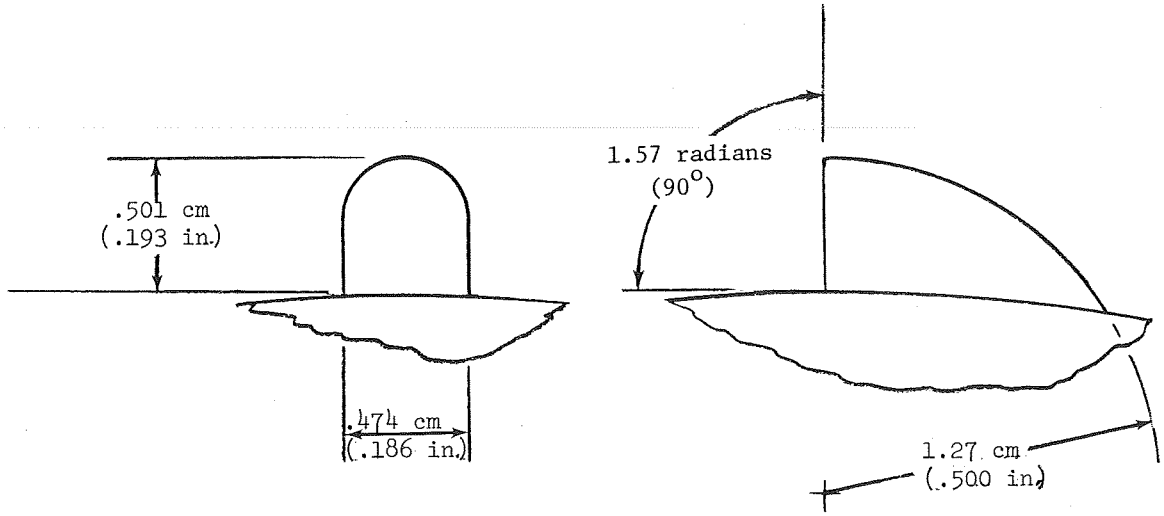

Figure 7.- Model 3 and 4 inlet protuberance geometry.

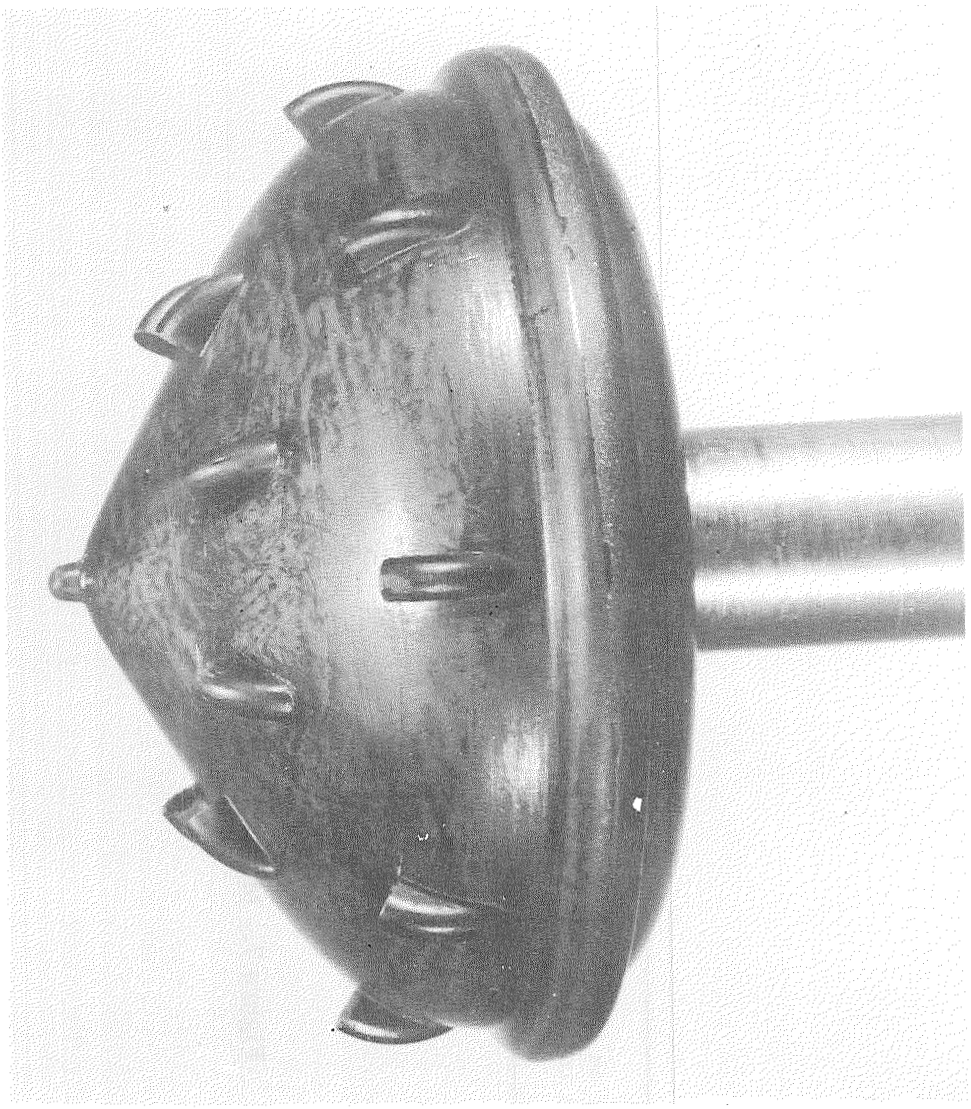

L-70-8908

Figure 8.- Model 4.

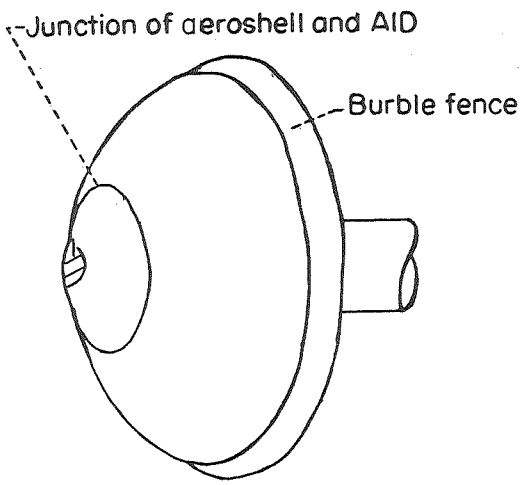

(a) T = 0.5 sec.

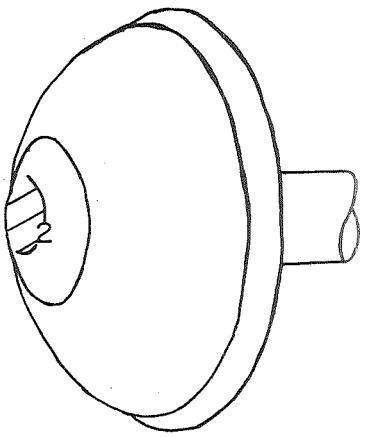

(b) T = 1.5 sec.

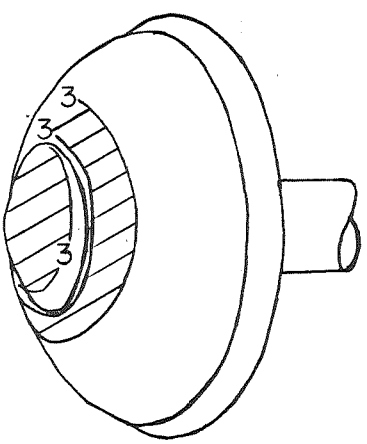

(c) T = 2.5 sec.

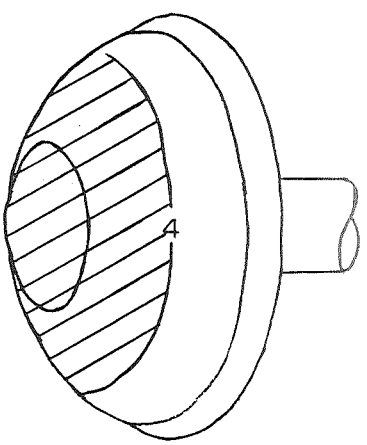

(d) T = 4.9 sec.

Figure 9.- Sketches of model showing typical phase-change pattern sequence. $\alpha = 0^{\circ}$.

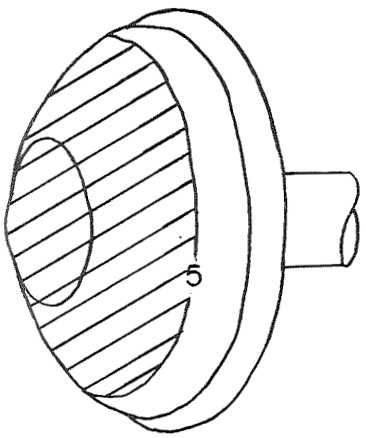

(e) T = 6.50 sec.

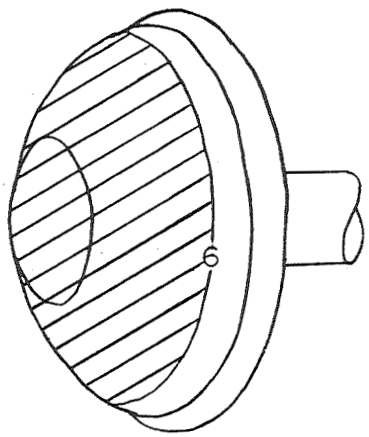

(f) T = 9.70 sec.

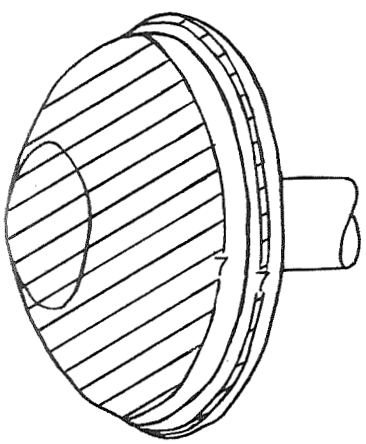

(g) T = 11.10 sec.

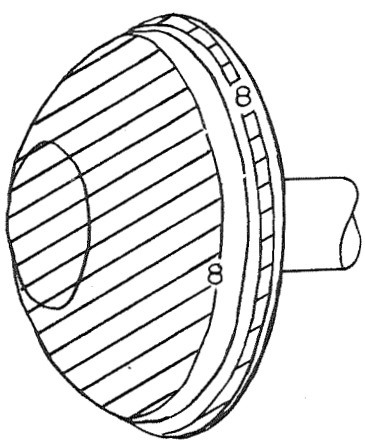

(h) T = 15.60 sec.

Figure 9.- Concluded.

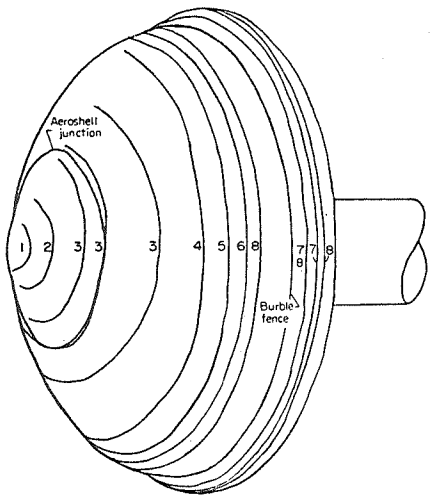

ALPHA= 0.000 MINF = 7.690
R/M= 2.01030E+06
HS= 2.46524E+02 WATTS/METER(SQ)-DEG-K

CONTOUR	T,SEC	H,WATTS/METER(SQ)-DEG-K	H/HS
1	.50	1.87934E+02	7.62336E-01
2	1.50	1.08504E+02	4.40135E-01
3	2.50	8.40466E+01	3.40927E-01
4	4.90	6.00333E+01	2.43519E-01
5	6.50	5.21235E+01	2.11434E-01
6	9.70	4.26682E+01	1.73079E-01
7	11.10	3.98867E+01	1.61797E-01
8	15.40	3.38633E+01	1.37363E-01

(a) $N_{Re,\infty} = 2.24 \times 10^5$.

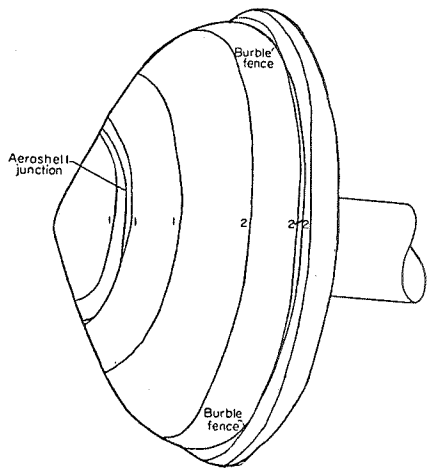

ALPHA= 0.000 MINF = 7.800
R/M= 3.27936E+06
HS= 3.26361E+02 WATTS/METER(SQ)-DEG-K

CONTOUR	T,SEC	H,WATTS/METER(SQ)-DEG-K	H/HS
1	1.20	1.18126E+02	3.61950E-01
2	6.10	5.23928E+01	1.60537E-01

(b) $N_{Re,\infty} = 3.70 \times 10^5$.

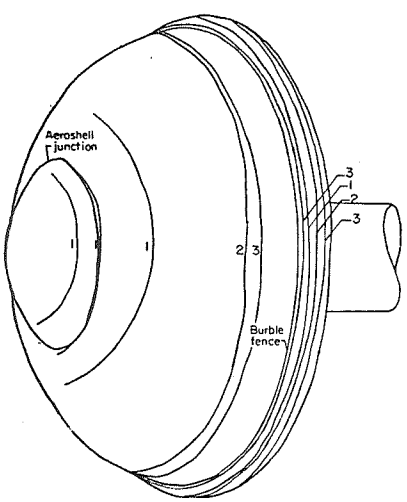

ALPHA= 0.000 MINF = 7.900
R/M= 5.86143E+06
HS= 4.41194E+02 WATTS/METER(SQ)-DEG-K

CONTOUR	T,SEC	H,WATTS/METER(SQ)-DEG-K	H/HS
1	.50	1.71812E+02	3.89425E-01
2	3.70	6.31593E+01	1.43155E-01
3	8.70	4.11888E+01	9.33575E-02

(c) $N_{Re,\infty} = 6.6 \times 10^5$.

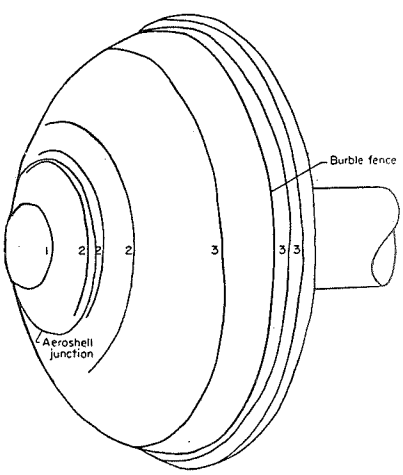

ALPHA= 0.000 MINF = 7.950
R/M= 1.04748E+07
HS= 5.72848E+02 WATTS/METER(SQ)-DEG-K

CONTOUR	T,SEC	H,WATTS/METER(SQ)-DEG-K	H/HS
1	.80	3.05087E+02	5.32579E-01
2	1.70	2.09288E+02	3.65346E-01
3	5.50	1.16355E+02	2.03118E-01

(d) $N_{Re,\infty} = 1.12 \times 10^6$.

Figure 10.- View of windward side of model showing constant-temperature contours. $\alpha = 0^o$.

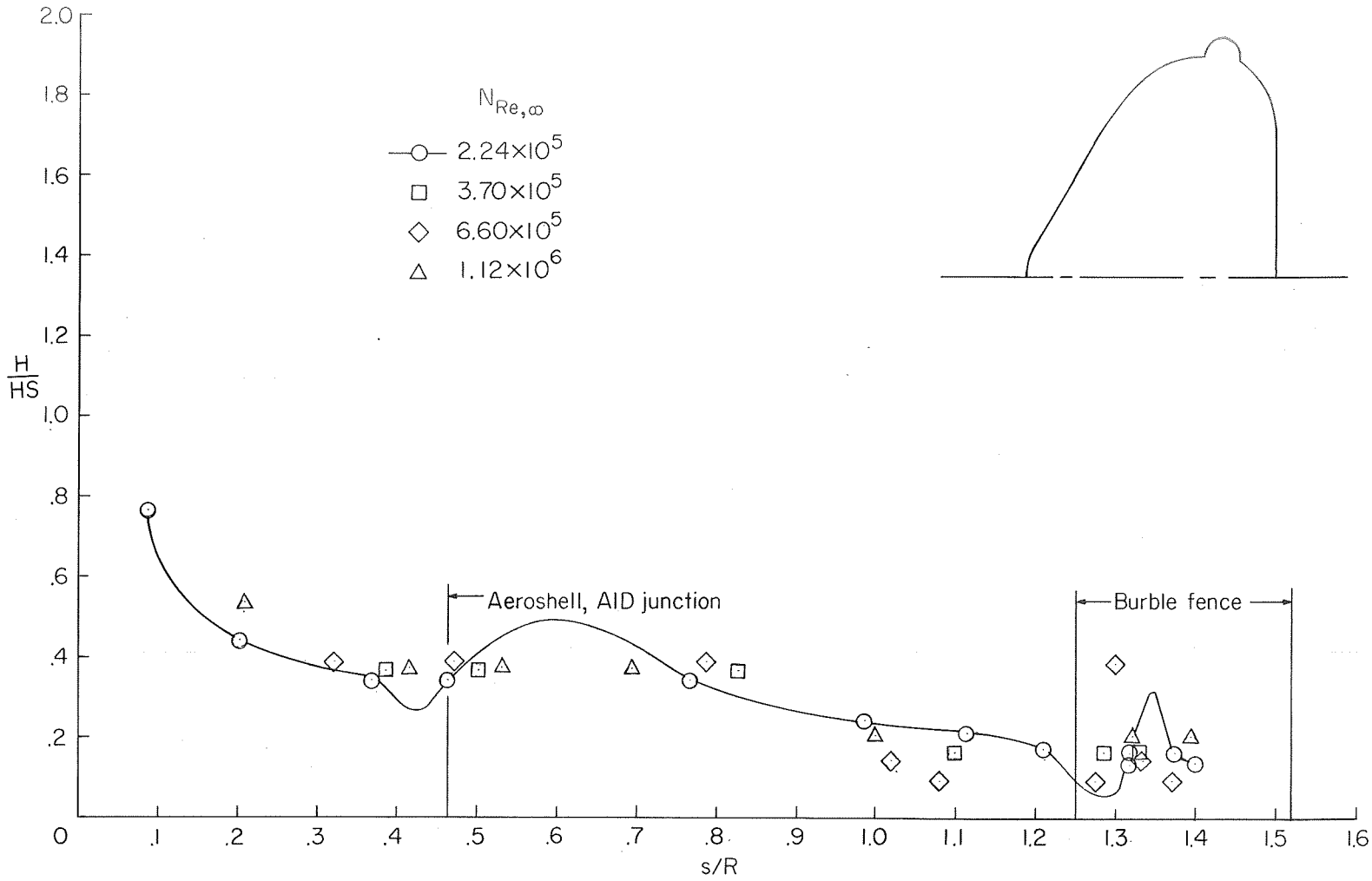

Figure 11.- Relative heat-transfer coefficients on model 1 at $\alpha = 0^{o}$ for several Reynolds numbers.

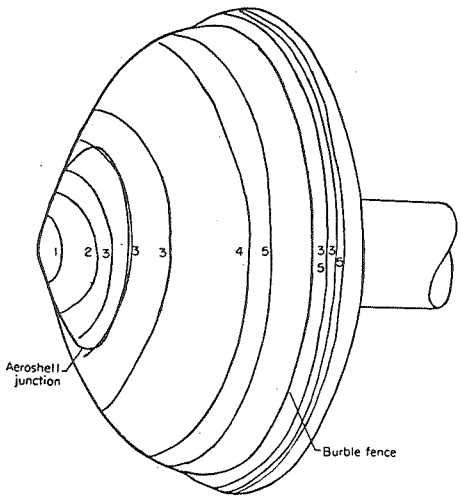

ALPHA= 5.000 MINF = 7.690
R/M= 1.88016E+06
HS= 2.46979E+02 WATTS/METER(SQ)-DEG-K

CONTOUR	T,SEC	H,WATTS/METER(SQ)-DEG-K	H/HS
1	.40	2.15573E+02	8.72838E-01
2	.80	1.52433E+02	6.17190E-01
3	1.70	1.04568E+02	4.23389E-01
4	3.90	6.90385E+01	2.79532E-01
5	7.70	4.91336E+01	1.98938E-01

(a) $N_{Re,\infty} = 2.1 \times 10^5$.

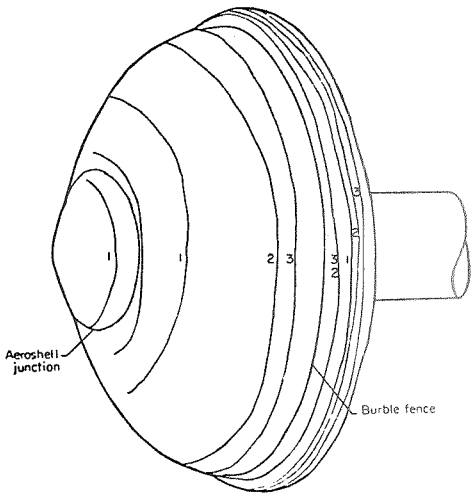

ALPHA= 5.000 MINF = 7.800
R/M= 3.29855E+06
HS= 3.26537E+02 WATTS/METER(SQ)-DEG-K

CONTOUR	T,SEC	H,WATTS/METER(SQ)-DEG-K	H/HS
1	.20	2.83123E+02	8.67045E-01
2	2.60	7.85241E+01	2.40475E-01
3	7.70	4.56293E+01	1.39737E-01

(b) $N_{Re,\infty} = 3.7 \times 10^5$.

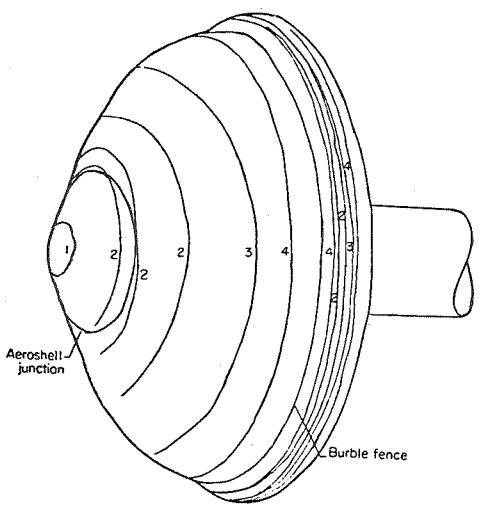

ALPHA= 5.000 MINF = 7.900
R/M= 5.99666E+06
HS= 4.41284E+02 WATTS/METER(SQ)-DEG-K

CONTOUR	T,SEC	H,WATTS/METER(SQ)-DEG-K	H/HS
1	.30	3.19480E+02	7.23980E-01
2	.80	1.95641E+02	4.43345E-01
3	2.00	1.23734E+02	2.80396E-01
4	6.50	6.86354E+01	1.55536E-01

(c) $N_{Re,\infty} = 7.72 \times 10^5$.

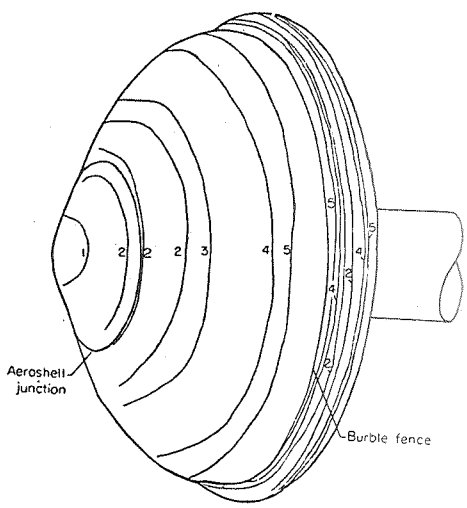

ALPHA= 5.000 MINF = 7.950
R/M= 1.07896E+07
HS= 5.74412E+02 WATTS/METER(SQ)-DEG-K

CONTOUR	T,SEC	H,WATTS/METER(SQ)-DEG-K	H/HS
1	.30	5.41021E+02	9.41869E-01
2	1.10	2.88247E+02	5.01813E-01
3	2.00	2.18179E+02	3.79830E-01
4	3.30	1.73429E+02	3.01925E-01
5	5.70	1.34799E+02	2.34673E-01

(d) $N_{Re,\infty} = 1.2 \times 10^6$.

Figure 12.- View of windward side of model 1 showing constant-temperature contours. $\alpha = 5^o$.

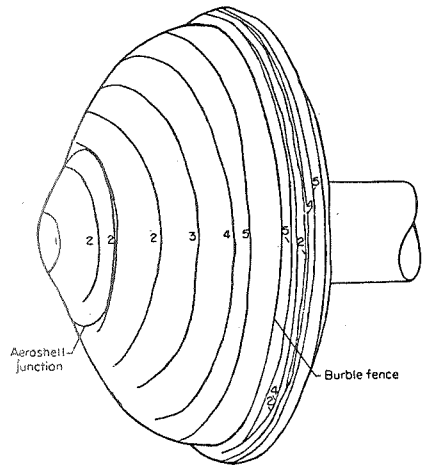

ALPHA=10.000 MINF = 7.690
R/M= 1.96128E+06
HS= 2.46847E+02 WATTS/METER(SQ)-DEG-K

CONTOUR	T,SEC	H,WATTS/METER(SQ)-DEG-K	H/HS
1	.60	1.76920E+02	7.16720E-01
2	1.40	1.15822E+02	4.69203E-01
3	2.70	8.34010E+01	3.37865E-01
4	4.30	6.60875E+01	2.67726E-01
5	9.20	4.51814E+01	1.83034E-01

(a) $N_{Re,\infty} = 2.24 \times 10^5$.

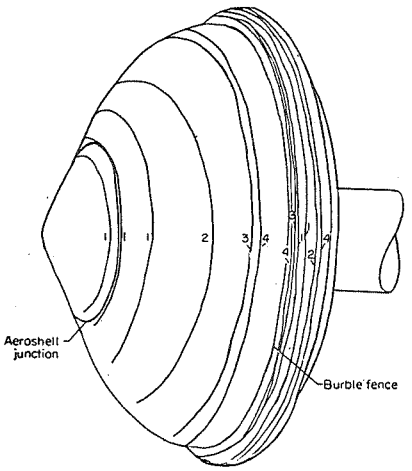

ALPHA=10.000 MINF = 7.800
R/M= 3.27819E+06
HS= 3.34180E+02 WATTS/METER(SQ)-DEG-K

CONTOUR	T,SEC	H,WATTS/METER(SQ)-DEG-K	H/HS
1	.50	1.69398E+02	5.06906E-01
2	1.20	1.09346E+02	3.27206E-01
3	2.80	7.15837E+01	2.14207E-01
4	6.30	4.77225E+01	1.42805E-01

(b) $N_{Re,\infty} = 3.7 \times 10^5$.

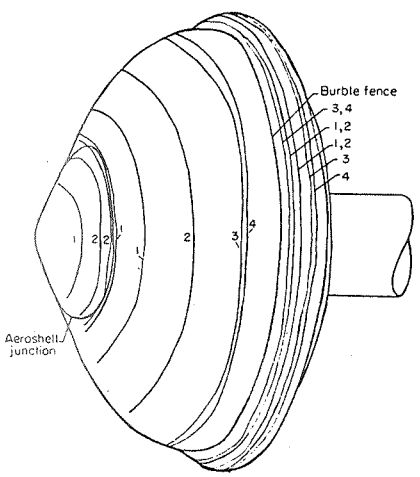

ALPHA=10.000 MINF = 7.900
R/M= 5.92840E+06
HS= 4.41576E+02 WATTS/METER(SQ)-DEG-K

CONTOUR	T,SEC	H,WATTS/METER(SQ)-DEG-K	H/HS
1	.30	3.18715E+02	7.21765E-01
2	.80	1.95172E+02	4.41989E-01
3	2.90	1.02509E+02	2.32144E-01
4	5.90	7.18681E+01	1.62754E-01

(c) $N_{Re,\infty} = 6.7 \times 10^5$.

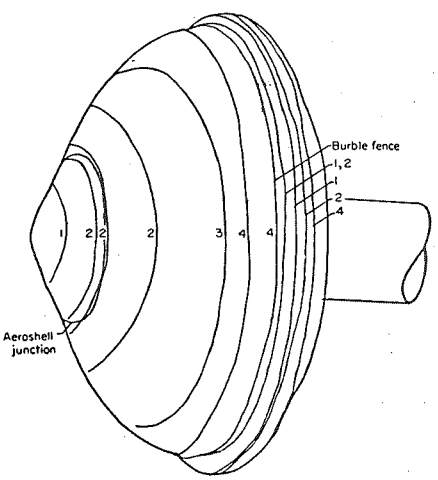

ALPHA=10.000 MINF = 7.950
R/M= 1.04137E+07
HS= 5.72535E+02 WATTS/METER(SQ)-DEG-K

CONTOUR	T,SEC	H,WATTS/METER(SQ)-DEG-K	H/HS
1	.20	6.44360E+02	1.12545E+00
2	1.00	2.88166E+02	5.03317E-01
3	2.70	1.75373E+02	3.06309E-01
4	6.30	1.14808E+02	2.00526E-01

(d) $N_{Re,\infty} = 1.12 \times 10^6$.

Figure 13.- View of windward side of model 1 showing constant-temperature contours. $\alpha = 10^o$.

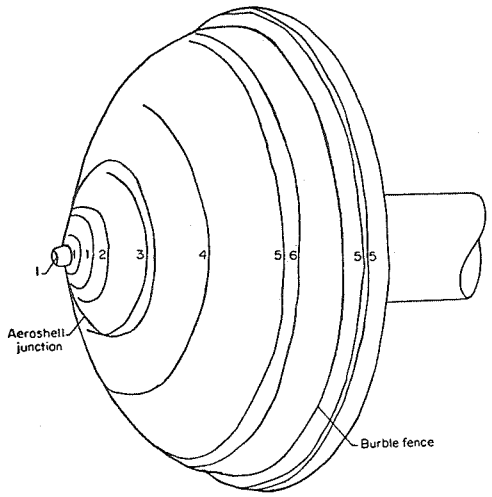

ALPHA= 0.000 MINF = 7.690
R/M= 2.04842E+06
HS= 2.46248E+02 WATTS/METER(SQ)-DEG-K

CONTOUR	T,SEC	H,WATTS/METER(SQ)-DEG-K	H/HS
1	.10	4.81077E+02	1.95363E+00
2	.60	1.96399E+02	7.97565E-01
3	2.20	1.02566E+02	4.16515E-01
4	2.90	8.93338E+01	3.62779E-01
5	7.10	5.70934E+01	2.31853E-01
6	10.30	4.74020E+01	1.92497E-01

(a) $N_{Re,\infty} = 2.24 \times 10^5$.

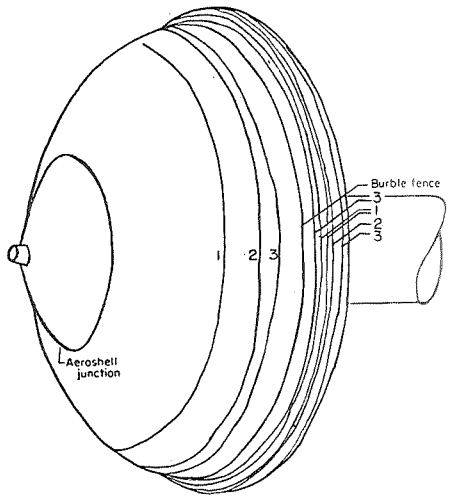

ALPHA= 0.000 MINF = 7.900
R/M= 5.86143E+06
HS= 4.41194E+02 WATTS/METER(SQ)-DEG-K

CONTOUR	T,SEC	H,WATTS/METER(SQ)-DEG-K	H/HS
1	1.30	1.06553E+02	2.41511E-01
2	2.90	7.13410E+01	1.61700E-01
3	9.20	4.00539E+01	9.07851E-02

(b) $N_{Re,\infty} = 6.72 \times 10^5$.

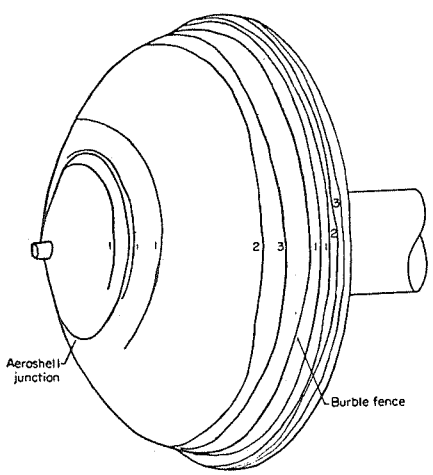

ALPHA= 0.000 MINF = 7.950
R/M= 1.04137E+07
HS= 5.71484E+02 WATTS/METER(SQ)-DEG-K

CONTOUR	T,SEC	H,WATTS/METER(SQ)-DEG-K	H/HS
1	.30	2.97686E+02	5.20900E-01
2	2.50	1.03121E+02	1.80445E-01
3	8.50	5.59255E+01	9.78601E-02

(c) $N_{Re,\infty} = 1.12 \times 10^6$.

Figure 14.- View of windward side of model 2 showing constant-temperature contours. $\alpha = 0^o$.

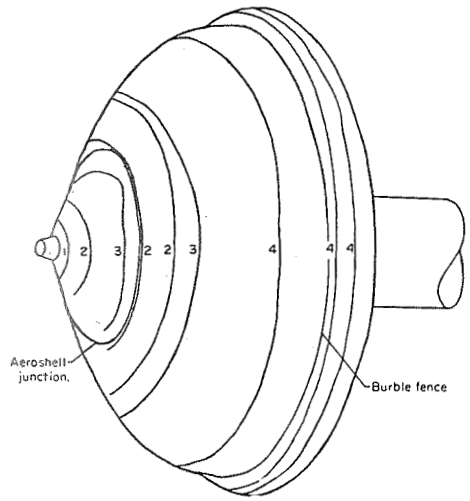

ALPHA= 5.000 MINF = 7.800
R/M= 3.58824E+06
HS= 3.27041E+02 WATTS/METER(SQ)-DEG-K

CONTOUR	T,SEC	H,WATTS/METER(SQ)-DEG-K	H/HS
1	.30	2.46467E+02	7.53627E-01
2	.70	1.61351E+02	4.93364E-01
3	2.40	8.71393E+01	2.66447E-01

(a) $N_{Re,\infty} = 2.4 \times 10^5$.

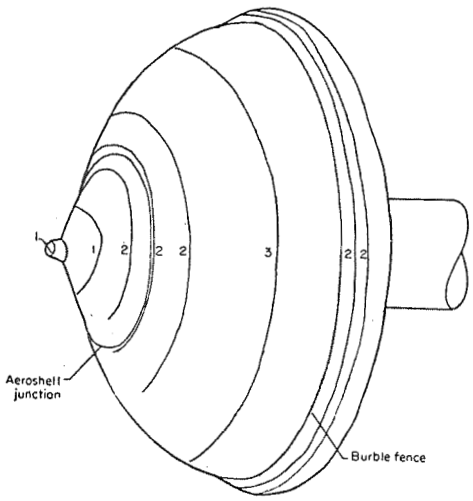

ALPHA= 5.000 MINF = 7.690
R/M= 2.07451E+06
HS= 2.46054E+02 WATTS/METER(SQ)-DEG-K

CONTOUR	T,SEC	H,WATTS/METER(SQ)-DEG-K	H/HS
1	.30	2.66673E+02	1.08380E+00
2	1.20	1.33337E+02	5.41901E-01
3	2.20	9.84756E+01	4.00220E-01
4	7.40	5.36938E+01	2.18220E-01

(b) $N_{Re,\infty} = 4.03 \times 10^5$.

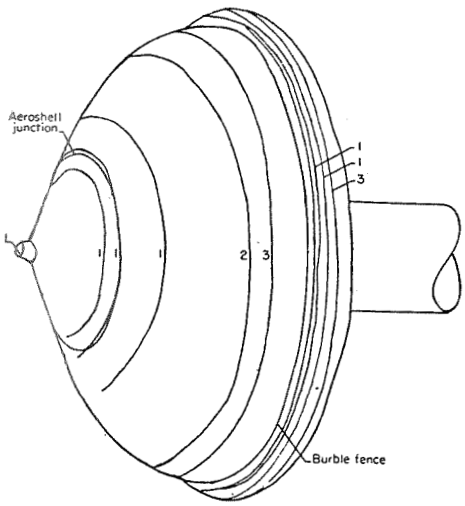

ALPHA= 5.000 MINF = 7.900
R/M= 5.99666E+06
HS= 4.41284E+02 WATTS/METER(SQ)-DEG-K

CONTOUR	T,SEC	H,WATTS/METER(SQ)-DEG-K	H/HS
1	.60	2.21338E+02	5.01511E-01
2	2.20	1.15575E+02	2.61905E-01
3	4.90	7.74418E+01	1.75492E-01

(c) $N_{Re,\infty} = 6.72 \times 10^5$.

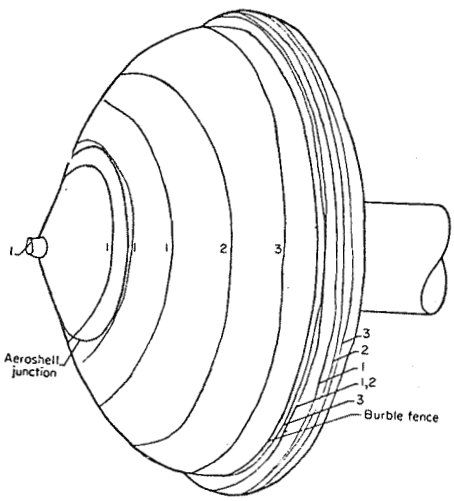

ALPHA= 5.000 MINF = 7.950
R/M= 1.00020E+07
HS= 5.72869E+02 WATTS/METER(SQ)-DEG-K

CONTOUR	T,SEC	H,WATTS/METER(SQ)-DEG-K	H/HS
1	.40	4.29074E+02	7.48991E-01
2	1.50	2.21573E+02	3.86777E-01
3	4.30	1.30866E+02	2.28440E-01

(d) $N_{Re,\infty} = 1.12 \times 10^6$.

Figure 15.- View of windward side of model 2 showing constant-temperature contours. $\alpha = 5^o$.

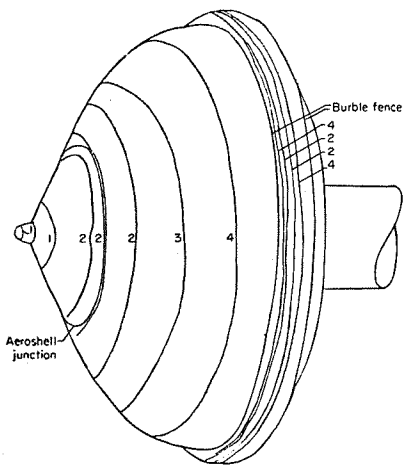

ALPHA=10.000 MINF = 7.690
R/M= 2.10116E+06
HS= 2.45859E+02 WATTS/METER(SQ)-DEG-K

CONTOUR	T,SEC	H,WATTS/METER(SQ)-DEG-K	H/HS
1	.40	2.31045E+02	9.39748E-01
2	1.40	1.23499E+02	5.02316E-01
3	2.90	8.58081E+01	3.49014E-01
4	7.20	5.44579E+01	2.21501E-01

(a) $N_{Re,\infty} = 2.24 \times 10^5$.

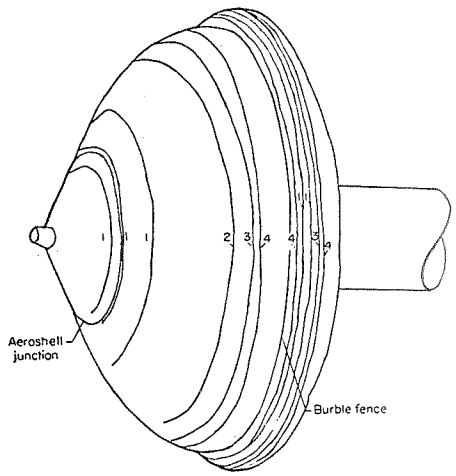

ALPHA=10.000 MINF = 7.800
R/M= 3.15007E+06
HS= 3.26551E+02 WATTS/METER(SQ)-DEG-K

CONTOUR	T,SEC	H,WATTS/METER(SQ)-DEG-K	H/HS
1	.40	1.98676E+02	6.08407E-01
2	1.20	1.14706E+02	3.51264E-01
3	2.50	7.94704E+01	2.43363E-01
4	5.60	5.30984E+01	1.62604E-01

(b) $N_{Re,\infty} = 3.6 \times 10^5$.

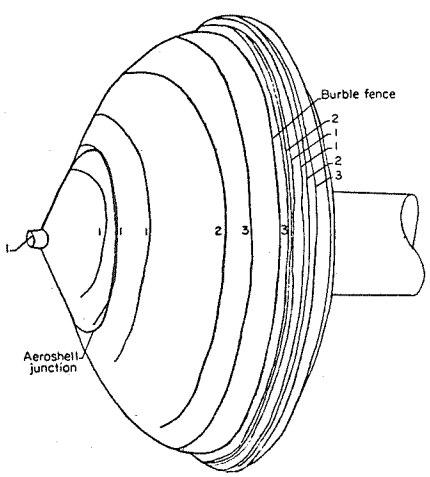

ALPHA=10.000 MINF = 7.900
R/M= 5.99666E+06
HS= 4.41284E+02 WATTS/METER(SQ)-DEG-K

CONTOUR	T,SEC	H,WATTS/METER(SQ)-DEG-K	H/HS
1	.40	2.79492E+02	6.33362E-01
2	1.80	1.31754E+02	2.98570E-01
3	5.20	7.75172E+01	1.75663E-01

(c) $N_{Re,\infty} = 6.72 \times 10^5$.

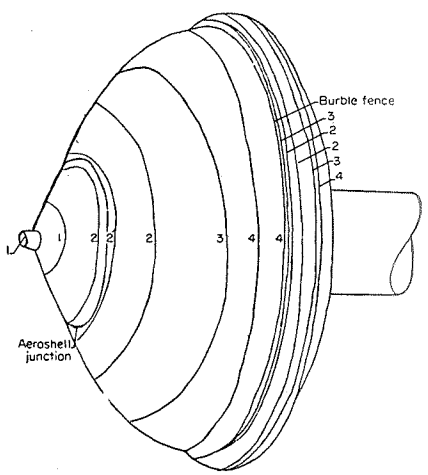

ALPHA=10.000 MINF = 7.950
R/M= 1.05989E+07
HS= 5.73468E+02 WATTS/METER(SQ)-DEG-K

CONTOUR	T,SEC	H,WATTS/METER(SQ)-DEG-K	H/HS
1	.40	4.68240E+02	8.16506E-01
2	.80	3.31096E+02	5.77357E-01
3	2.30	1.95270E+02	3.40507E-01
4	6.00	1.20899E+02	2.10821E-01

(d) $N_{Re,\infty} = 1.12 \times 10^6$.

Figure 16.- View of windward side of model 2 showing constant-temperature contours. $\alpha = 10^o$.

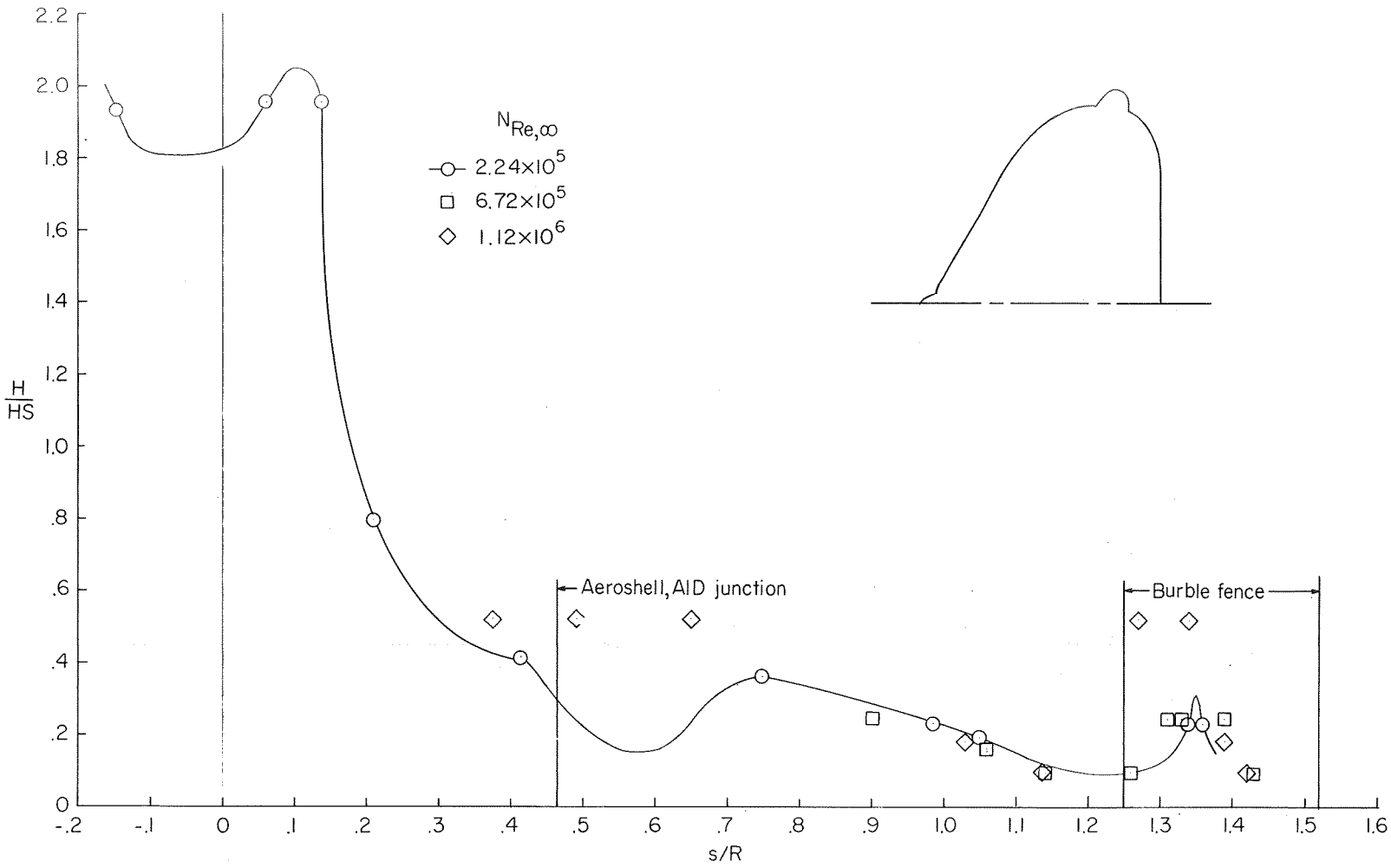

Figure 17.- Relative heat-transfer coefficients on model 2 at $\alpha = 0^{o}$ for several Reynolds numbers.

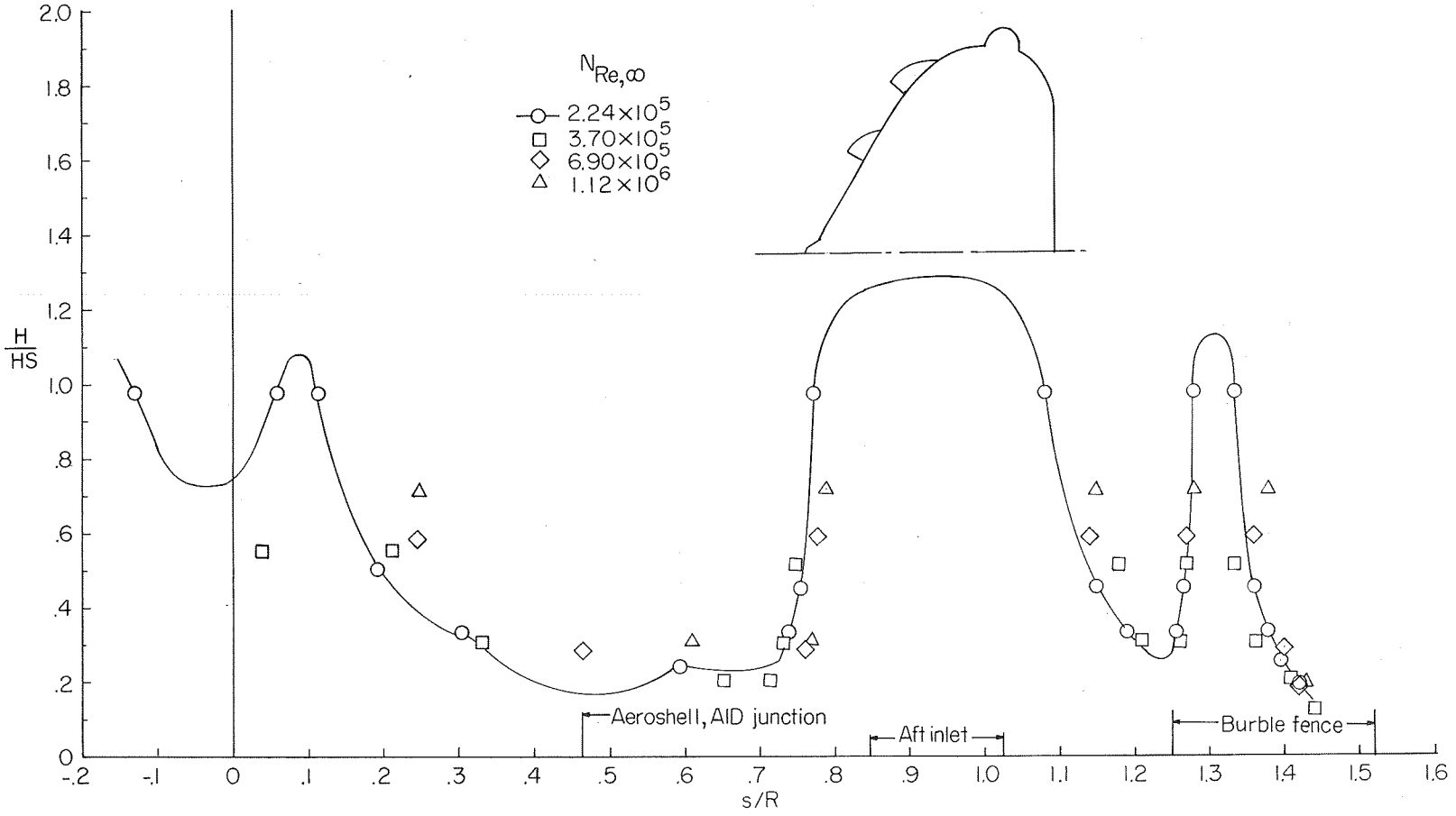

(a) Model 3.

Figure 18.- Relative heat-transfer coefficients on models 3 and 4 at $\alpha = 0^{\circ}$ for several Reynolds numbers.

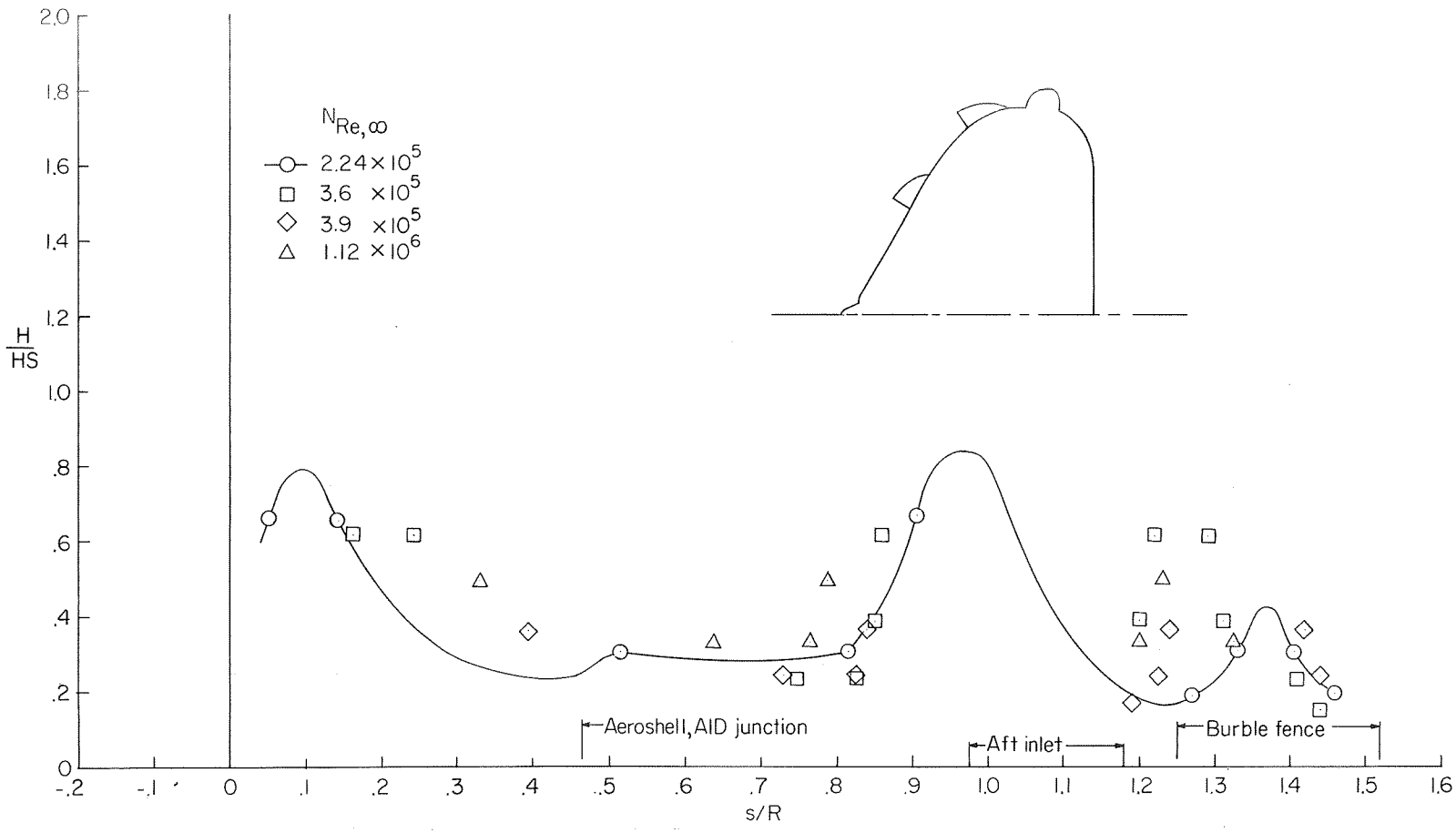

(b) Model 4.

Figure 18.- Concluded.

ALPHA= 0.000 MINF = 7.690
R/M= 1.86903E+06
HS= 2.46843E+02 WATTS/METER(SQ)-DEG-K

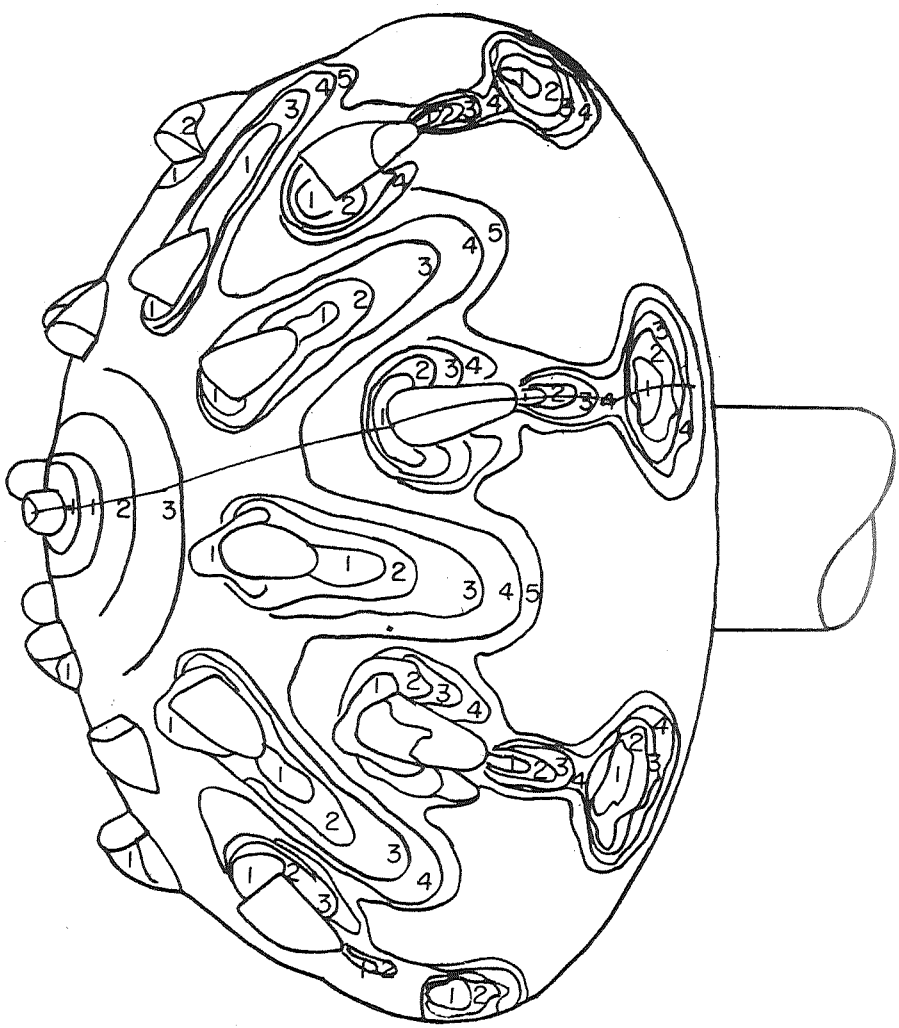

CONTOUR	T,SEC	H,WATTS/METER(SQ)-DEG-K	H/HS
1	.30	2.40558E+02	9.74540E-01
2	1.40	1.11357E+02	4.51124E-01
3	2.60	8.17136E+01	3.31035E-01
4	4.70	6.07760E+01	2.46213E-01
5	7.80	4.71774E+01	1.91123E-01

(a) $N_{Re,\infty} \approx 2.24 \times 10^5$.

Figure 19.- View of windward side of model 3 showing constant-temperature contours. $\alpha = 0^o$.

ALPHA= 0.000 MINF = 7.800
R/M= 3.31793E+06
HS= 3.26715E+02 WATTS/METER(SQ)-DEG-K

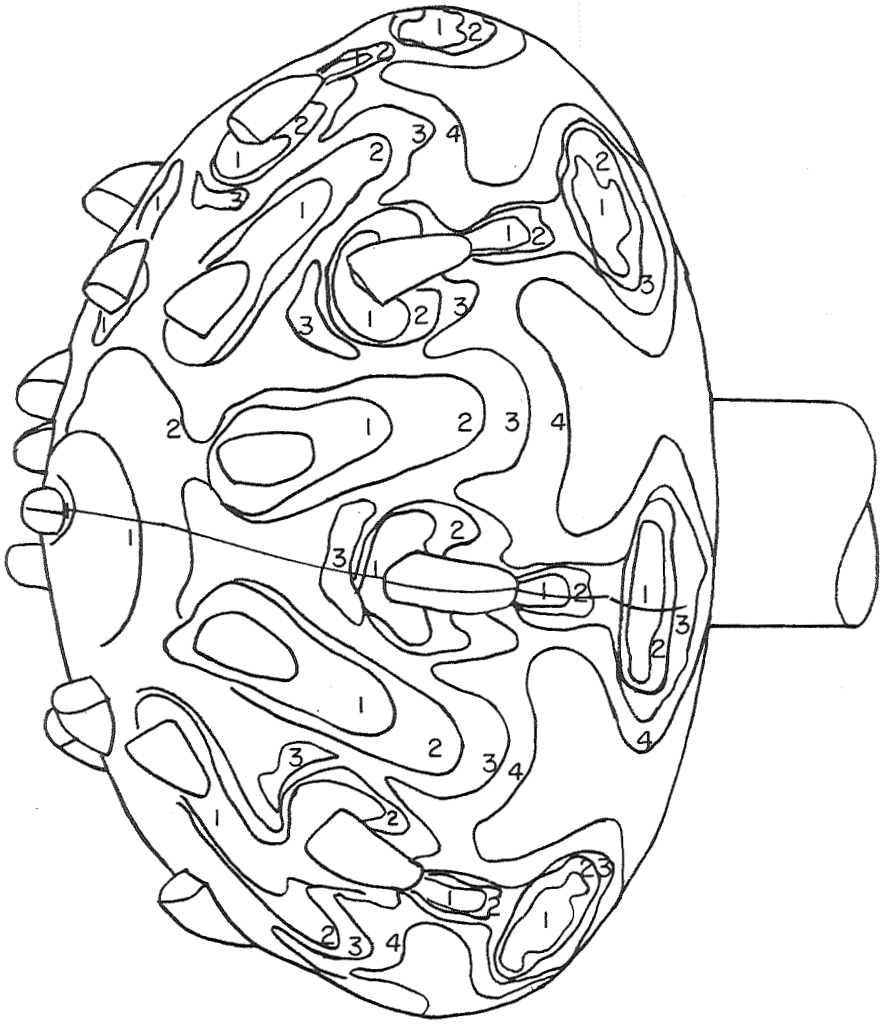

CONTOUR	T,SEC	H,WATTS/METER(SQ)-DEG-K	H/HS
1	.50	1.67359E+02	5.12250E-01
2	1.40	1.00016E+02	3.06128E-01
3	3.10	6.72132E+01	2.05724E-01
4	8.50	4.05906E+01	1.24239E-01

(b) $N_{Re,\infty} \approx 3.7 \times 10^5$.

Figure 19.- Continued.

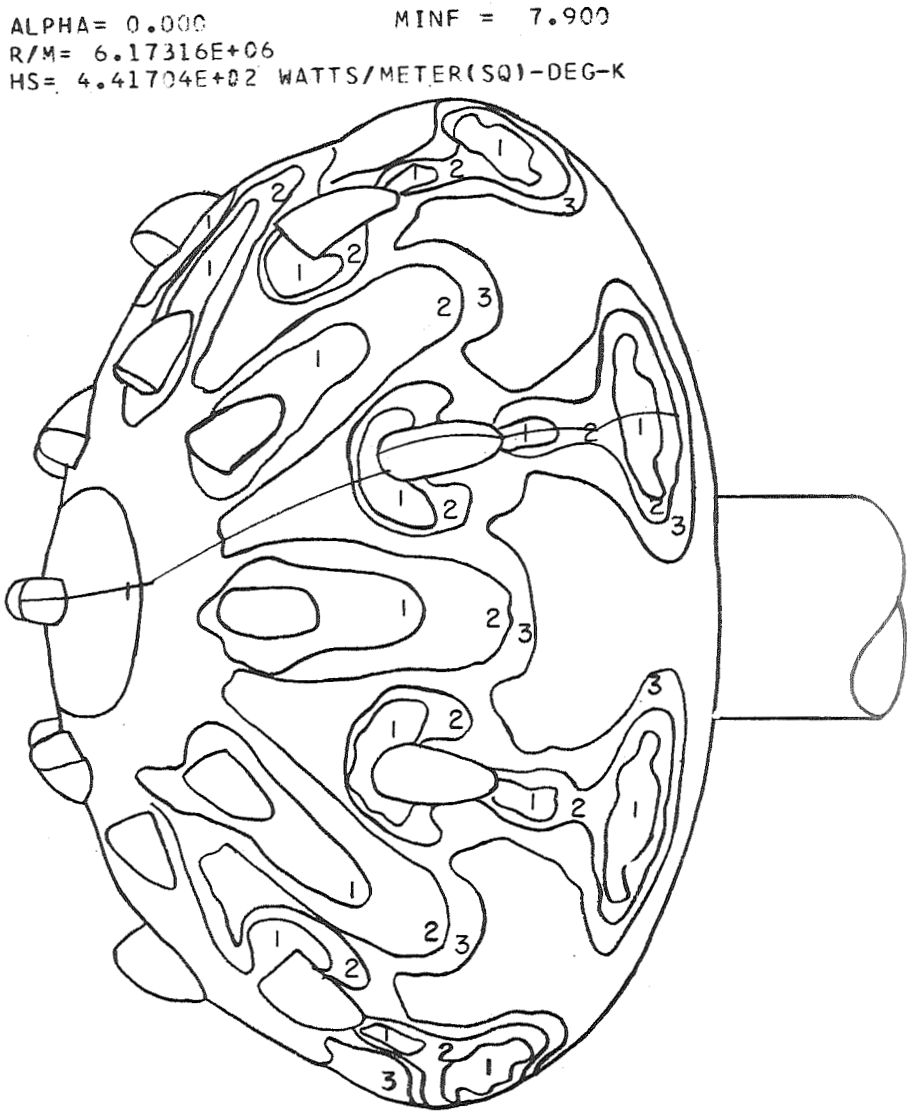

CONTOUR	T, SEC	H, WATTS/METER(SQ)-DEG-K	H/HS
1	.40	2.59484E+02	5.87462E-01
2	1.70	1.25868E+02	2.84961E-01
3	4.00	8.20562E+01	1.85772E-01

(c) $N_{Re,\infty} \approx 6.9 \times 10^5$.

Figure 19.- Continued.

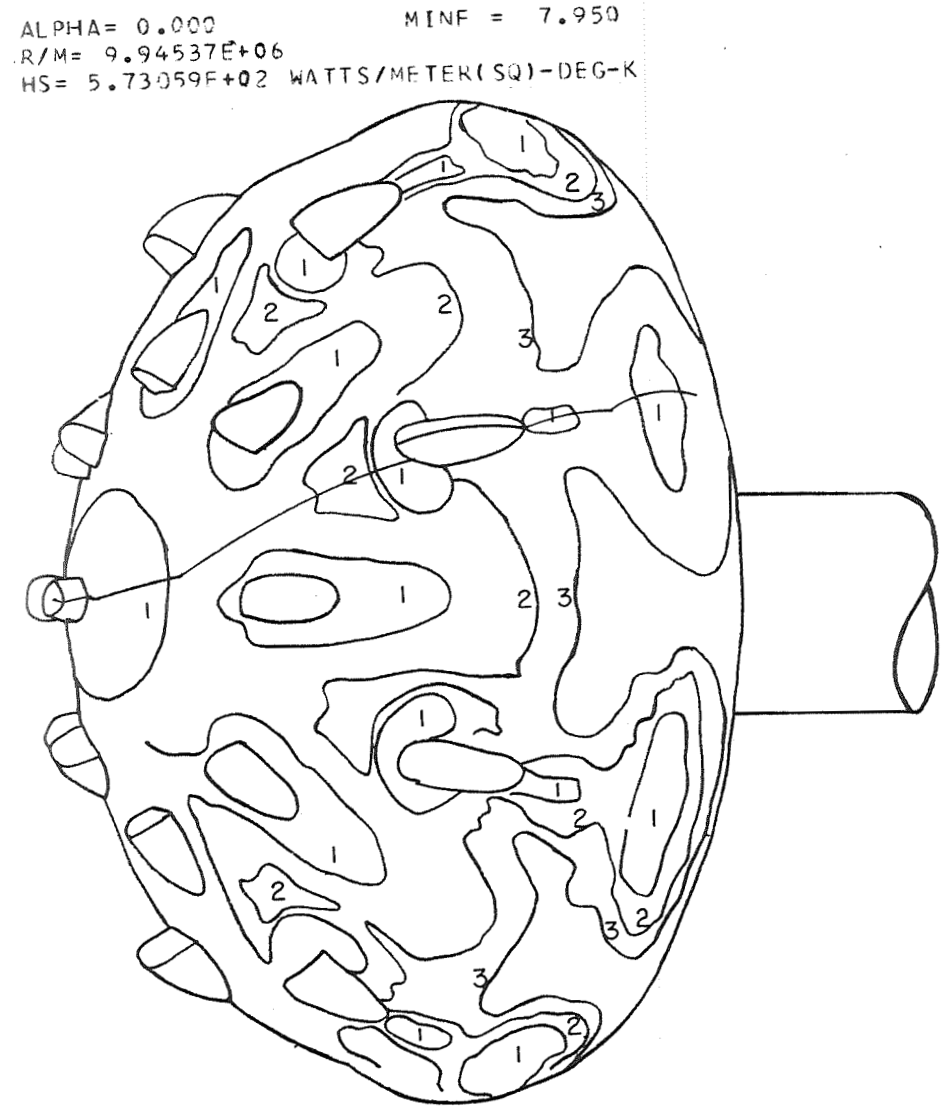

CONTOUR	T,SEC	H,WATTS/METER(SQ)-DEG-K	H/HS
1	.40	4.09114E+02	7.13912E-01
2	2.10	1.78552E+02	3.11577E-01
3	5.40	1.11347E+02	1.94302E-01

(d) $N_{Re,\infty} \approx 1.12 \times 10^6$.

Figure 19.- Concluded.

ALPHA= 5.000 MINF = 7.690
R/M=.1.92581E+06
HS= 2.47090E+02 WATTS/METER(SQ)-DEG-K

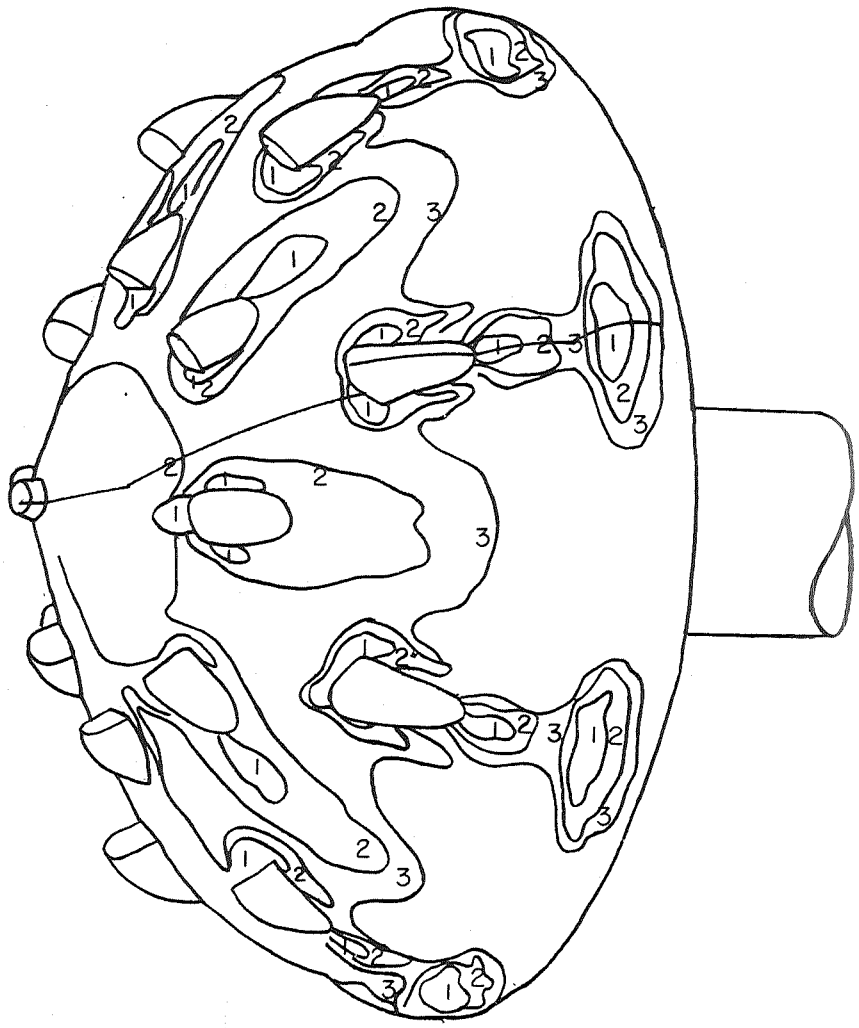

CONTOUR	T,SEC	H,WATTS/METER(SQ)-DEG-K	H/HS
1	.60	1.58532E+02	6.41595E-01
2	2.70	7.47326E+01	3.02451E-01
3	6.20	4.93170E+01	1.99591E-01

(a) $N_{Re,\infty} \approx 2.24 \times 10^5$.

Figure 20.- View of windward side of model 3 showing constant-temperature contour. $\alpha = 5^o$.

ALPHA= 5.000 MINF = 7.800
R/M= 3.29855E+06
HS= 3.26537E+02 WATTS/METER(SQ)-DEG-K

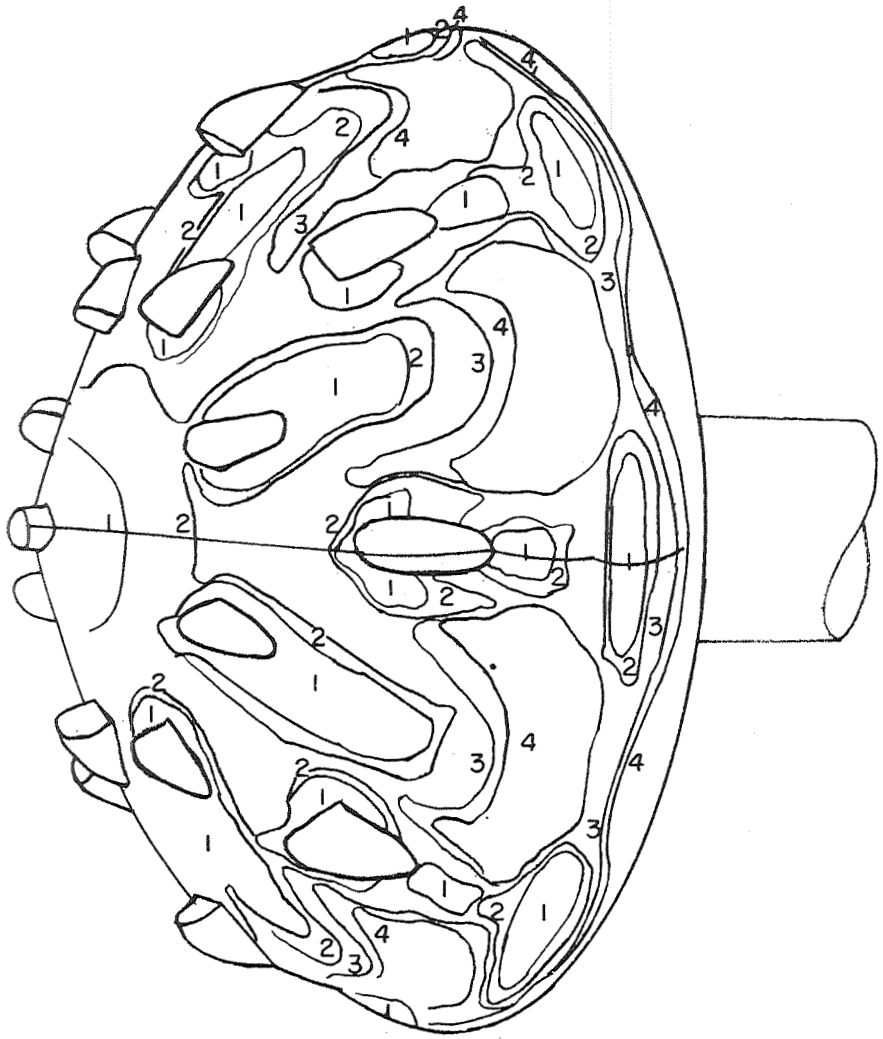

CONTOUR	T,SEC	H,WATTS/METER(SQ)-DEG-K	H/HS
1	.30	2.27876E+02	6.97855E-01
2	1.20	1.13938E+02	3.48928E-01
3	2.90	7.32926E+01	2.24454E-01
4	4.30	6.01901E+01	1.84328E-01

(b) $N_{Re,\infty} \approx 3.7 \times 10^5$.

Figure 20.- Continued.

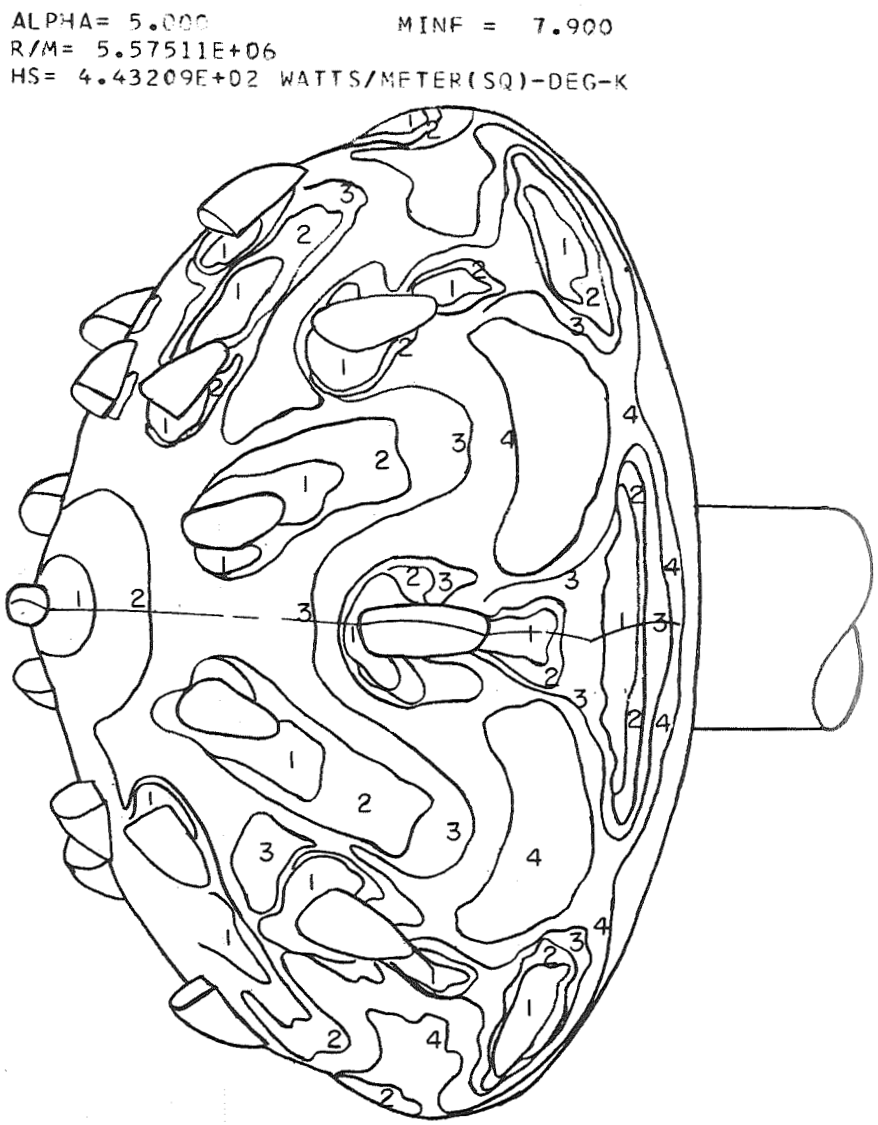

CONTOUR	T,SEC	H,WATTS/METER(SQ)-DEG-K	H/HS
1	.20	3.94764E+02	8.90697E-01
2	.60	2.27917E+02	5.14244E-01
3	1.70	1.35403E+02	3.05506E-01
4	5.50	7.52786E+01	1.69849E-01

(c) $N_{Re,\infty} \approx 6.3 \times 10^5$.

Figure 20.- Continued.

ALPHA= 5.000 MINF = 7.950
R/M= 1.07254E+07
HS= 5.74096E+02 WATTS/METER(SQ)-DEG-K

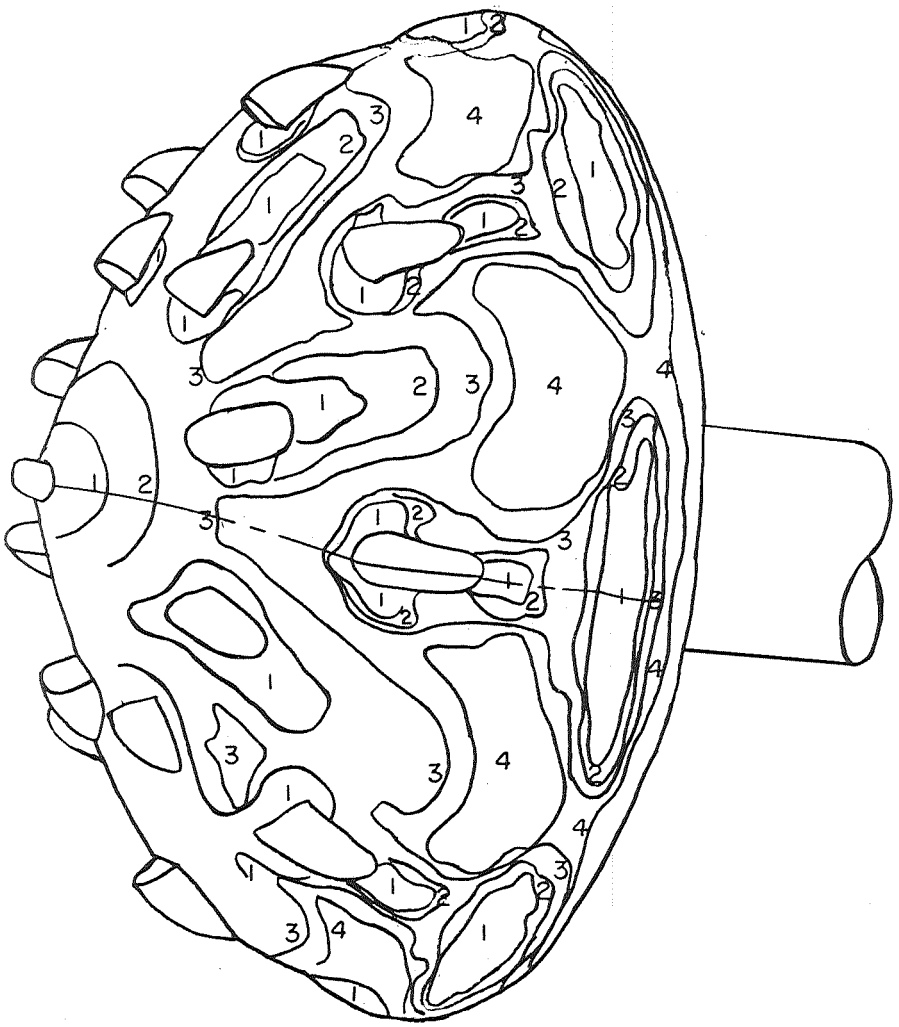

CONTOUR	T, SEC	H, WATTS/METER(SQ)-DEG-K	H/HS
1	.20	6.40731E+02	1.11607E+00
2	.90	3.02043E+02	5.26120E-01
3	2.40	1.84963E+02	3.22181E-01
4	4.70	1.32173E+02	2.30227E-01

(d) $N_{Re,\infty} \approx 1.2 \times 10^6$.

Figure 20.- Concluded.

ALPHA=10.000 MINF = 7.690
R/M= 1.94934E+06
HS= 2.46928E+02 WATTS/METER(SQ)-DEG-K

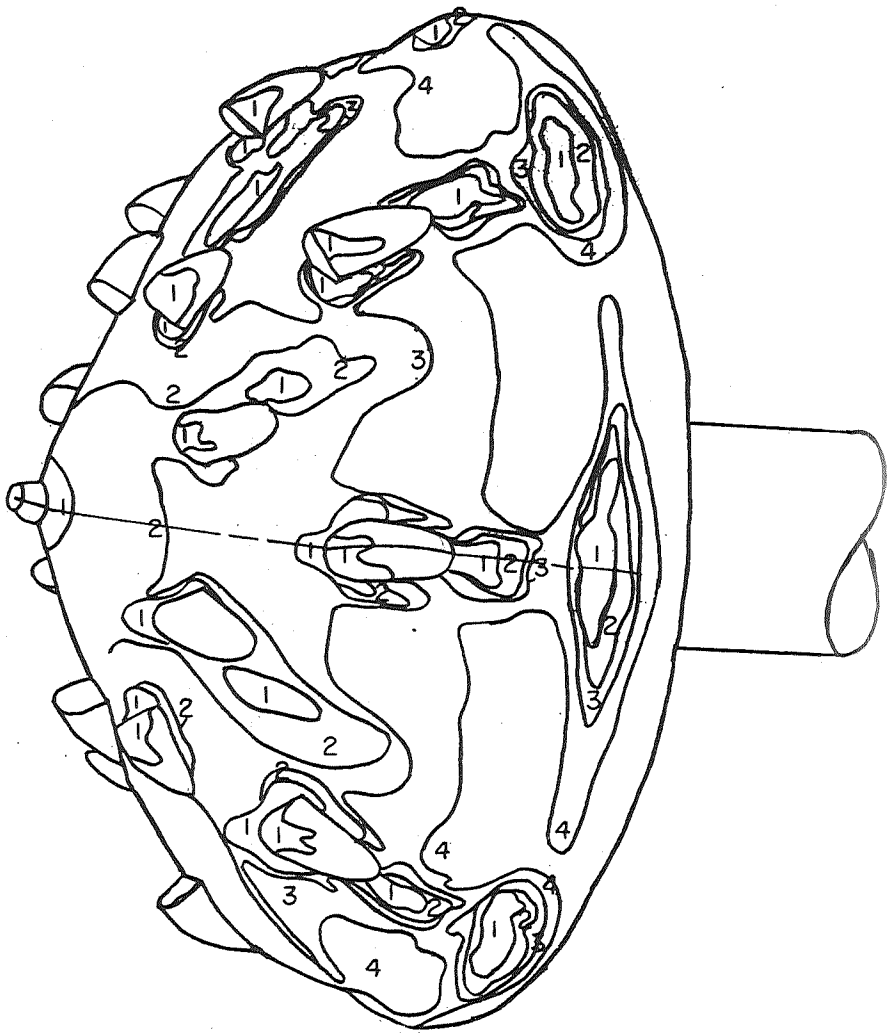

CONTOUR	T,SEC	H,WATTS/METER(SQ)-DEG-K	H/HS
1	.50	1.92486E+02	7.79521E-01
2	1.90	9.87430E+01	3.99886E-01
3	3.20	7.60866E+01	3.08133E-01
4	9.10	4.51193E+01	1.82723E-01

(a) $N_{Re,\infty} \approx 2.24 \times 10^5$.

Figure 21.- View of windward side of model 3 showing constant-temperature contour. $\alpha = 10^{\circ}$.

ALPHA=10.000 MINF = 7.800
R/M= 2.99772E+06
HS= 3.14520E+02 WATTS/METER(SQ)-DEG-K

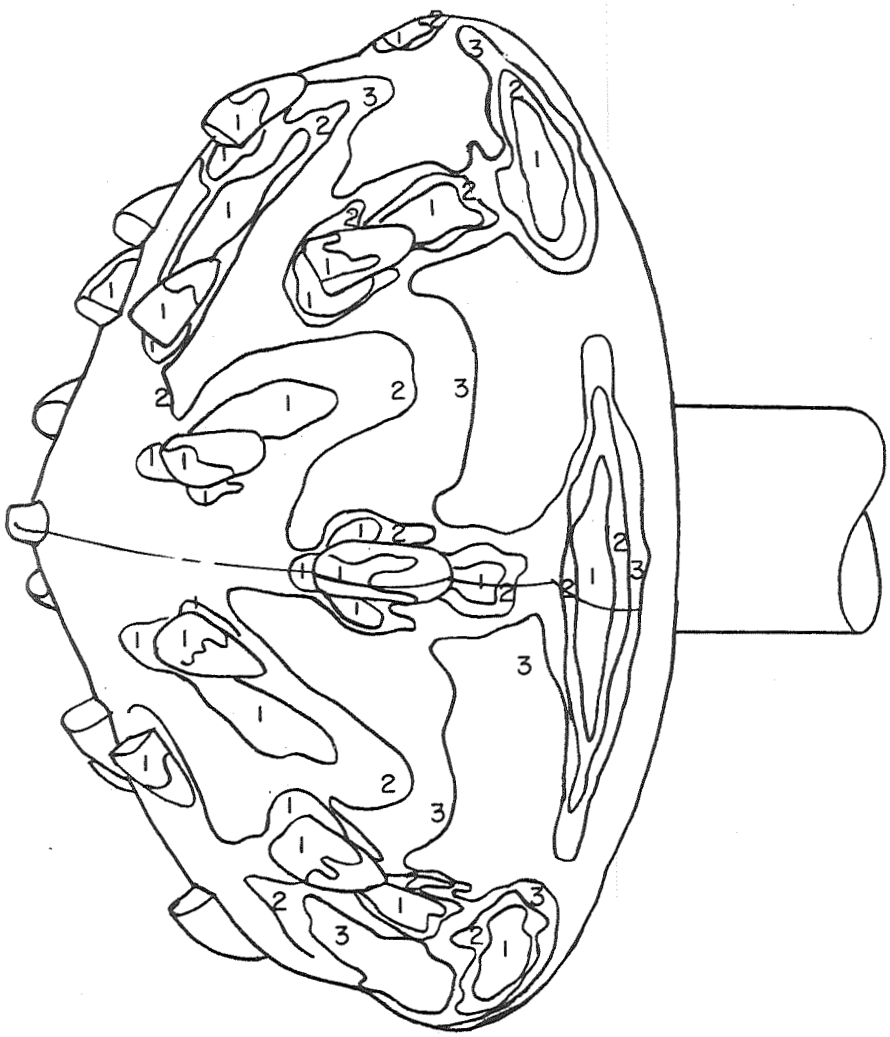

CONTOUR	T,SEC	H,WATTS/METER(SQ)-DEG-K	H/HS
1	.30	2.22239E+02	7.06598E-01
2	1.30	1.06760E+02	3.39439E-01
3	3.40	6.60149E+01	2.09891E-01

(b) $N_{Re,\infty} \approx 3.4 \times 10^5$.

Figure 21.- Continued.

ALPHA=10.000 MINF = 7.900
R/M= 5.82842E+06
HS= 4.42016E+02 WATTS/METER(SQ)-DEG-K

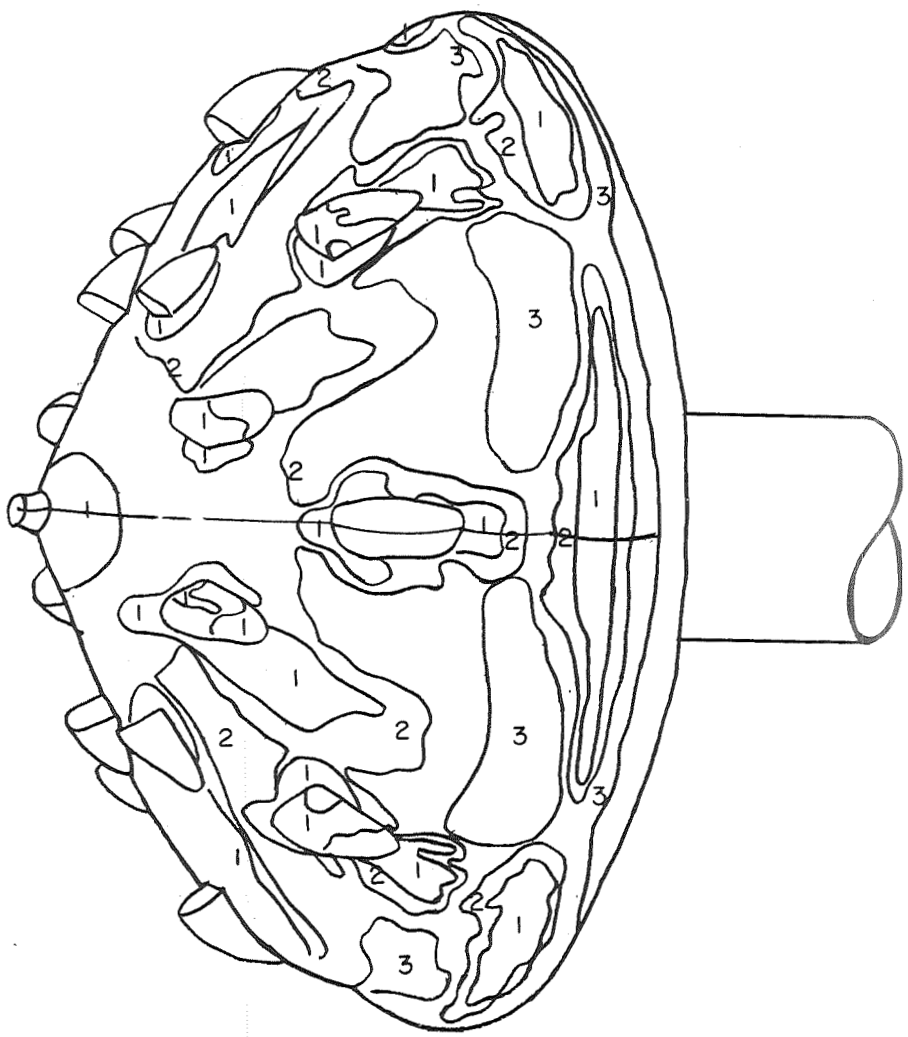

CONTOUR	T,SEC	H,WATTS/METER(SQ)-DEG-K	H/HS
1	.40	2.65497E+02	6.00651E-01
2	1.30	1.47271E+02	3.33181E-01
3	5.50	7.15993E+01	1.61983E-01

(c) $N_{Re,\infty} \approx 6.72 \times 10^5$.

Figure 21.- Continued.

ALPHA=10.000 MINF = 7.950
R/M= 1.04707E+07
HS= 5.82416E+02 WATTS/METER(SQ)-DEG-K

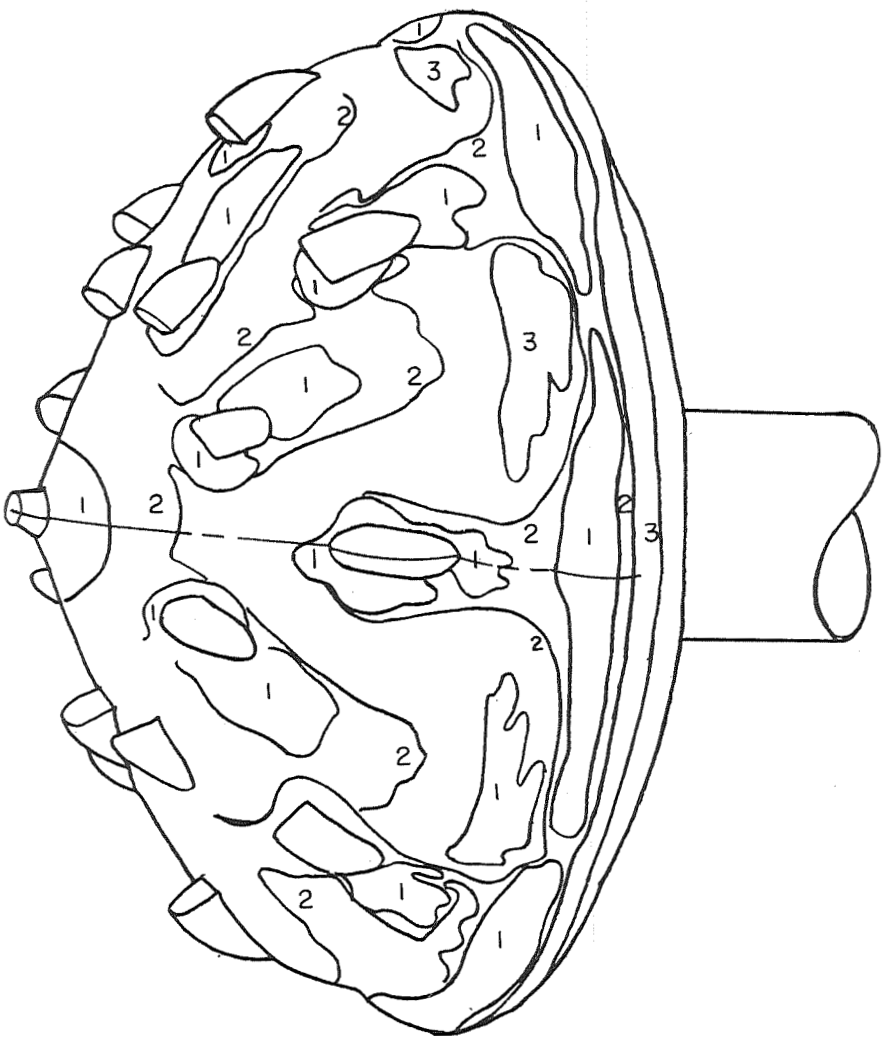

CONTOUR	T,SEC	H,WATTS/METER(SQ)-DEG-K	H/HS
1	.50	3.94061E+02	6.76597E-01
2	1.40	2.35496E+02	4.04344E-01
3	5.40	1.19909E+02	2.05882E-01

(d) $N_{Re,\infty} \approx 1.12 \times 10^6$.

Figure 21.- Concluded.

ALPHA= 0.000 MINF = 7.690
R/M= 2.03558E+06
HS= 2.46346E+02 WATTS/METER(SQ)-DEG-K

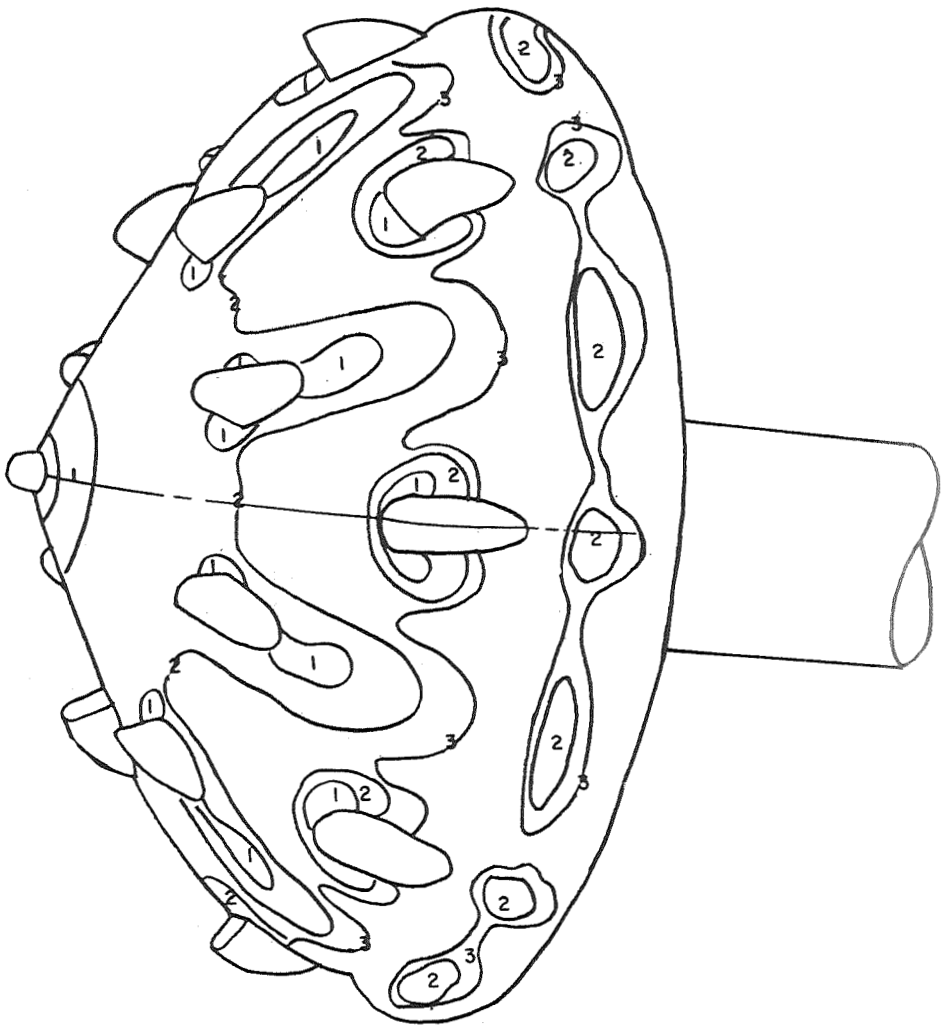

CONTOUR	T,SEC	H,WATTS/METER(SQ)-DEG-K	H/HS
1	.80	1.64336E+02	6.67095E-01
2	3.80	7.54026E+01	3.06084E-01
3	9.30	4.81988E+01	1.95655E-01

(a) $N_{Re,\infty} \approx 2.24 \times 10^5$.

Figure 22.- View of windward side of model 4 showing constant-temperature contours. $\alpha = 10^{\circ}$.

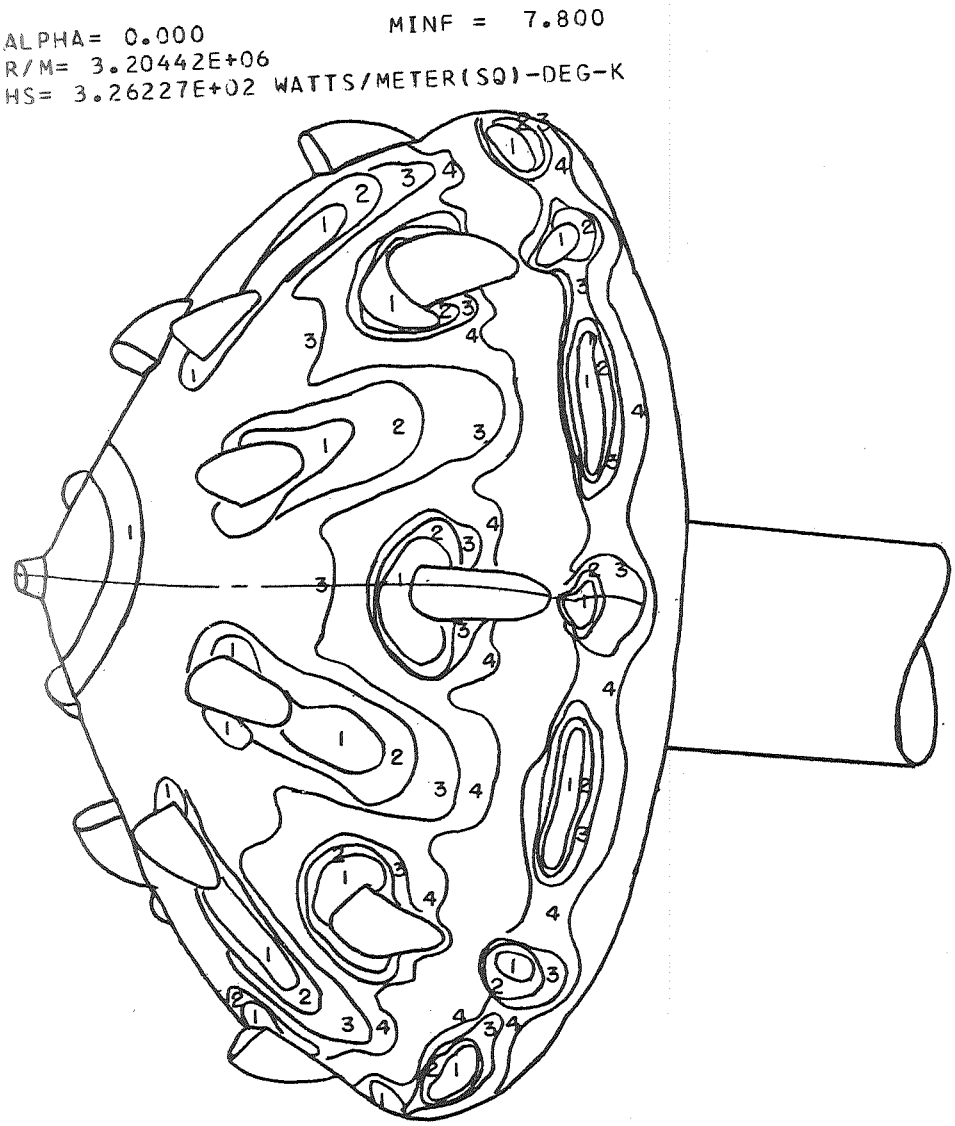

CONTOUR	T, SEC	H, WATTS/METER(SQ)-DEG-K	H/HS
1	.40	1.99574E+02	6.11766E-01
2	1.00	1.26222E+02	3.86915E-01
3	2.80	7.54320E+01	2.31226E-01
4	6.60	4.91318E+01	1.50606E-01

(b) $N_{Re,\infty} \approx 3.6 \times 10^5$.

Figure 22.- Continued.

ALPHA= 0.000 MINF = 7.950
R/M= 9.84207E+06
HS= 5.73440E+02 WATTS/METER(SQ)-DEG-K

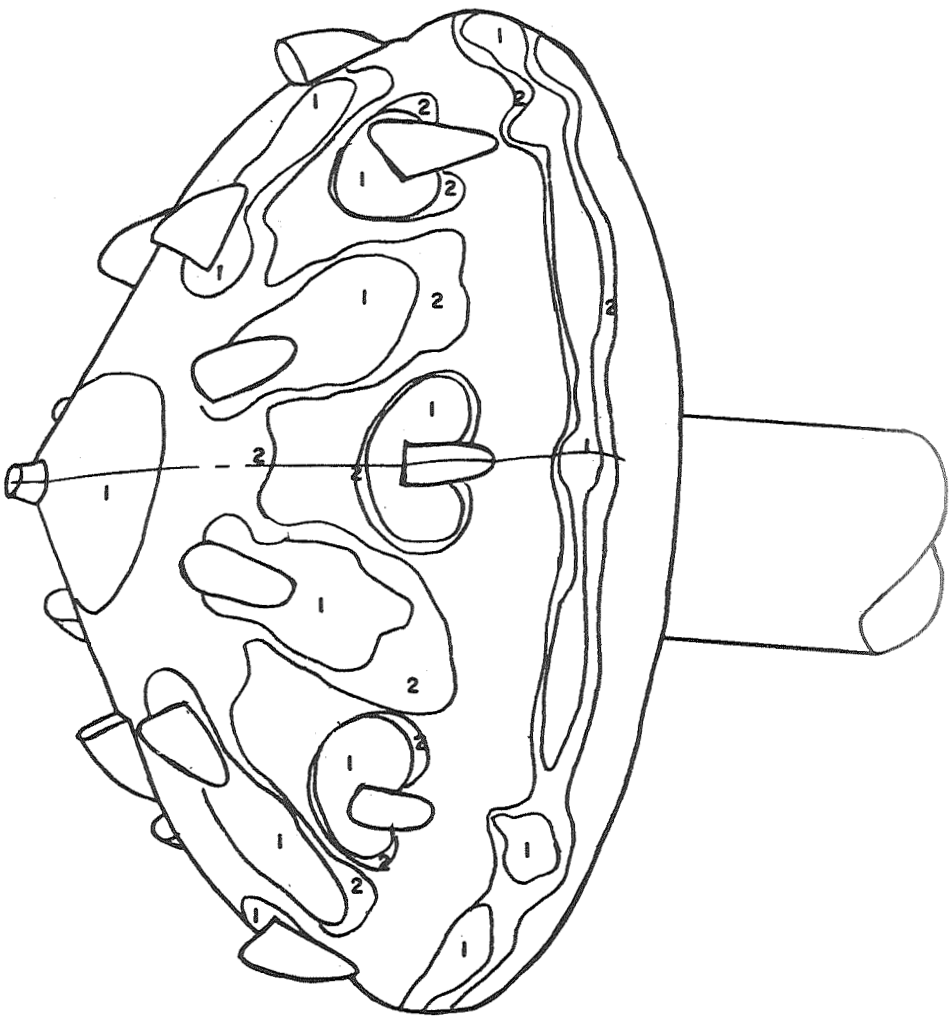

CONTOUR	T, SEC	H, WATTS/METER(SQ)-DEG-K	H/HS
1	.90	2.84321E+02	4.95817E-01
2	2.00	1.90728E+02	3.32604E-01

(c) $N_{Re,\infty} \approx 6.9 \times 10^5$.

Figure 22.- Continued.

ALPHA= 0.000 MINF = 7.900
R/M= 6.13717E+06
HS= 4.41465E+02 WATTS/METER(SQ)-DEG-K

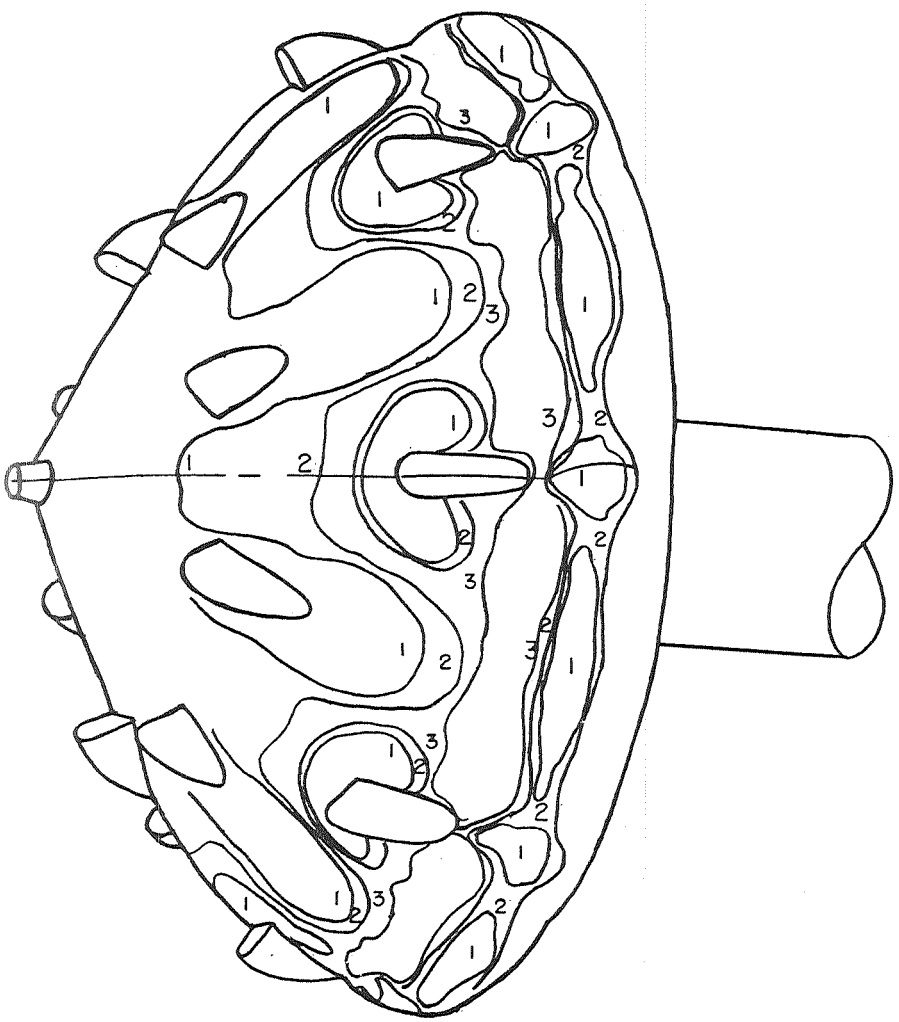

CONTOUR	T,SEC	H,WATTS/METER(SQ)-DEG-K	H/HS
1	1.20	1.60537E+02	3.63645E-01
2	2.70	1.07024E+02	2.42430E-01
3	5.50	7.49865E+01	1.69858E-01

(d) $N_{Re,\infty} \approx 1.12 \times 10^6$.

Figure 22.- Concluded.

ALPHA= 5.000 MINF = 7.690
R/M= 2.03558E+06
HS= 2.46346E+02 WATTS/METER(SQ)-DEG-K

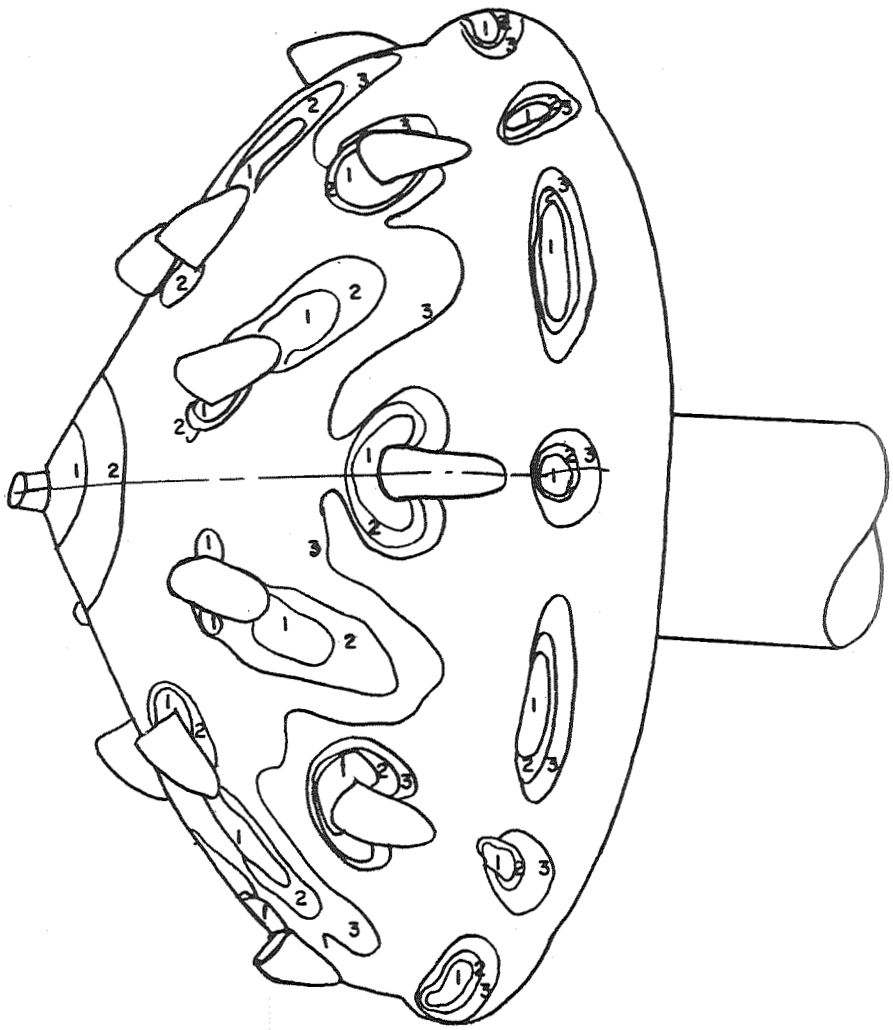

CONTOUR	T,SEC	H,WATTS/METER(SQ)-DEG-K	H/HS
1	1.00	1.42927E+02	5.80187E-01
2	2.10	9.86288E+01	4.00367E-01
3	6.00	5.83496E+01	2.36861E-01

(a) $N_{Re,\infty} \approx 2.24 \times 10^5$.

Figure 23.- View of windward side of model 4 showing constant-temperature contours. $\alpha = 5^o$.

ALPHA= 5.000 MINF = 7.800
R/M= 3.37723E+06
HS= 3.27251E+02 WATTS/METER(SQ)-DEG-K

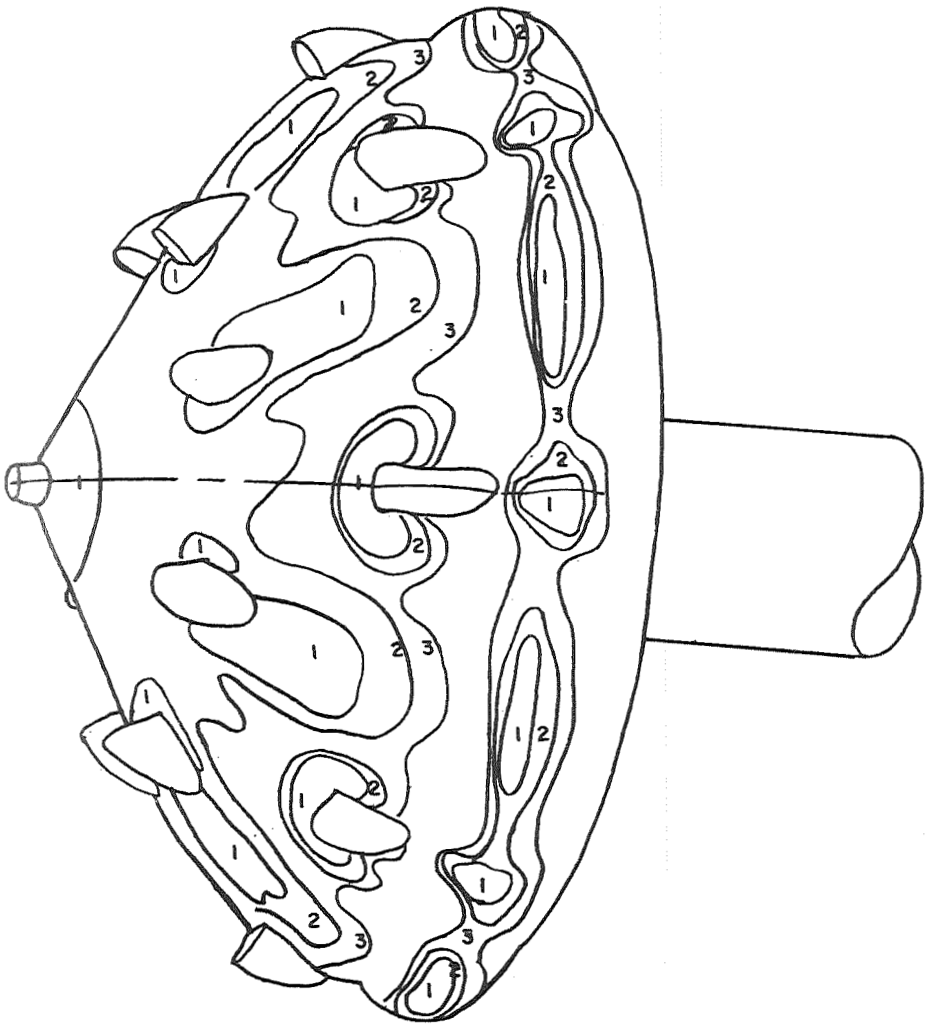

CONTOUR	T,SEC	H,WATTS/METER(SQ)-DEG-K	H/HS
1	.60	1.74870E+02	5.34362E-01
2	2.00	9.57804E+01	2.92682E-01
3	5.30	5.88375E+01	1.79793E-01

(b) $N_{Re,\infty} \approx 3.8 \times 10^5$.

Figure 23.- Continued.

ALPHA= 5.000 MINF = 7.900
R/M= 5.86143E+06
HS= 4.41870E+02 WATTS/METER(SQ)-DEG-K

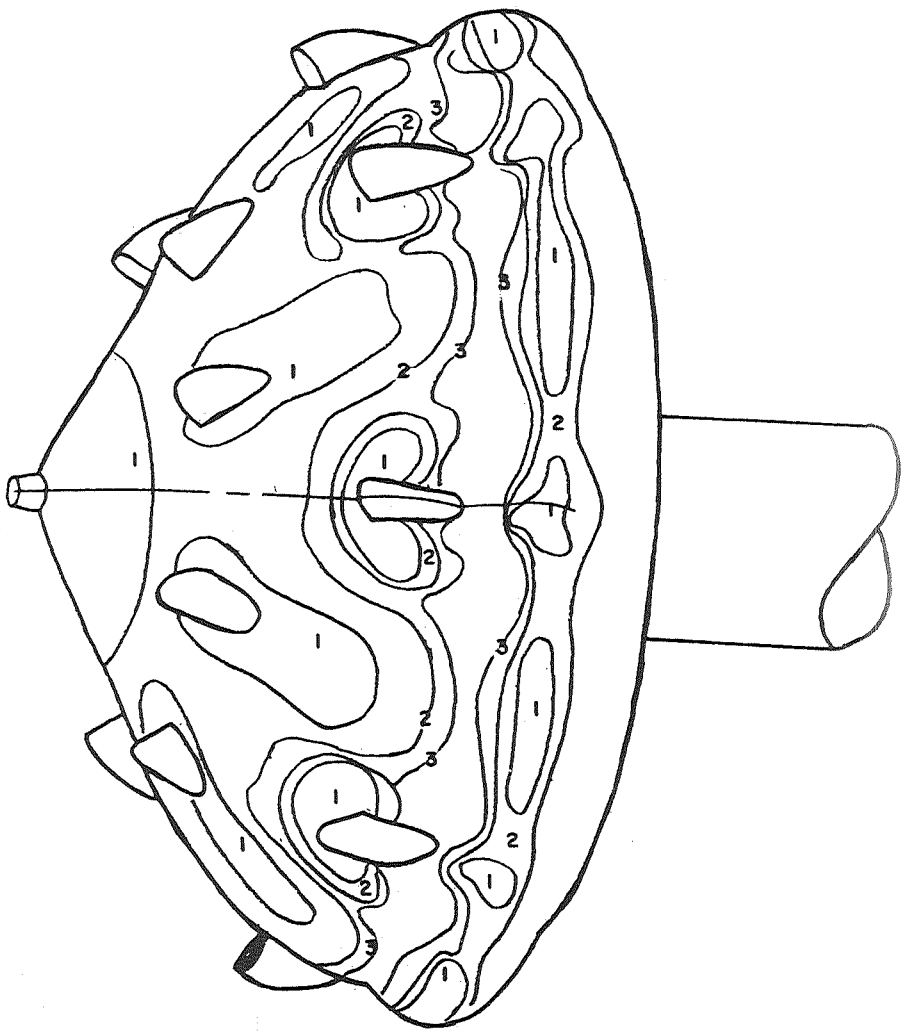

CONTOUR	T,SEC	H,WATTS/METER(SQ)-DEG-K	H/HS
1	.80	1.88889E+02	4.27477E-01
2	2.50	1.06852E+02	2.41817E-01
3	5.50	7.20394E+01	1.63033E-01

(c) $N_{Re,\infty} \approx 6.7 \times 10^5$.

Figure 23.- Continued.

ALPHA= 5.000 MINF = 7.950
R/M= 9.25557E+06
HS= 5.75577E+02 WATTS/METER(SQ)-DEG-K

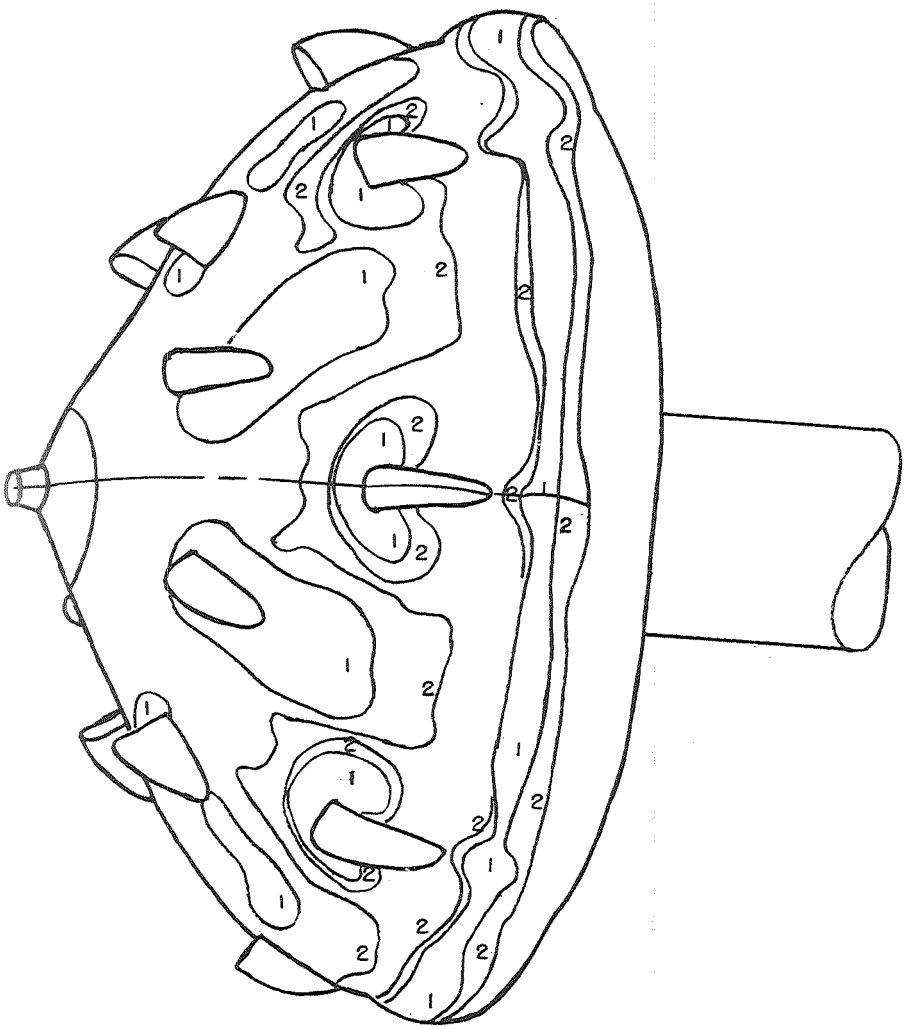

CONTOUR	T,SEC	H,WATTS/METER(SQ)-DEG-K	H/HS
1	.70	2.97206E+02	5.16362E-01
2	2.00	1.75830E+02	3.05484E-01

(d) $N_{Re,\infty} \approx 1.04 \times 10^6$.

Figure 23.- Concluded.

ALPHA=10.000 MINF = 7.690
R/M= 2.03558E+06
HS= 2.46346E+02 WATTS/METER(SQ)-DEG-K

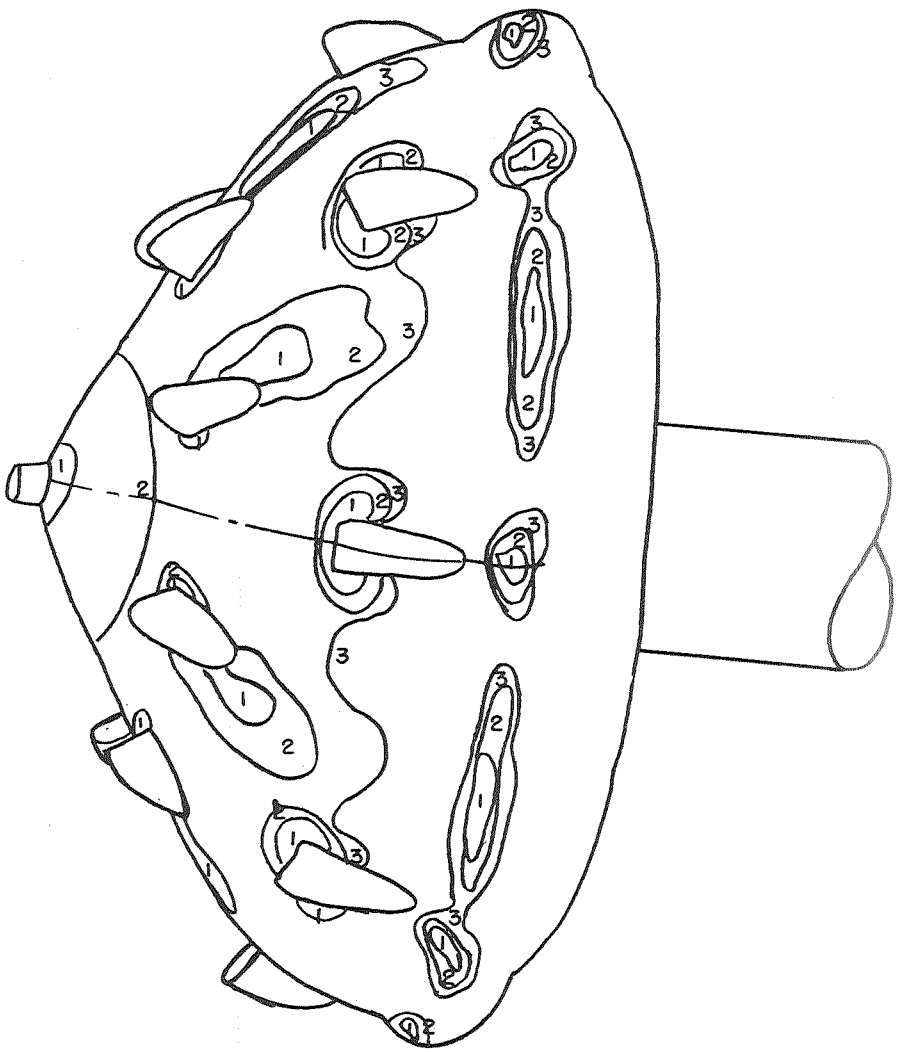

CONTOUR	T,SEC	H,WATTS/METER(SQ)-DEG-K	H/HS
1	.60	1.92378E+02	7.80925E-01
2	2.00	1.05370E+02	4.27730E-01
3	4.90	6.73181E+01	2.73267E-01

(a) $N_{Re,\infty} \approx 2.24 \times 10^5$.

Figure 24.- View of windward side of model 4 showing constant-temperature contour. $\alpha = 10^{\circ}$.

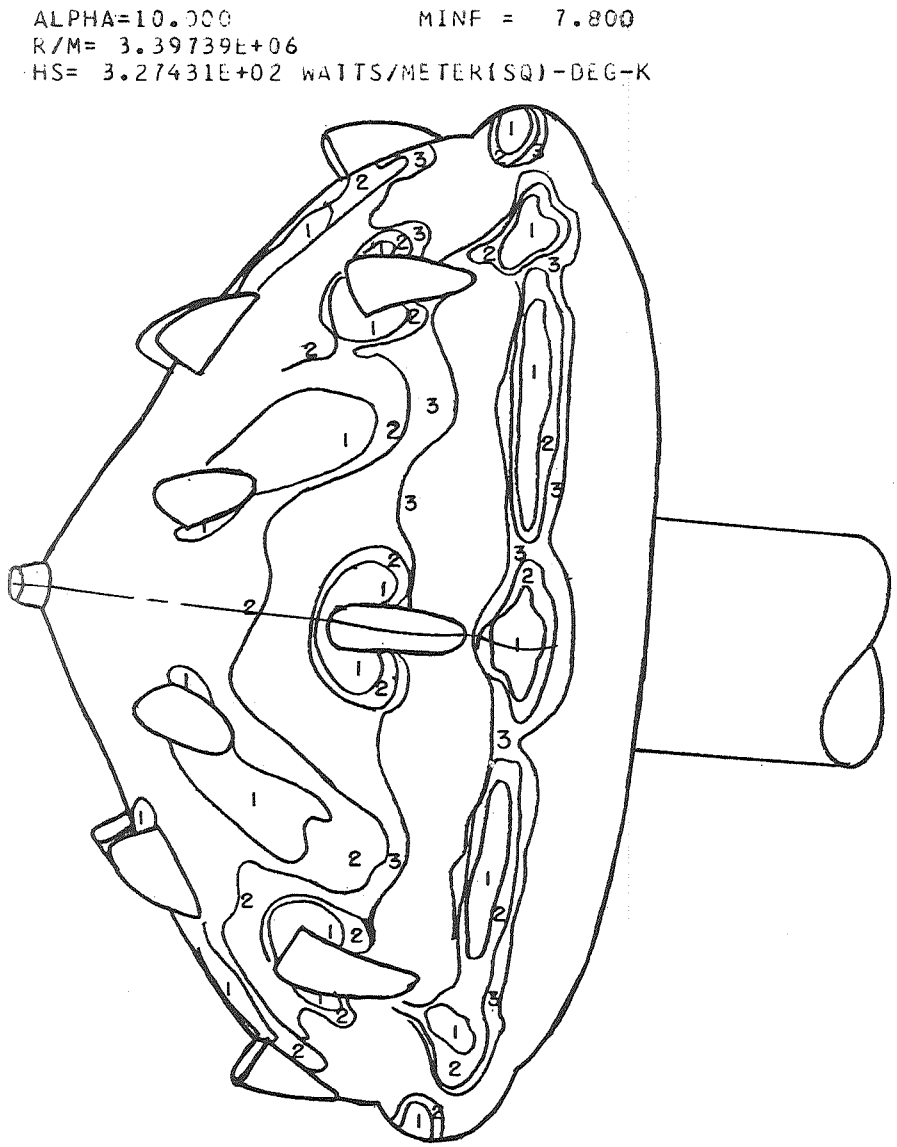

CONTOUR	T,SEC	H,WATTS/METER(SQ)-DEG-K	H/HS
1	.60	1.68812E+02	5.15565E-01
2	1.70	1.00289E+02	3.06291E-01
3	4.10	6.45783E+01	1.97227E-01

(b) $N_{Re,\infty} \approx 3.8 \times 10^5$.

Figure 24.- Continued.

ALPHA=10.000 MINF = 7.900
R/M= 6.13717E+06
HS= 4.41465E+02 WATTS/METER(SQ)-DEG-K

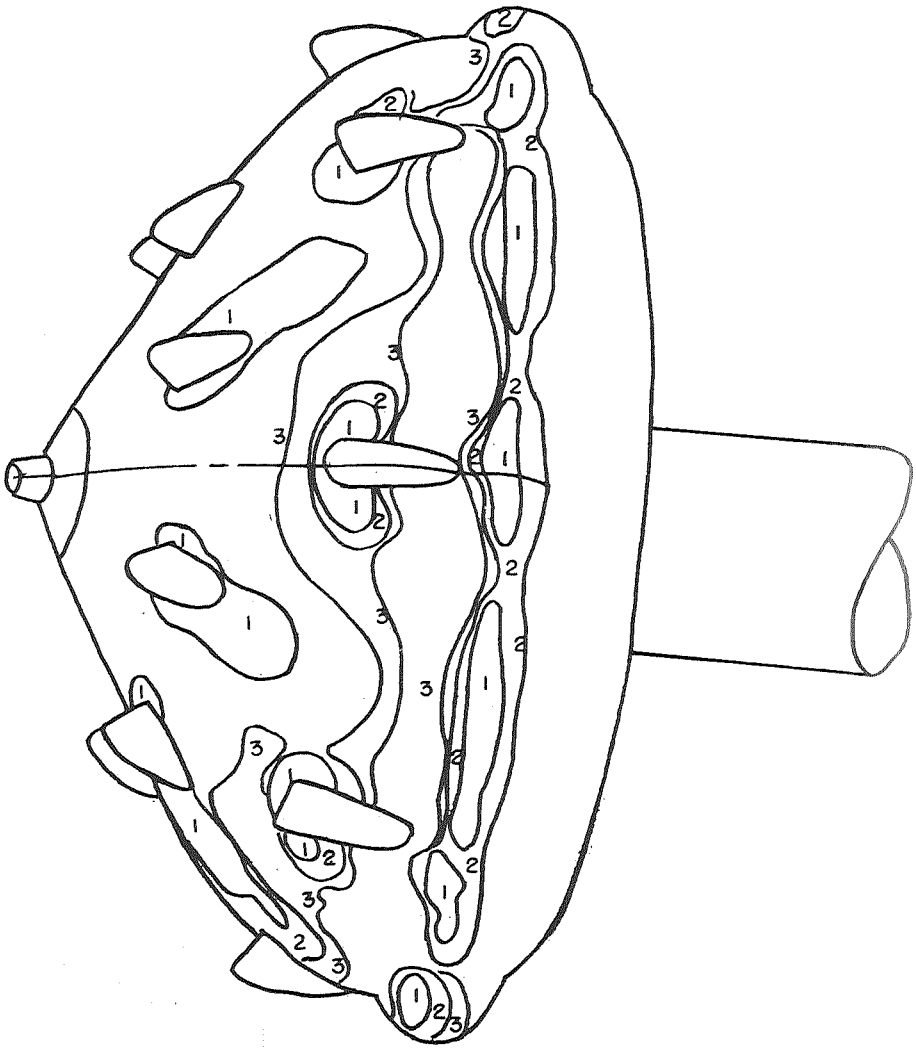

CONTOUR	T,SEC	H,WATTS/METER(SQ)-DEG-K	H/HS
1	.50	2.56447E+02	5.80901E-01
2	2.00	1.28224E+02	2.90450E-01
3	3.90	9.18229E+01	2.07996E-01

(c) $N_{Re,\infty} \approx 6.9 \times 10^5$.

Figure 24.- Continued.

ALPHA=10.000 MINF = 7.950
R/M= 9.67021E+06
HS= 5.74016E+02 WATTS/METER(SQ)-DEG-K

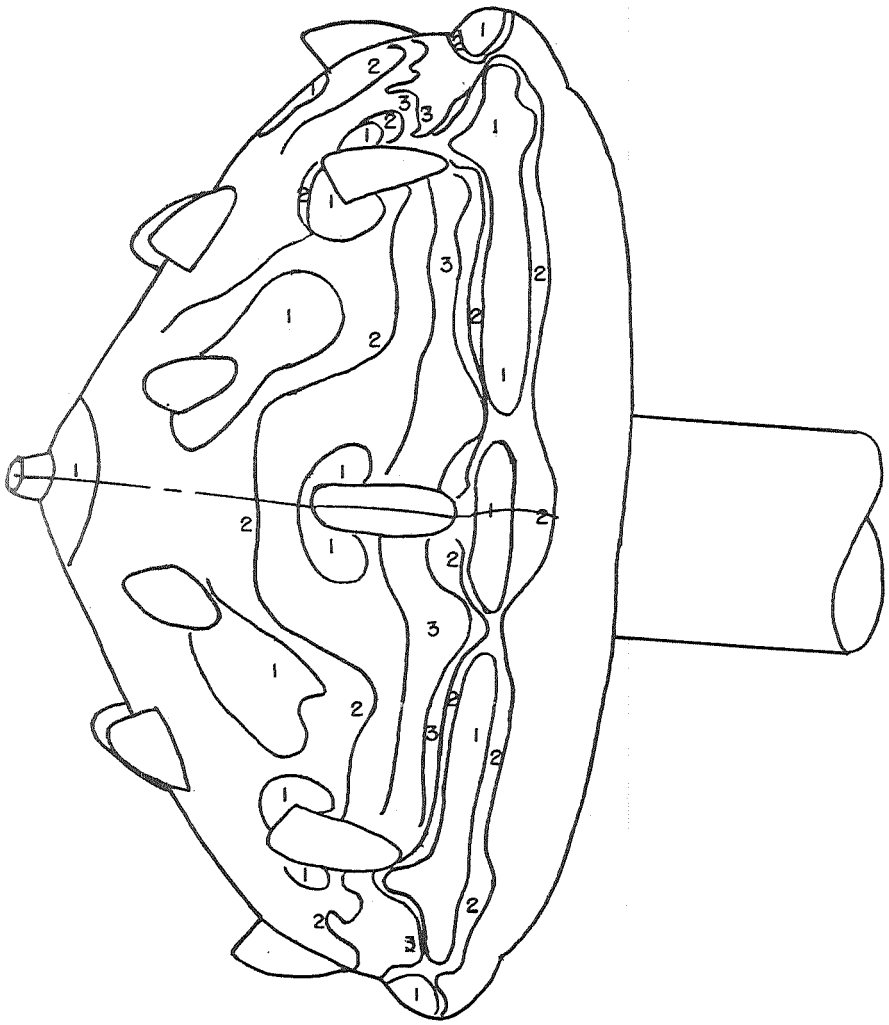

CONTOUR	T, SEC	H, WATTS/METER(SQ)-DEG-K	H/HS
1	.70	3.14226E+02	5.47417E-01
2	1.80	1.95954E+02	3.41375E-01
3	3.80	1.34865E+02	2.34950E-01

(d) $N_{Re,\infty} \approx 1.12 \times 10^6$.

Figure 24.- Concluded.

ALPHA= 0.000 MINF = 7.690
R/M= 2.09371E+06
HS= 2.59040E+02 WATTS/METER(SQ)-DEG-K

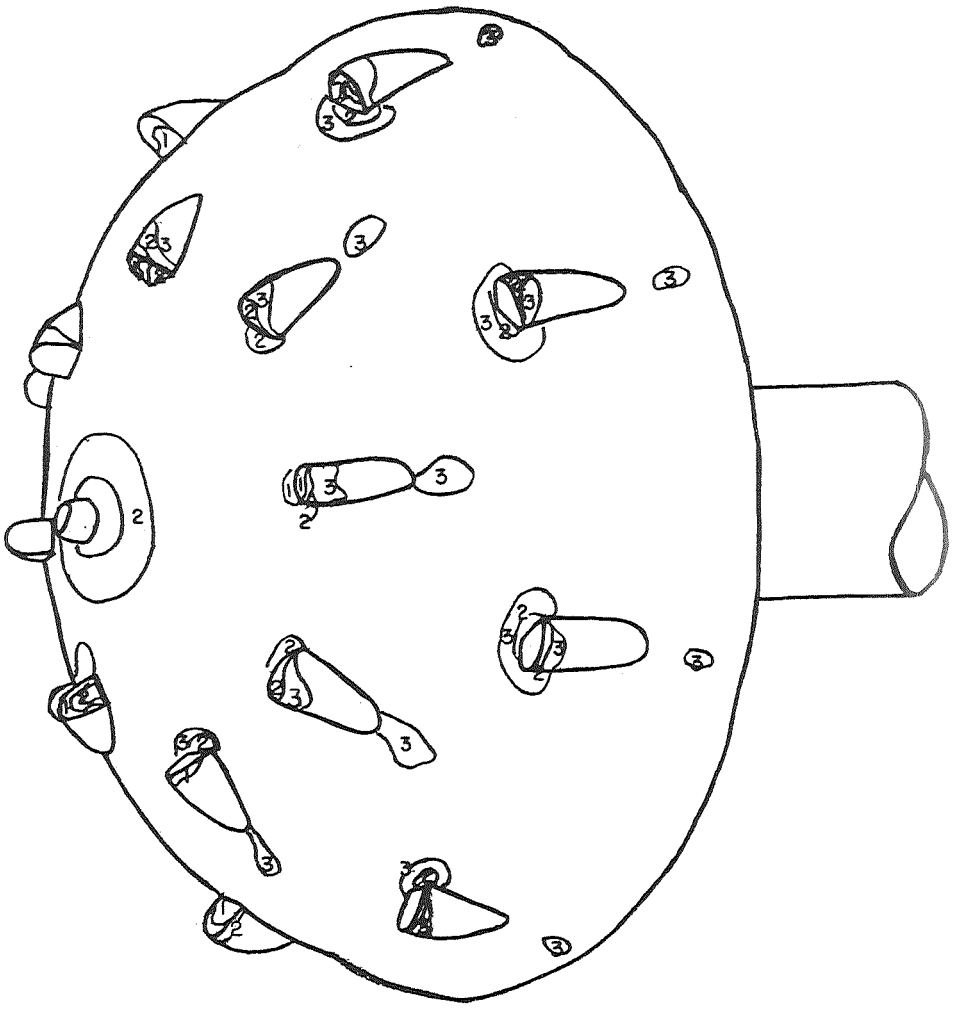

CONTOUR	T,SEC	H,WATTS/METER(SQ)-DEG-K	H/HS
1	1.60	4.07566E+02	1.57337E+00
2	1.80	3.84257E+02	1.48339E+00
3	6.30	2.05394E+02	7.92906E-01

(a) $N_{Re,\infty} \approx 2.24 \times 10^5$.

Figure 25.- Heat-transfer coefficient over protuberance on model 4 at $\alpha = 0^o$.

ALPHA= 0.000 MINF = 7.800
R/M= 3.29855E+06
HS= 3.28316E+02 WATTS/METER(SQ)-DEG-K

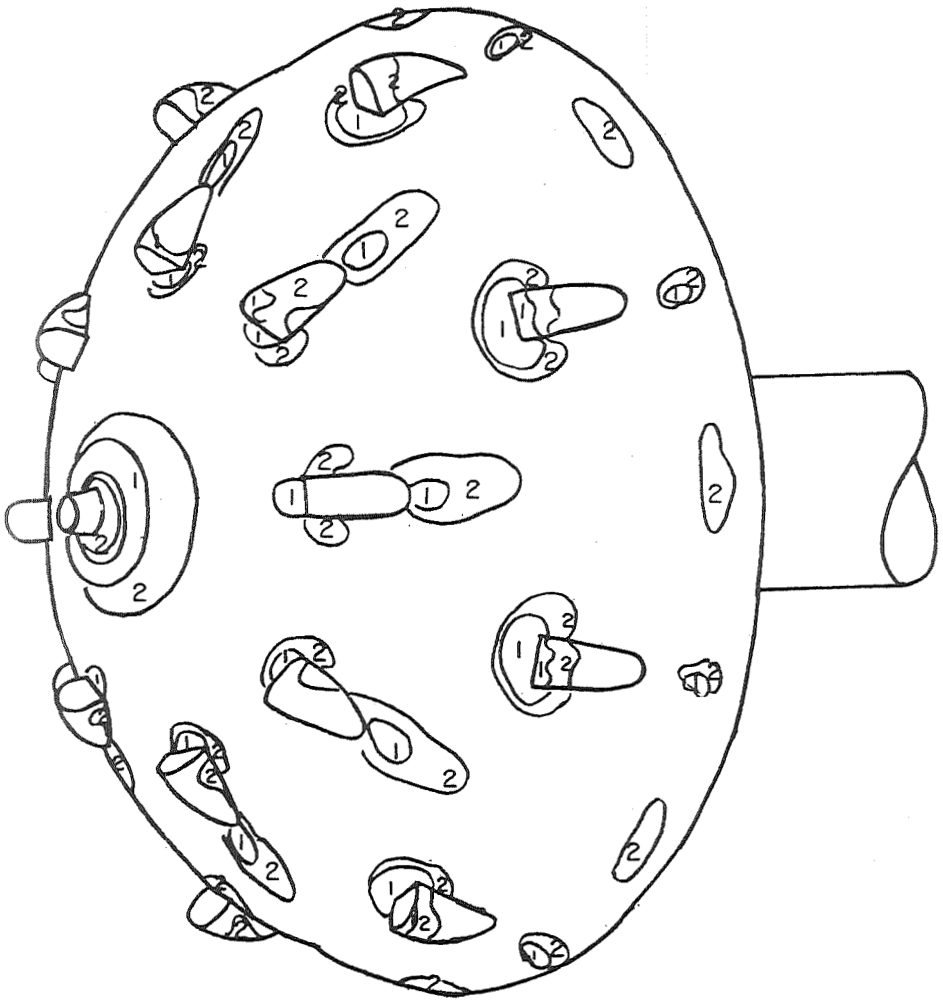

CONTOUR	T,SEC	H,WATTS/METER(SQ)-DEG-K	H/HS
1	2.70	2.88608E+02	8.79056E-01
2	5.50	2.02213E+02	6.15910E-01

(b) $N_{Re,\infty} \approx 3.6 \times 10^5$.

Figure 25.- Continued.

ALPHA= 0.000 MINF = 7.900
R/M= 5.86143E+06
HS= 4.42647E+02 WATTS/METER(SQ)-DEG-K

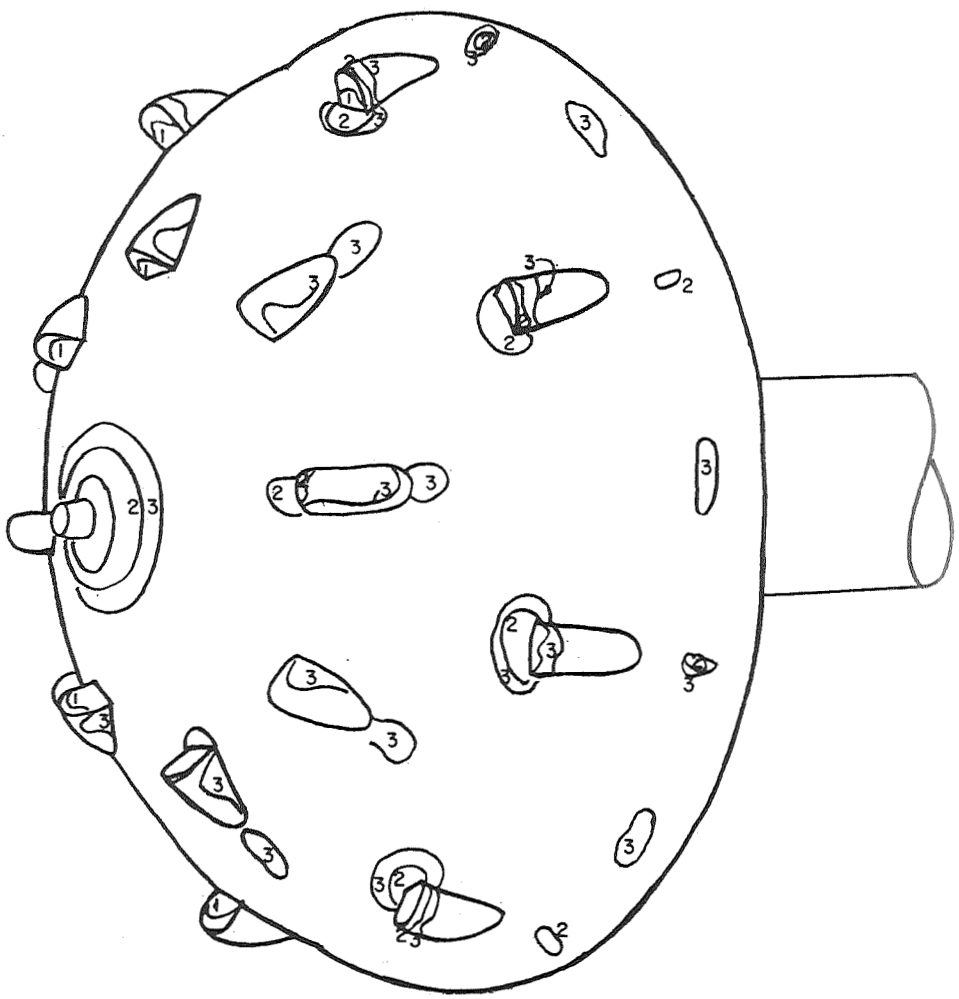

CONTOUR	T,SEC	H,WATTS/METER(SQ)-DEG-K	H/HS
1	2.60	7.05419E+02	1.59364E+00
2	5.60	4.80662E+02	1.08588E+00
3	8.50	3.90143E+02	8.81387E-01

(c) $N_{Re,\infty} \approx 6.5 \times 10^5$.

Figure 25.- Continued.

ALPHA= 0.000 MINF = 7.950
R/M= 1.01168E+07
HS= 5.72441E+02 WATTS/METER(SQ)-DEG-K

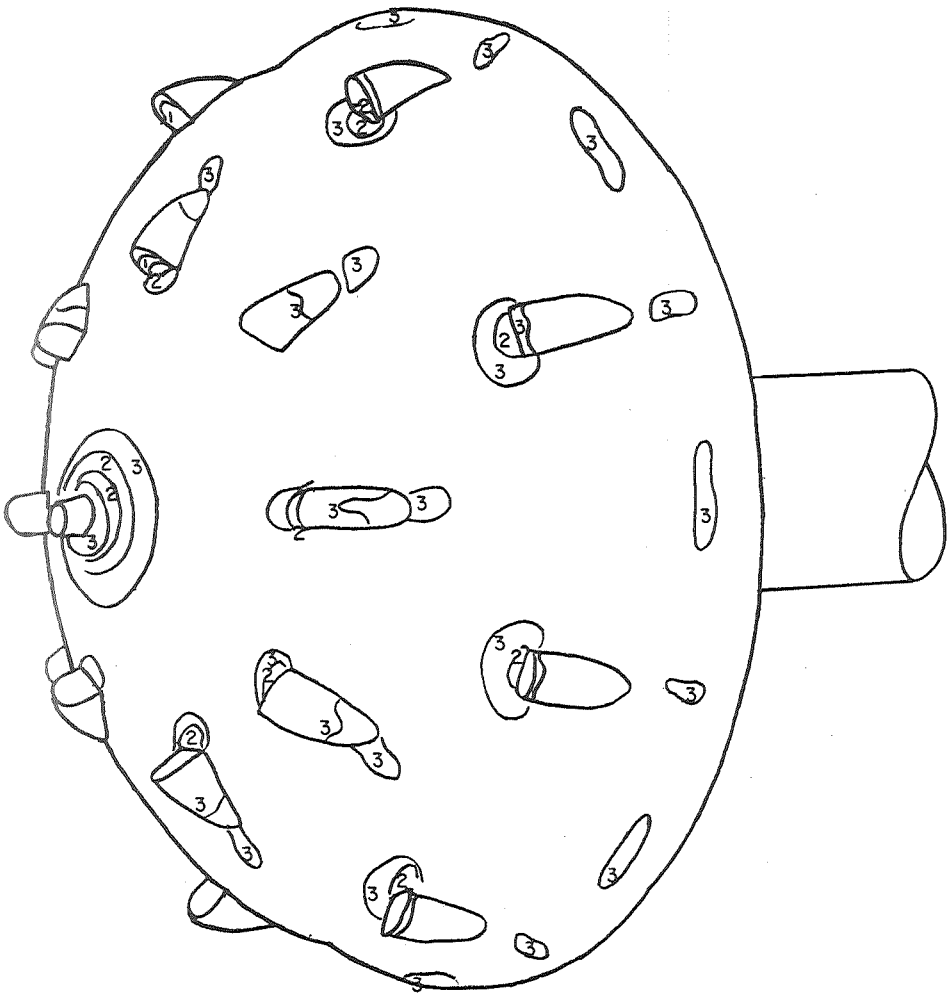

CONTOUR	T,SEC	H,WATTS/METER(SQ)-DEG-K	H/HS
1	1.30	1.02743E+03	1.79483E+00
2	2.00	8.28343E+02	1.44704E+00
3	4.50	5.52229E+02	9.64692E-01

(d) $N_{Re,\infty} \approx 1.12 \times 10^6$.

Figure 25.- Concluded.

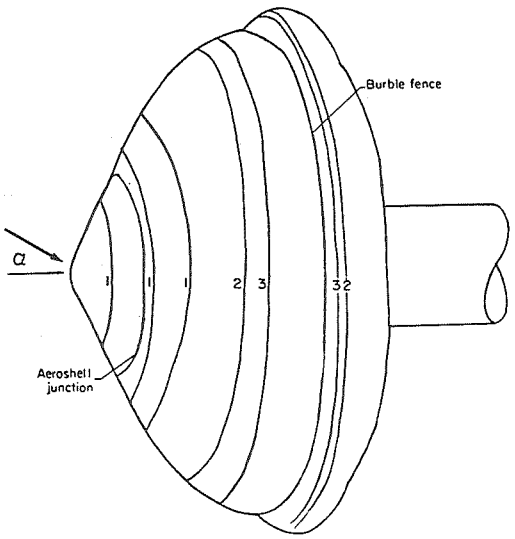

ALPHA= 5.000 MINF = 7.690
R/M= 1.88016E+06
HS= 2.46979E+02 WATTS/METER(SQ)-DEG-K

CONTOUR	T,SEC	H,WATTS/METER(SQ)-DEG-K	H/HS
1	1.40	1.15228E+02	4.66552E-01
2	4.70	6.28890E+01	2.54633E-01
3	8.60	4.64916E+01	1.88241E-01

(a) $N_{Re,\infty} = 2.24 \times 10^5$.

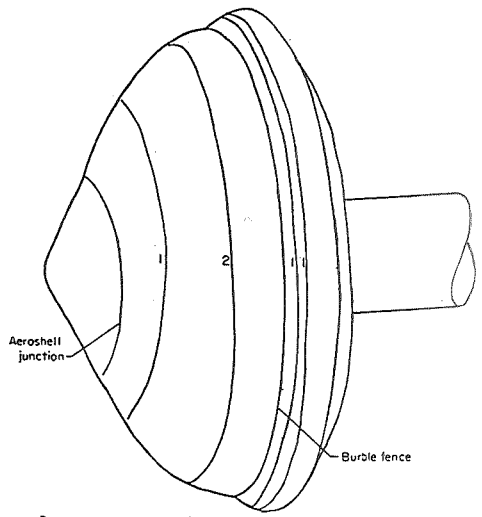

ALPHA= 5.000 MINF = 7.800
R/M= 3.29855E+06
HS= 3.26537E+02 WATTS/METER(SQ)-DEG-K

CONTOUR	T,SEC	H,WATTS/METER(SQ)-DEG-K	H/HS
1	1.40	1.07010E+02	3.27712E-01
2	3.70	6.58247E+01	2.01584E-01

(b) $N_{Re,\infty} = 3.7 \times 10^5$.

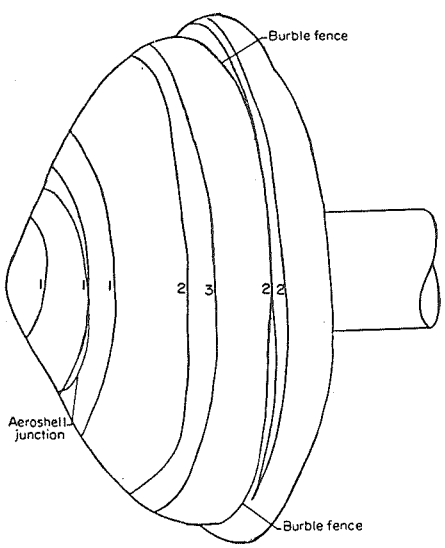

ALPHA= 5.000 MINF = 7.900
R/M= 5.99666E+06
HS= 4.41284E+02 WATTS/METER(SQ)-DEG-K

CONTOUR	T,SEC	H,WATTS/METER(SQ)-DEG-K	H/HS
1	.60	2.25907E+02	5.11931E-01
2	2.70	1.06493E+02	2.41327E-01
3	5.50	7.46146E+01	1.69085E-01

(c) $N_{Re,\infty} = 6.72 \times 10^5$.

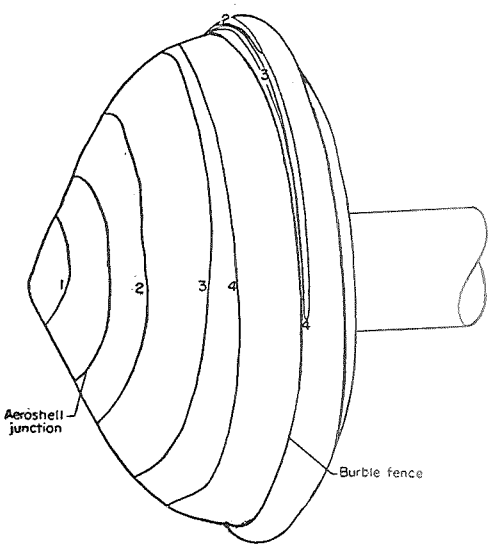

ALPHA= 5.000 MINF = 7.950
R/M= 1.07896E+07
HS= 5.74412E+02 WATTS/METER(SQ)-DEG-K

CONTOUR	T,SEC	H,WATTS/METER(SQ)-DEG-K	H/HS
1	.70	3.54181E+02	6.16598E-01
2	1.90	2.19323E+02	3.81822E-01
3	3.40	1.67335E+02	2.91316E-01
4	5.70	1.31960E+02	2.29730E-01

(d) $N_{Re,\infty} = 1.2 \times 10^6$.

Figure 26.- Constant-temperature contours on model 1, 90° from the windward side. $\alpha = 5^\circ$.

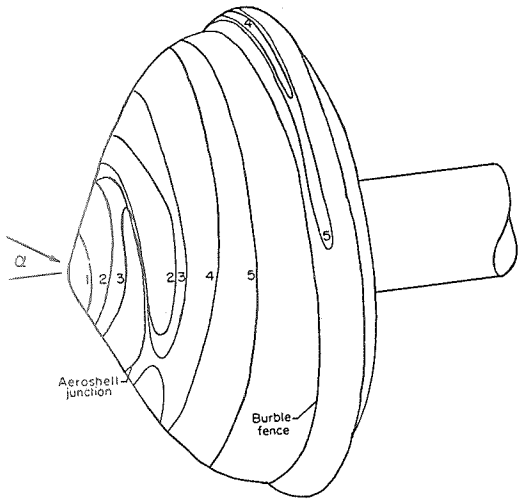

ALPHA=10.000 MINF = 7.690
R/M= 1.96128E+06
HS= 2.46847E+02 WATTS/METER(SQ)-DEG-K

CONTOUR	T,SEC	H,WATTS/METER(SQ)-DEG-K	H/HS
1	.80	1.53217E+02	6.20698E-01
2	1.70	1.05106E+02	4.25795E-01
3	2.50	8.66729E+01	3.51120E-01
4	4.30	6.60875E+01	2.67726E-01
5	8.40	4.72839E+01	1.91551E-01

(a) $N_{Re,\infty} = 2.24 \times 10^5$.

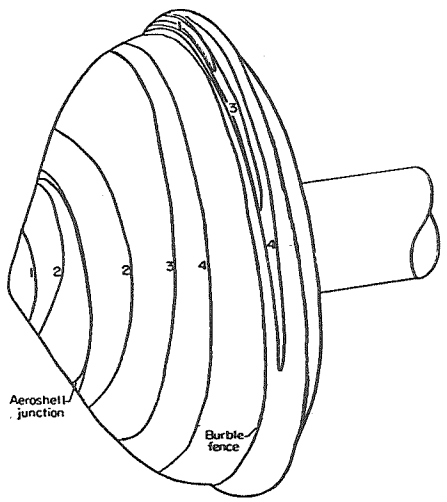

ALPHA=10.000 MINF = 7.800
R/M= 3.27819E+06
HS= 3.34180E+02 WATTS/METER(SQ)-DEG-K

CONTOUR	T,SEC	H,WATTS/METER(SQ)-DEG-K	H/HS
1	.30	2.18692E+02	6.54413E-01
2	.60	1.54639E+02	4.62740E-01
3	2.00	8.46990E+01	2.53453E-01
4	4.80	5.46730E+01	1.63603E-01

(b) $N_{Re,\infty} = 3.7 \times 10^5$.

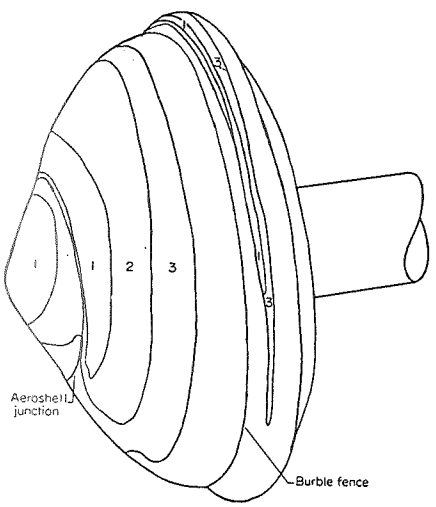

ALPHA=10.000 MINF = 7.900
R/M= 5.92840E+06
HS= 4.41576E+02 WATTS/METER(SQ)-DEG-K

CONTOUR	T,SEC	H,WATTS/METER(SQ)-DEG-K	H/HS
1	.70	2.08648E+02	4.72506E-01
2	1.90	1.26644E+02	2.86800E-01
3	4.00	8.72836E+01	1.97664E-01

(c) $N_{Re,\infty} = 6.7 \times 10^5$.

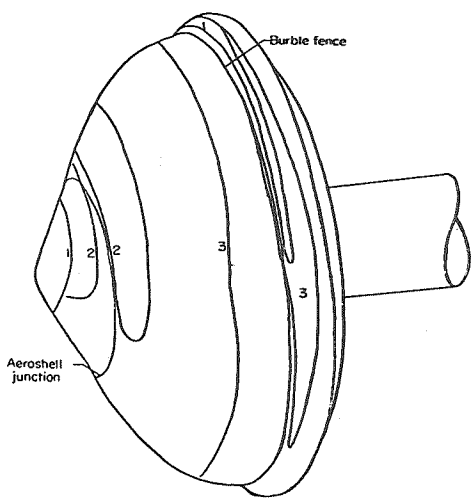

ALPHA=10.000 MINF = 7.950
R/M= 1.04137E+07
HS= 5.72535E+02 WATTS/METER(SQ)-DEG-K

CONTOUR	T,SEC	H,WATTS/METER(SQ)-DEG-K	H/HS
1	.70	3.44425E+02	6.01578E-01
2	1.60	2.27816E+02	3.97907E-01
3	7.70	1.03848E+02	1.81383E-01

(d) $N_{Re,\infty} = 1.1 \times 10^6$.

Figure 27.- Constant-temperature contours on model 1, 90^o from windward side. $\alpha = 10^o$.

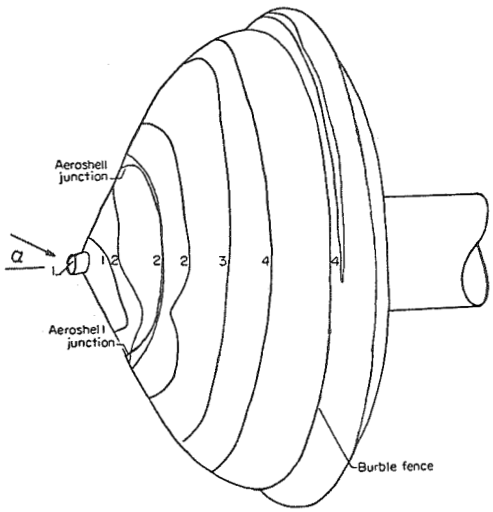

ALPHA= 5.000 MINF = 7.690
R/M= 2.07451E+06
HS= 2.46054E+02 WATTS/METER(SQ)-DEG-K

CONTOUR	T,SEC	H,WATTS/METER(SQ)-DEG-K	H/HS
1	.50	2.06564E+02	8.39509E-01
2	1.70	1.12025E+02	4.55288E-01
3	3.70	7.59345E+01	3.08610E-01
4	7.30	5.40603E+01	2.19710E-01

(a) $N_{Re,\infty} = 2.3 \times 10^5$.

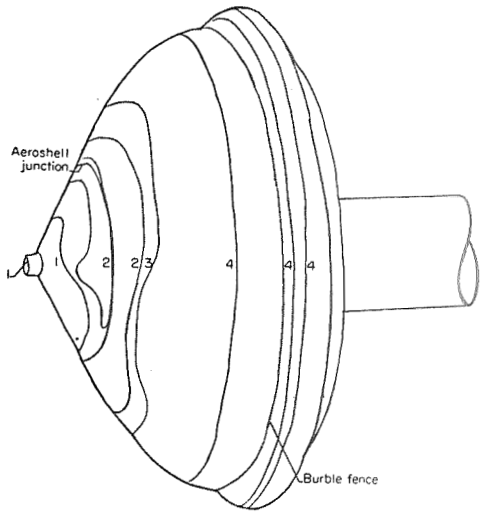

ALPHA= 5.000 MINF = 7.800
R/M= 3.58824E+06
HS= 3.27041E+02 WATTS/METER(SQ)-DEG-K

CONTOUR	T,SEC	H,WATTS/METER(SQ)-DEG-K	H/HS
1	.40	2.13447E+02	6.52660E-01
2	.80	1.50930E+02	4.61500E-01
3	1.40	1.14092E+02	3.48861E-01
4	6.10	5.46581E+01	1.67129E-01

(b) $N_{Re,\infty} = 4.0 \times 10^5$.

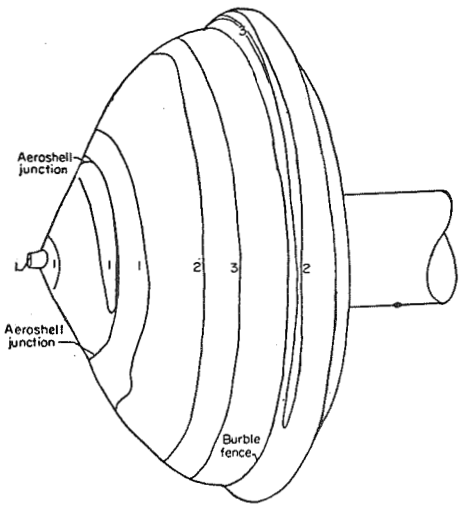

ALPHA= 5.000 MINF = 7.900
R/M= 5.99666E+06
HS= 4.41284E+02 WATTS/METER(SQ)-DEG-K

CONTOUR	T,SEC	H,WATTS/METER(SQ)-DEG-K	H/HS
1	.50	2.42431E+02	5.49377E-01
2	1.80	1.27772E+02	2.89547E-01
3	4.90	7.74418E+01	1.75492E-01

(c) $N_{Re,\infty} = 6.72 \times 10^5$.

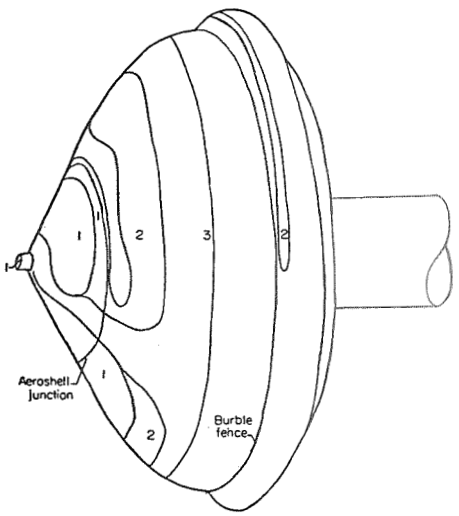

ALPHA= 5.000 MINF = 7.950
R/M= 1.00020E+07
HS= 5.72869E+02 WATTS/METER(SQ)-DEG-K

CONTOUR	T,SEC	H,WATTS/METER(SQ)-DEG-K	H/HS
1	.70	3.24349E+02	5.66184E-01
2	1.50	2.21573E+02	3.86777E-01
3	2.80	1.62175E+02	2.83092E-01

(d) $N_{Re,\infty} = 1.12 \times 10^6$.

Figure 28.- Constant-temperature contours on model 2, 90° from windward side. $\alpha = 5°$.

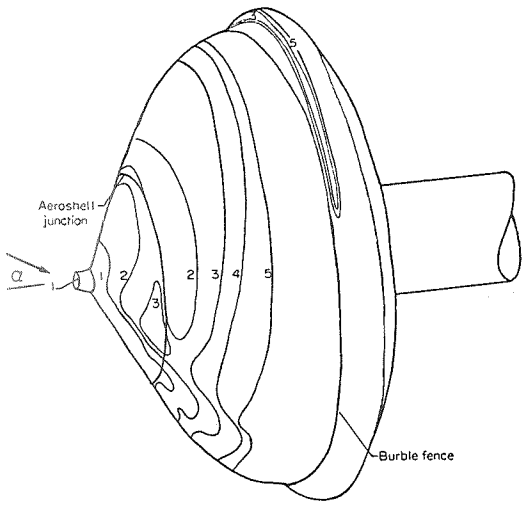

ALPHA=10.000 MINF = 7.690
R/M= 2.10116E+06
HS= 2.45859E+02 WATTS/METER(SQ)-DEG-K

CONTOUR	T,SEC	H,WATTS/METER(SQ)-DEG-K	H/HS
1	.70	1.74654E+02	7.10383E-01
2	1.90	1.06011E+02	4.31186E-01
3	3.90	7.39937E+01	3.00960E-01
4	6.00	5.96556E+01	2.42642E-01
5	7.30	5.40836E+01	2.19978E-01

(a) $N_{Re,\infty} = 2.4 \times 10^5$.

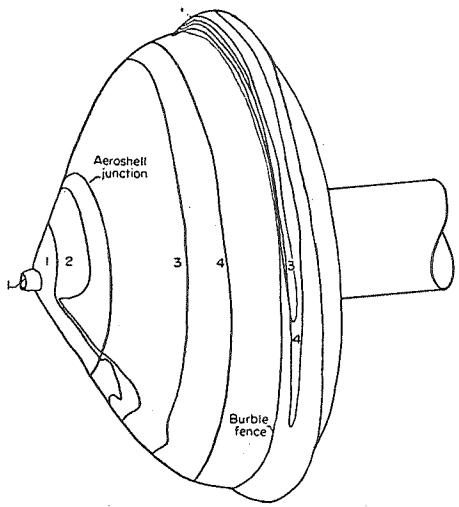

ALPHA=10.000 MINF = 7.800
R/M= 3.15007E+06
HS= 3.26551E+02 WATTS/METER(SQ)-DEG-K

CONTOUR	T,SEC	H,WATTS/METER(SQ)-DEG-K	H/HS
1	.20	2.80970E+02	8.60417E-01
2	.70	1.50185E+02	4.59912E-01
3	1.40	1.06197E+02	3.25207E-01
4	3.10	7.13666E+01	2.18546E-01

(b) $N_{Re,\infty} = 3.5 \times 10^5$.

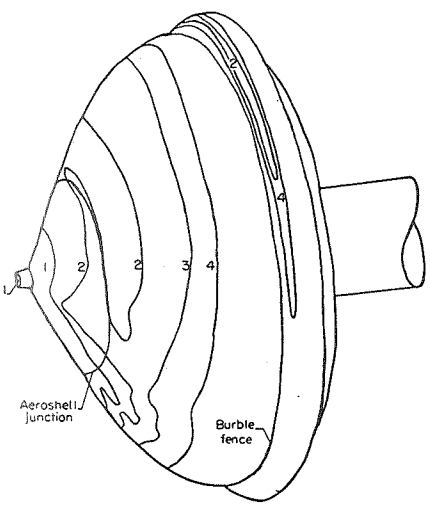

ALPHA=10.000 MINF = 7.900
R/M= 5.99666E+06
HS= 4.42779E+02 WATTS/METER(SQ)-DEG-K

CONTOUR	T,SEC	H,WATTS/METER(SQ)-DEG-K	H/HS
1	.20	3.95262E+02	8.92685E-01
2	.50	2.49985E+02	5.64583E-01
3	1.90	1.28240E+02	2.89625E-01
4	5.30	7.67824E+01	1.73410E-01

(c) $N_{Re,\infty} = 6.7 \times 10^5$.

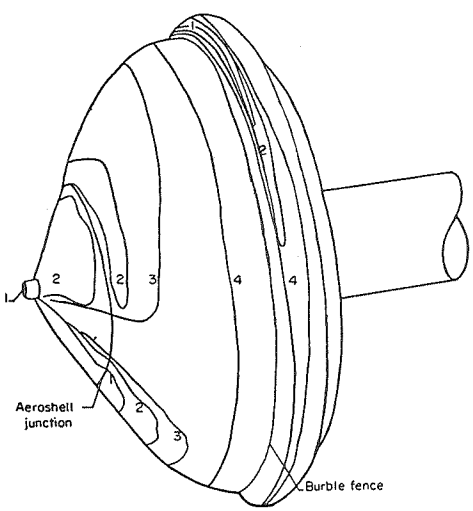

ALPHA=10.000 MINF = 7.950
R/M= 1.05989E+07
HS= 5.73468E+02 WATTS/METER(SQ)-DEG-K

CONTOUR	T,SEC	H,WATTS/METER(SQ)-DEG-K	H/HS
1	.20	6.62192E+02	1.15471E+00
2	1.00	2.96141E+02	5.16404E-01
3	2.20	1.99658E+02	3.48160E-01
4	6.20	1.18933E+02	2.07393E-01

(d) $N_{Re,\infty} = 1.1 \times 10^6$.

Figure 29.- Constant-temperature contours on model 2, 90^o from windward side. $\alpha = 10^o$.

ALPHA= 5.000 MINF = 7.690
R/M= 1.92581E+06
HS= 2.47090E+02 WATTS/METER(SQ)-DEG-K

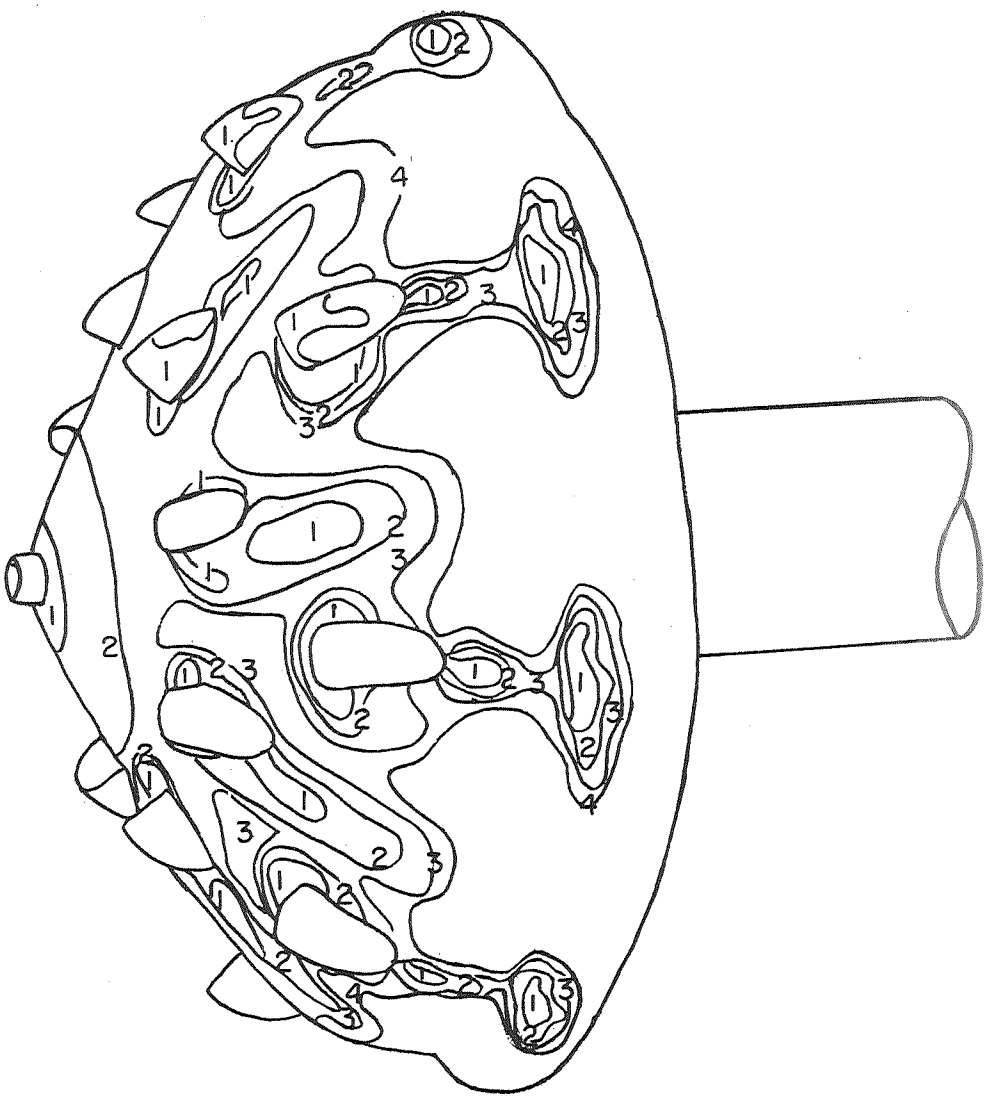

CONTOUR	T,SEC	H,WATTS/METER(SQ)-DEG-K	H/HS
1	.30	2.24198E+02	9.07352E-01
2	1.60	9.70805E+01	3.92895E-01
3	3.90	6.21813E+01	2.51654E-01
4	7.30	4.54497E+01	1.83940E-01

(a) $N_{Re,\infty} \approx 2.2 \times 10^5$.

Figure 30.- View of model 3 showing constant-temperature contour 90° from most windward side. $\alpha = 5^\circ$.

ALPHA= 5.000 MINF = 7.800
R/M= 3.29855E+06
HS= 3.26537E+02 WATTS/METER(SQ)-DEG-K

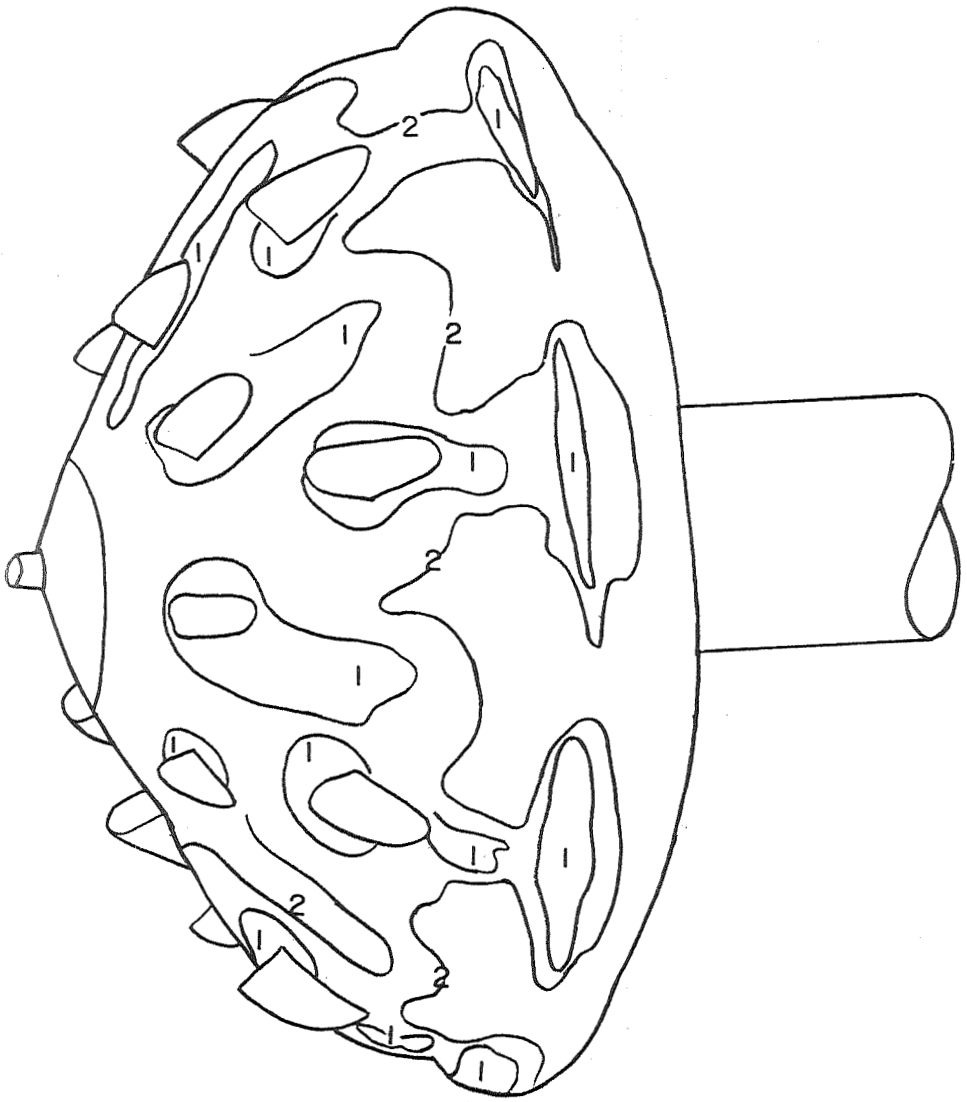

CONTOUR	T,SEC	H,WATTS/METER(SQ)-DEG-K	H/HS
1	.40	1.97346E+02	6.04361E-01
2	4.30	6.01901E+01	1.84328E-01

(b) $N_{Re,\infty} \approx 3.7 \times 10^5$.

Figure 30.- Continued.

ALPHA= 5.000 MINF = 7.900
R/M= 5.57511E+06
HS= 4.43209E+02 WATTS/METER(SQ)-DEG-K

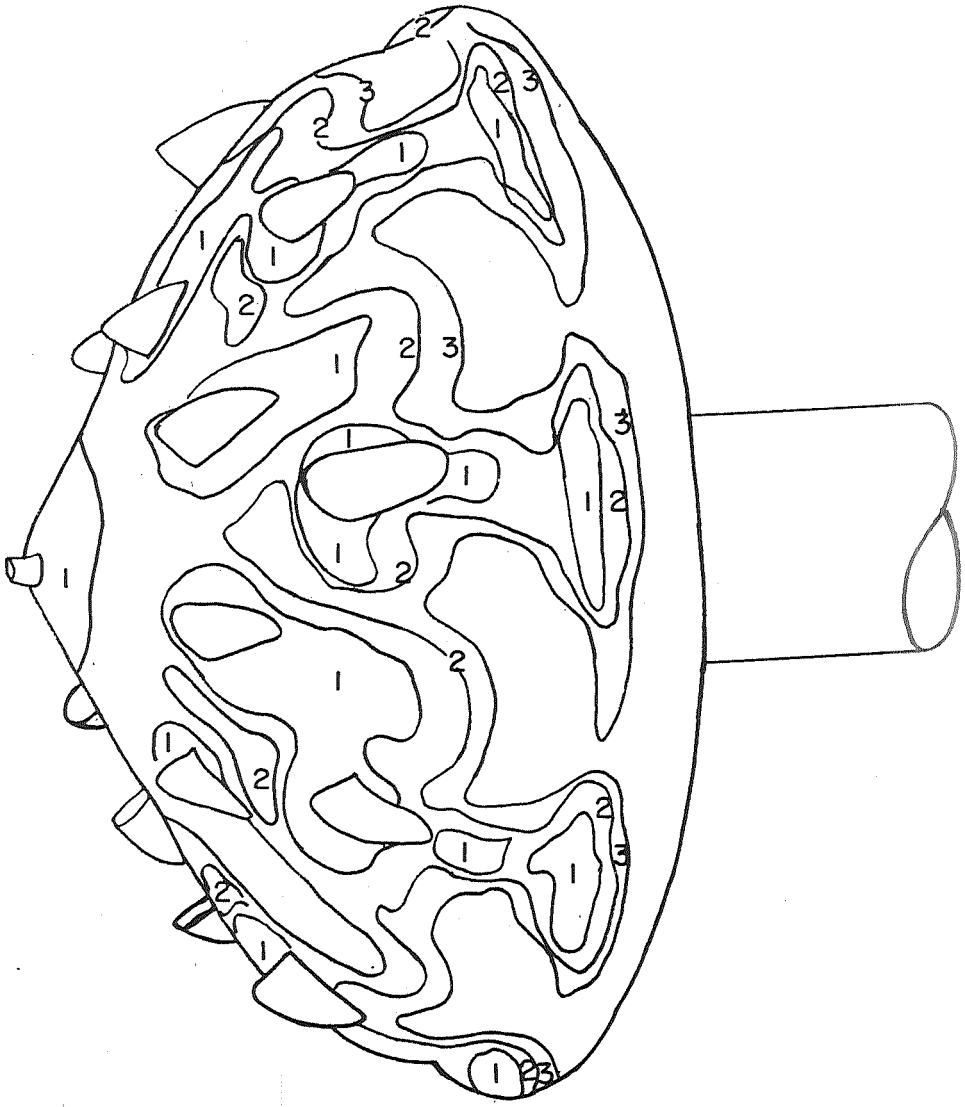

CONTOUR	T,SEC	H,WATTS/METER(SQ)-DEG-K	H/HS
1	.40	2.79141E+02	6.29818E-01
2	1.80	1.31588E+02	2.96899E-01
3	5.10	7.81750E+01	1.76384E-01

(c) $N_{Re,\infty} \approx 6.3 \times 10^5$.

Figure 30.- Continued.

ALPHA= 5.000 MINF = 7.950
R/M= 1.07254E+07
HS= 5.74096E+02 WATTS/METER(SQ)-DEG-K

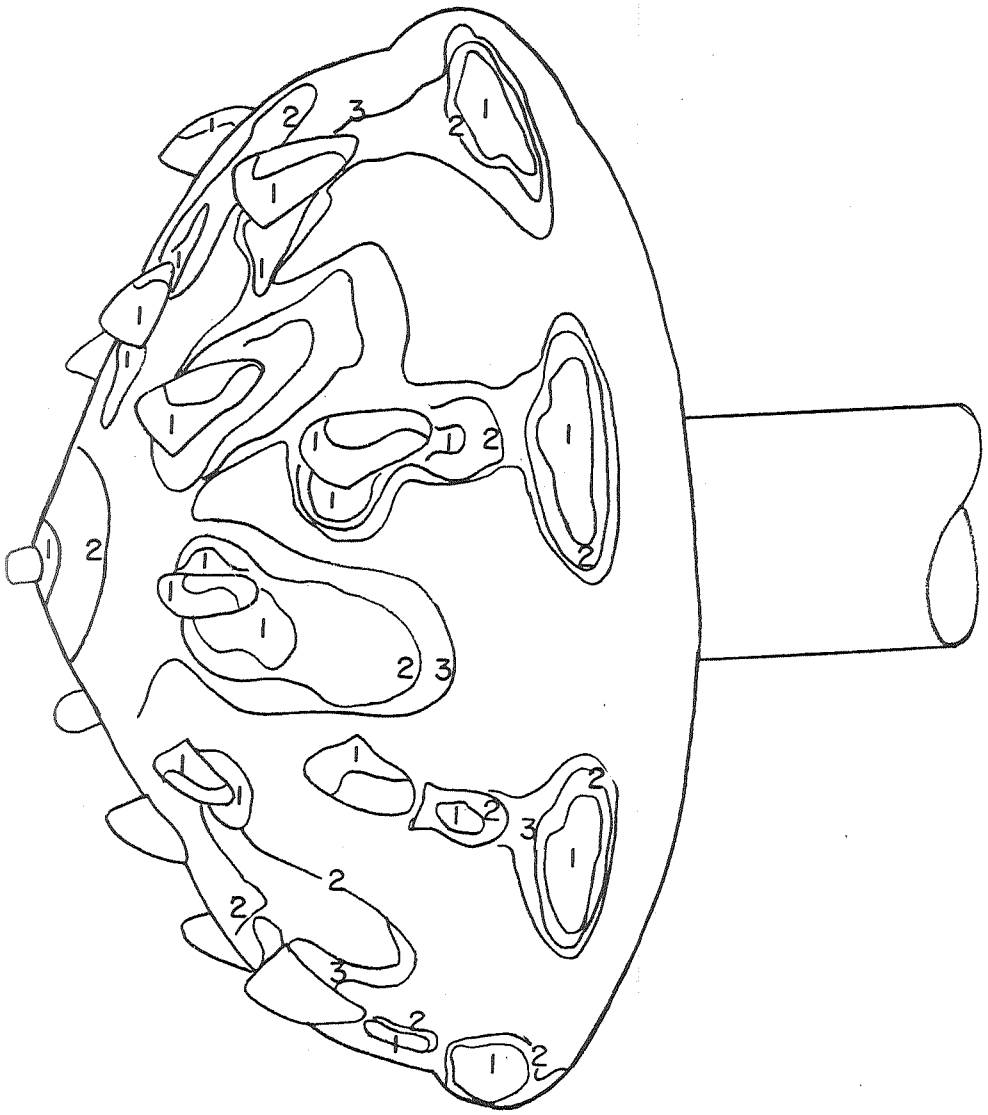

CONTOUR	T, SEC	H, WATTS/METER(SQ)-DEG-K	H/HS
1	.20	6.40731E+02	1.11607E+00
2	.90	3.02043E+02	.5.26120E-01
3	2.30	1.88941E+02	3.29111E-01

(d) $N_{Re,\infty} \approx 1.2 \times 10^6$.

Figure 30.- Concluded.

ALPHA=10.000 MINF = 7.690
R/M= 1.94934E+06
HS= 2.46928E+02 WATTS/METER(SQ)-DEG-K

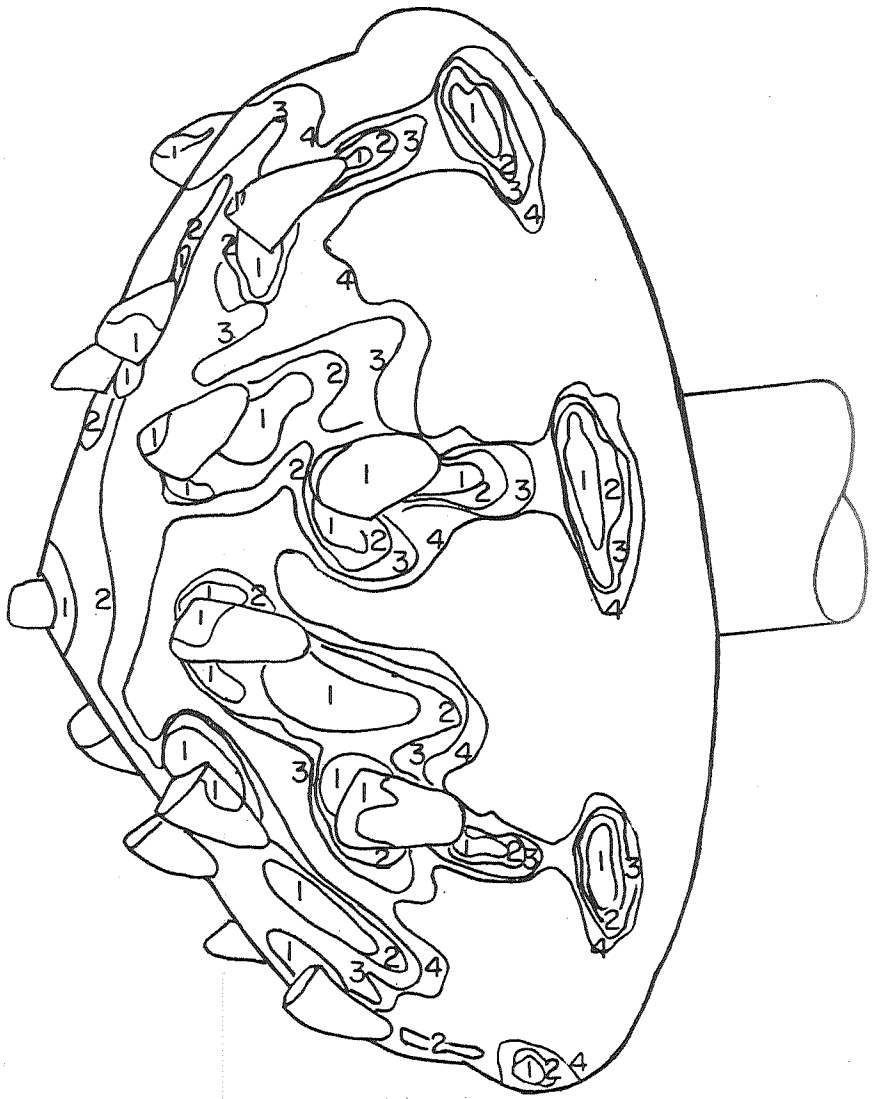

CONTOUR	T,SEC	H,WATTS/METER(SQ)-DEG-K	H/HS
1	.60	1.75715E+02	7.11602E-01
2	1.60	1.07603E+02	4.35765E-01
3	3.40	7.38149E+01	2.98933E-01
4	6.80	5.21950E+01	2.11377E-01

(a) $N_{Re,\infty} \approx 2.24 \times 10^5$.

Figure 31.- View of model 3 showing constant-temperature contour 90^o from most windward side. $\alpha = 5^o$.

ALPHA=10.000 MINF = 7.800
R/M= 2.99772E+06
HS= 3.14520E+02 WATTS/METER(SQ)-DEG-K

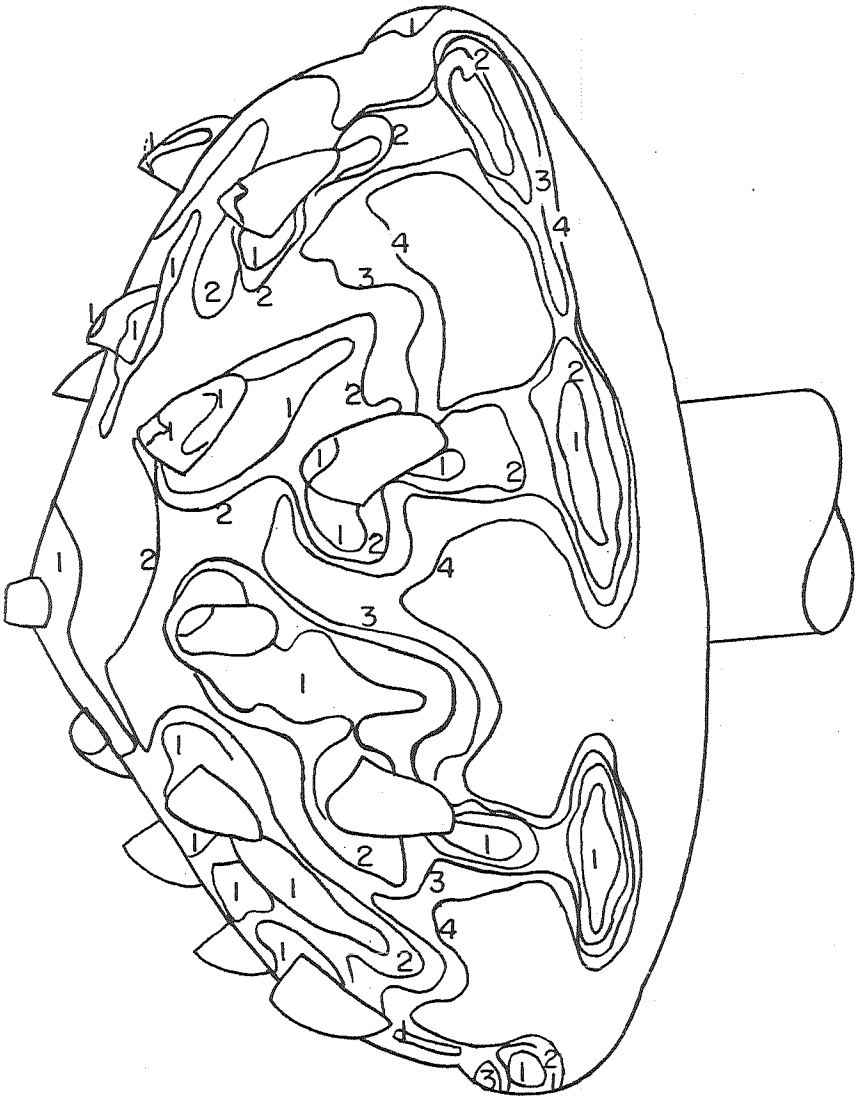

CONTOUR	T,SEC	H,WATTS/METER(SQ)-DEG-K	H/HS
1	.30	2.22239E+02	7.06598E-01
2	1.30	1.06760E+02	3.39439E-01
3	2.80	7.27449E+01	2.31289E-01
4	5.70	5.09852E+01	1.62105E-01

(b) $N_{Re,\infty} \approx 3.4 \times 10^5$.

Figure 31.- Continued.

ALPHA=10.000 MINF = 7.900
R/M= 5.82842E+06
HS= 4.42016E+02 WATTS/METER(SQ)-DEG-K

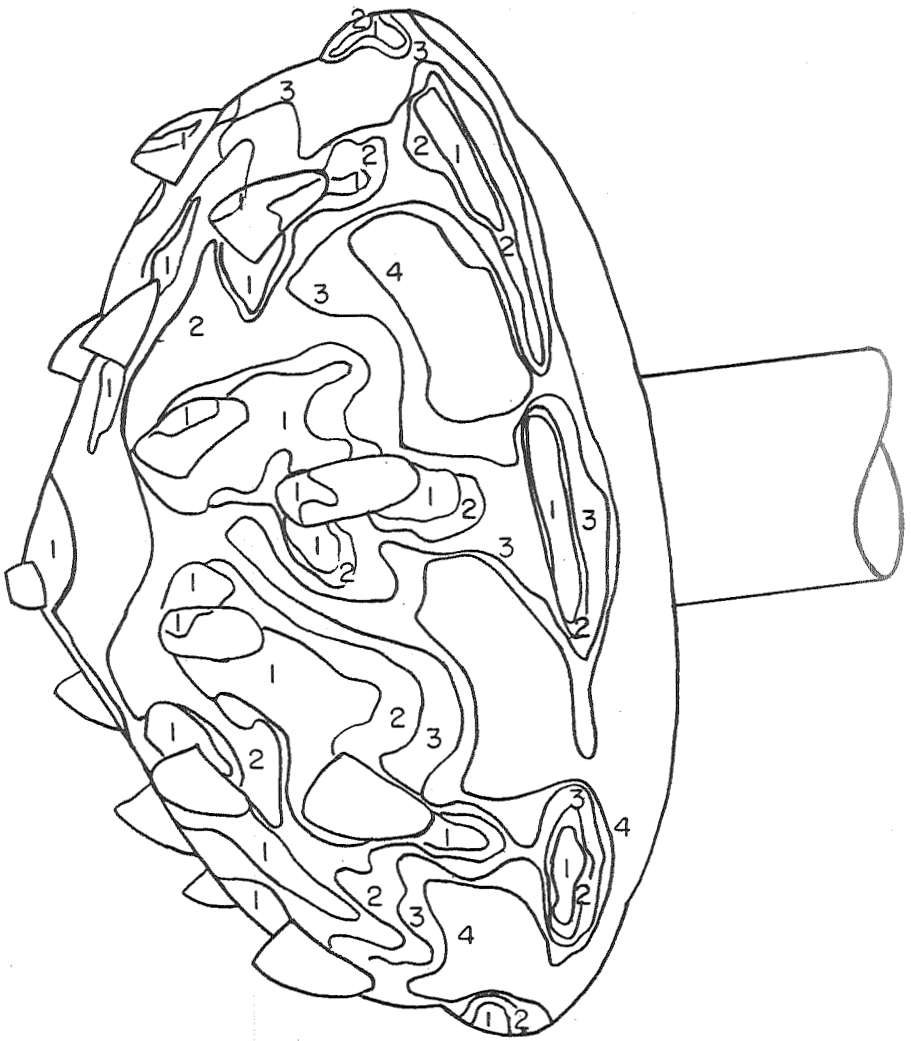

CONTOUR	T,SEC	H,WATTS/METER(SQ)-DEG-K	H/HS
1	.20	3.75470E+02	8.49448E-01
2	.90	1.76998E+02	4.00434E-01
3	2.70	1.02190E+02	2.31191E-01
4	5.60	7.09571E+01	1.60531E-01

(c) $N_{Re,\infty} \approx 6.5 \times 10^5$.

Figure 31.- Continued.

ALPHA=10.000 MINF = 7.950
R/M= 1.04707E+07
HS= 5.82416E+02 WATTS/METER(SQ)-DEG-K

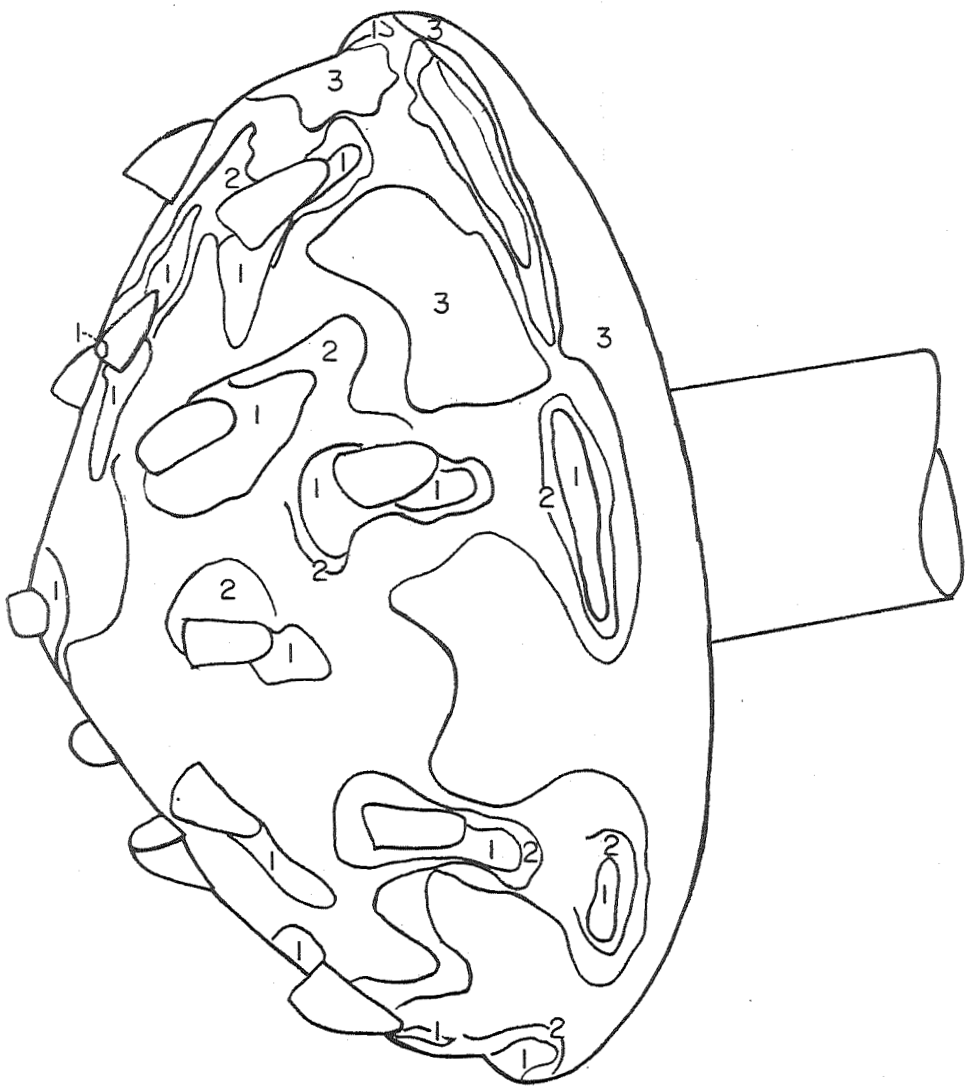

CONTOUR	T,SEC	H,WATTS/METER(SQ)-DEG-K	H/HS
1	.20	6.23065E+02	1.06979E+00
2	1.00	2.78643E+02	4.78426E-01
3	3.40	1.51115E+02	2.59463E-01

(d) $N_{Re,\infty} \approx 1.1 \times 10^6$.

Figure 31.- Concluded.

ALPHA= 5.000 MINF = 7.690
R/M= 2.03558E+06
HS= 2.46346E+02 WATTS/METER(SQ)-DEG-K

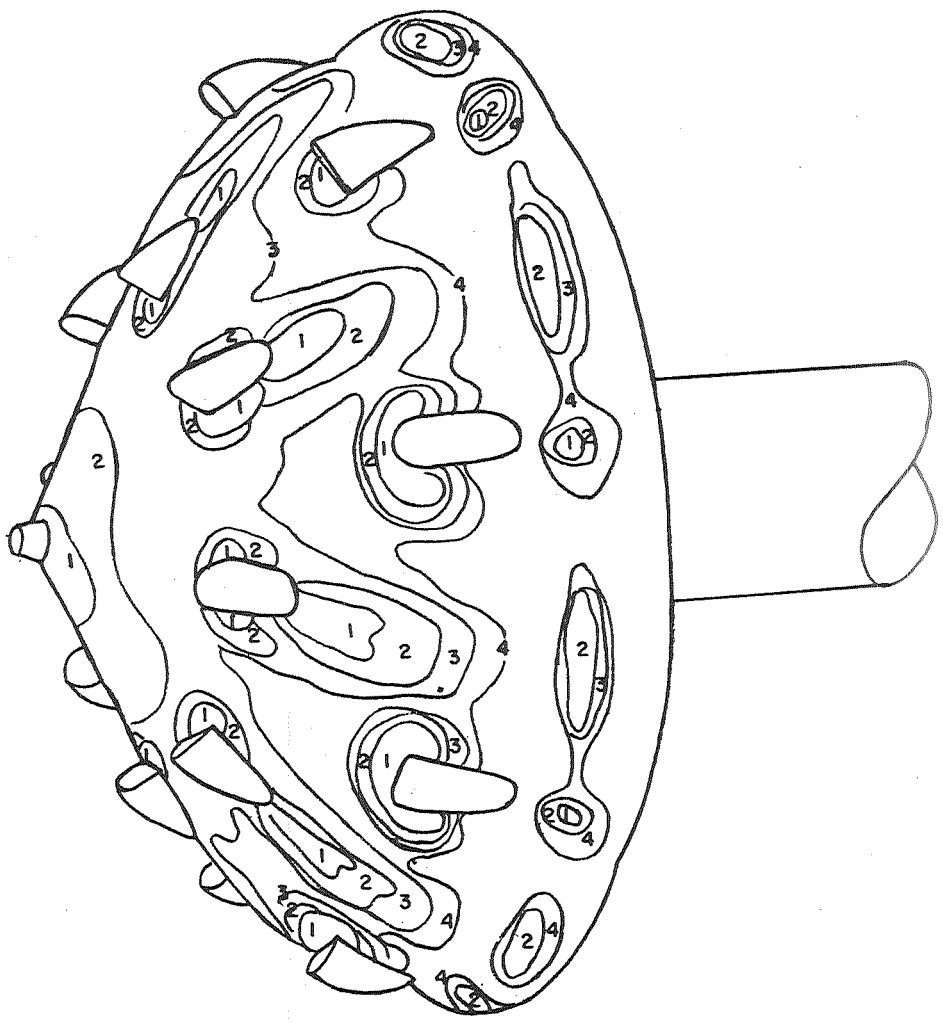

CONTOUR	T.SEC	H.WATTS/METER(SQ)-DEG-K	H/HS
1	.50	2.02129E+02	8.20509E-01
2	2.60	8.86394E+01	3.59817E-01
3	5.90	5.88420E+01	2.38859E-01
4	11.30	4.25181E+01	1.72595E-01

(a) $N_{Re,\infty} \approx 2.2 \times 10^5$.

Figure 32.- View of model 4 showing constant-temperature contour 90° from most windward side. $\alpha = 5^\circ$.

ALPHA= 5.000 MINF = 7.800
R/M= 3.37723E+06
HS= 3.27251E+02 WATTS/METER(SQ)-DEG-K

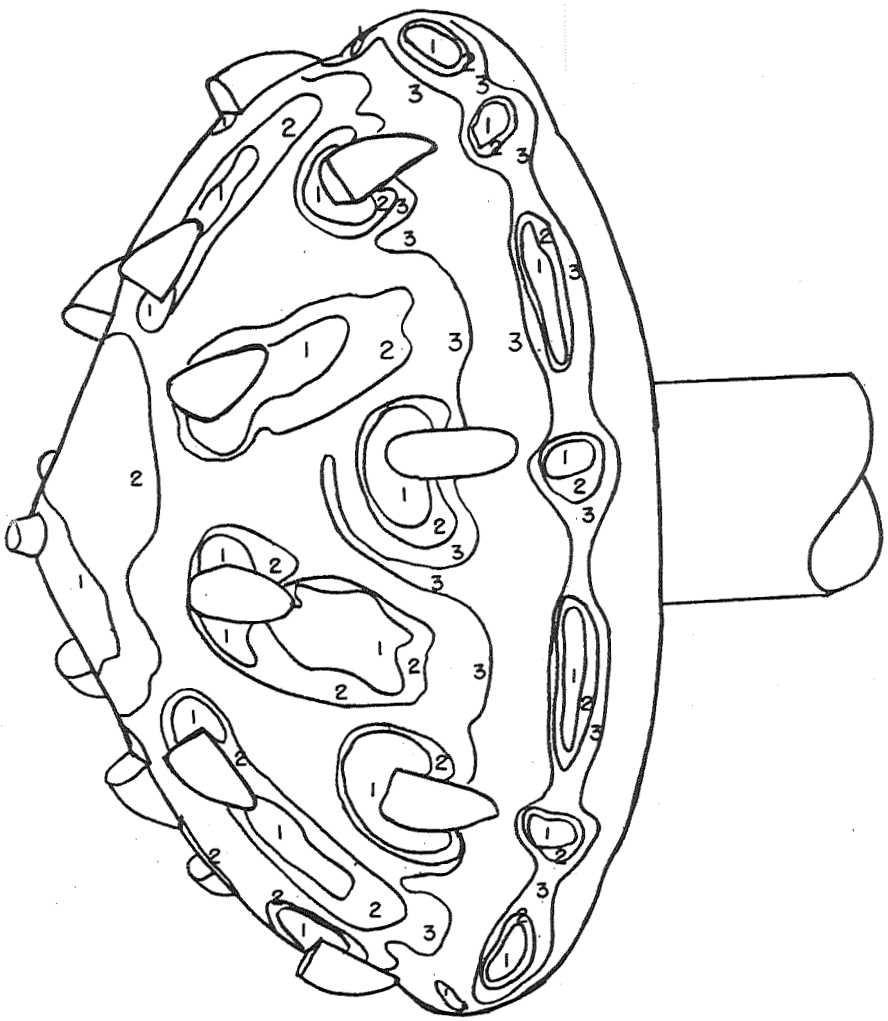

CONTOUR	T, SEC	H, WATTS/METER(SQ)-DEG-K	H/HS
1	.60	1.74870E+02	5.34362E-01
2	1.70	1.03888E+02	3.17458E-01
3	5.80	5.62442E+01	1.71869E-01

(b) $N_{Re,\infty} \approx 3.8 \times 10^5$.

Figure 32.- Continued.

ALPHA= 5.000 MINF = 7.900
R/M= 5.86143E+06
HS= 4.41870E+02 WATTS/METER(SQ)-DEG-K

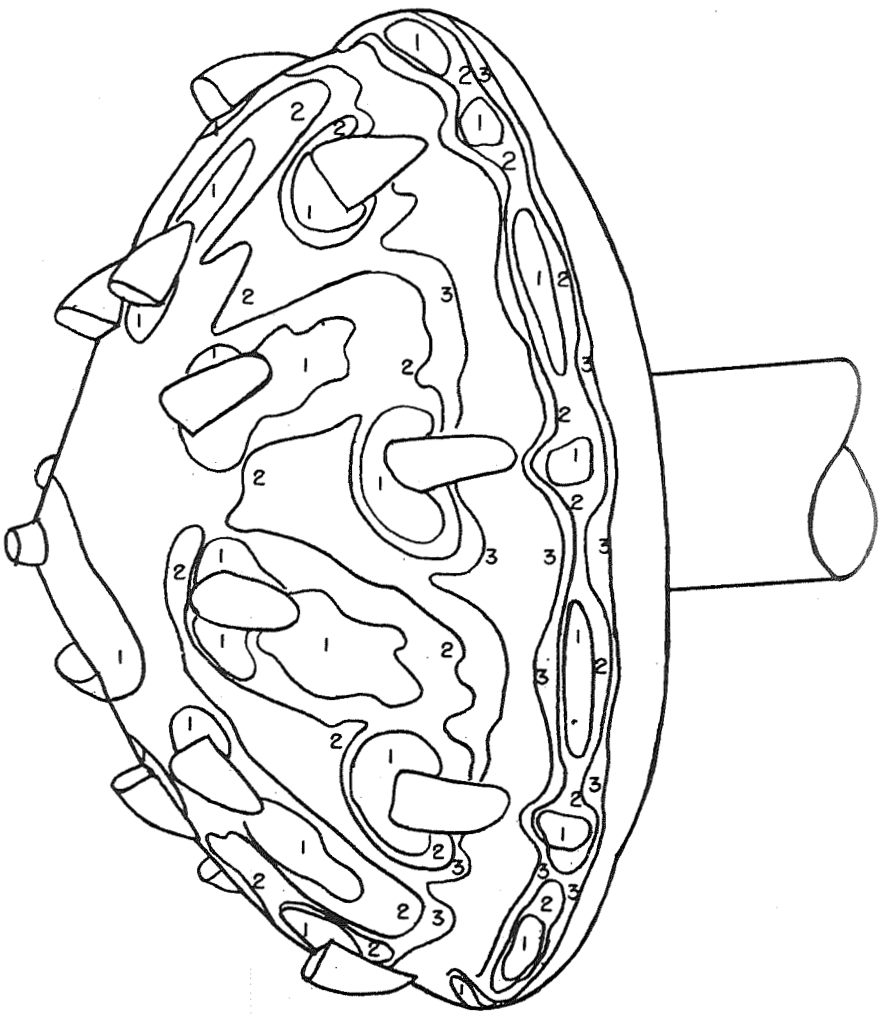

CONTOUR	T,SEC	H,WATTS/METER(SQ)-DEG-K	H/HS
1	.50	2.38928E+02	5.40720E-01
2	1.90	1.22567E+02	2.77383E-01
3	5.20	7.40883E+01	1.67670E-01

(c) $N_{Re,\infty} \approx 6.7 \times 10^5$.

Figure 32.- Continued.

ALPHA= 5.000 MINF = 7.950
R/M= 9.25557E+06
HS= 5.75577E+02 WATTS/METER(SQ)-DEG-K

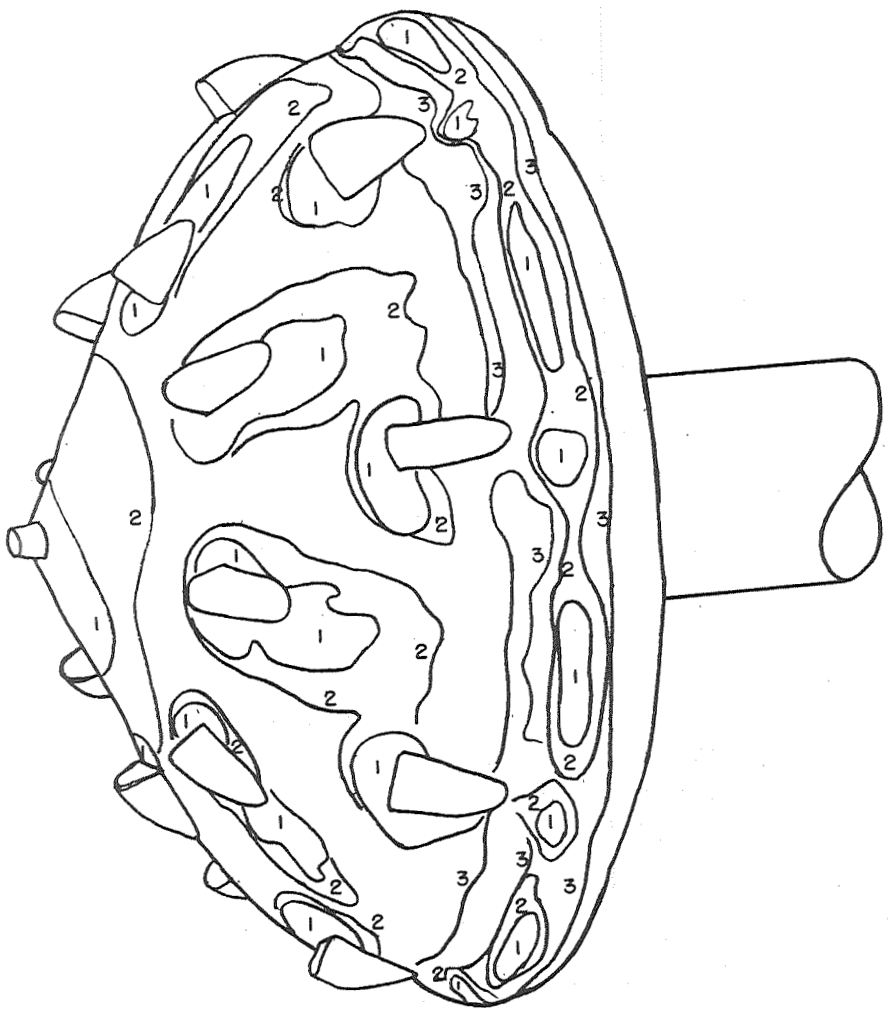

CONTOUR	T,SEC	H,WATTS/METER(SQ)-DEG-K	H/HS
1	.30	4.53990E+02	7.88757E-01
2	1.10	2.37089E+02	4.11915E-01
3	5.50	1.06029E+02	1.84214E-01

(d) $N_{Re,\infty} \approx 1.0 \times 10^6$.

Figure 32.- Concluded.

ALPHA=10.000 MINF = 7.690
R/M= 2.03558E+06
HS= 2.46346E+02 WATTS/METER(SQ)-DEG-K

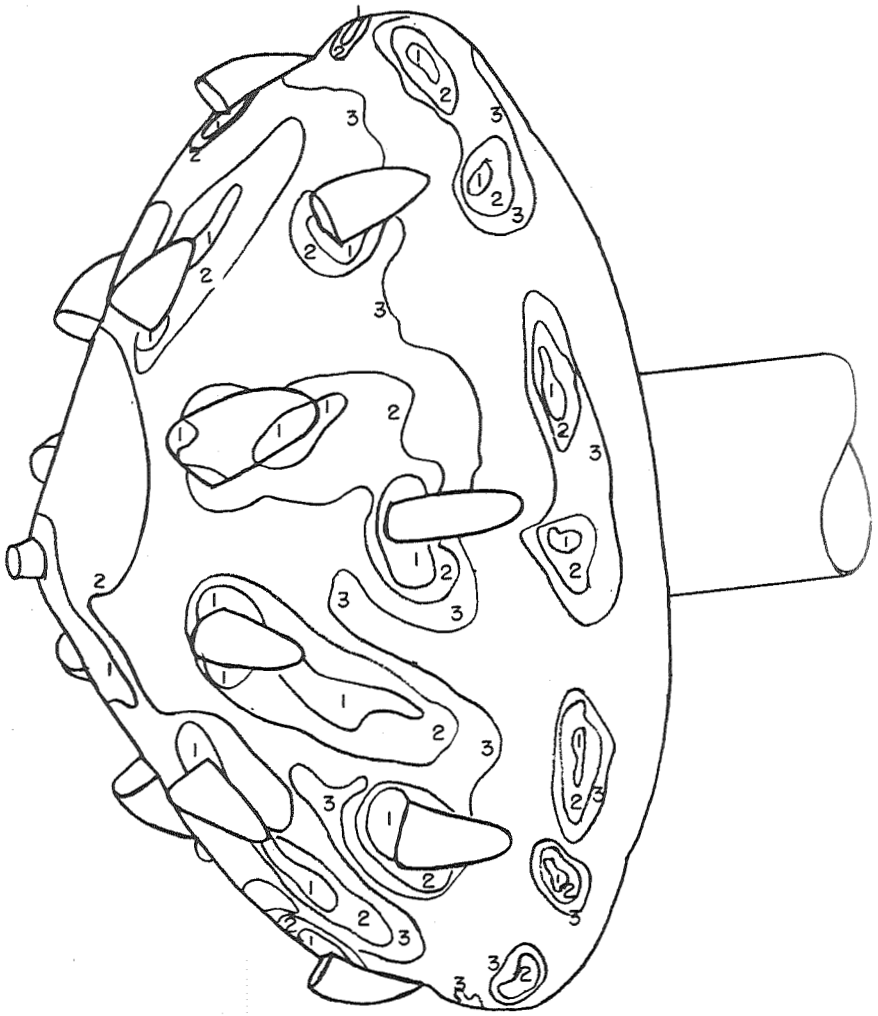

CONTOUR	T.SEC	H.WATTS/METER(SQ)-DEG-K	H/HS
1	.70	1.78107E+02	7.22996E-01
2	3.40	8.08148E+01	3.28054E-01
3	9.60	4.80944E+01	1.95231E-01

(a) $N_{Re,\infty} \approx 2.2 \times 10^5$.

Figure 33.- View of model 4 showing constant-temperature contour 90° from most windward side. $\alpha = 10^\circ$.

ALPHA=10.000 MINF = 7.800
R/M= 3.39739E+06
HS= 3.27431E+02 WATTS/METER(SQ)-DEG-K

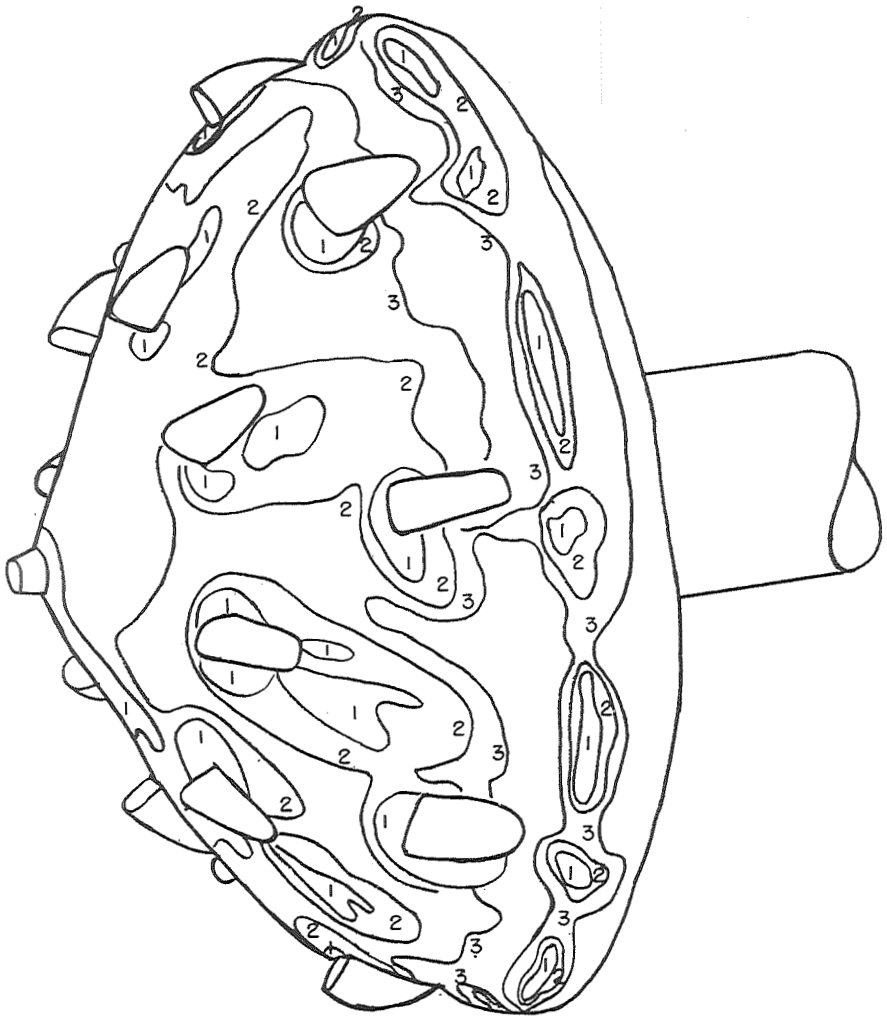

CONTOUR	T,SEC	H,WATTS/METER(SQ)-DEG-K	H/HS
1	.50	1.84924E+02	5.64773E-01
2	2.20	8.81591E+01	2.69245E-01
3	6.40	5.16878E+01	1.57859E-01

(b) $N_{Re,\infty} \approx 3.8 \times 10^5$.

Figure 33.- Continued.

ALPHA=10.000 MINF = 7.900
R/M= 6.13717E+06
HS= 4.41465E+02 WATTS/METER(SQ)-DEG-K

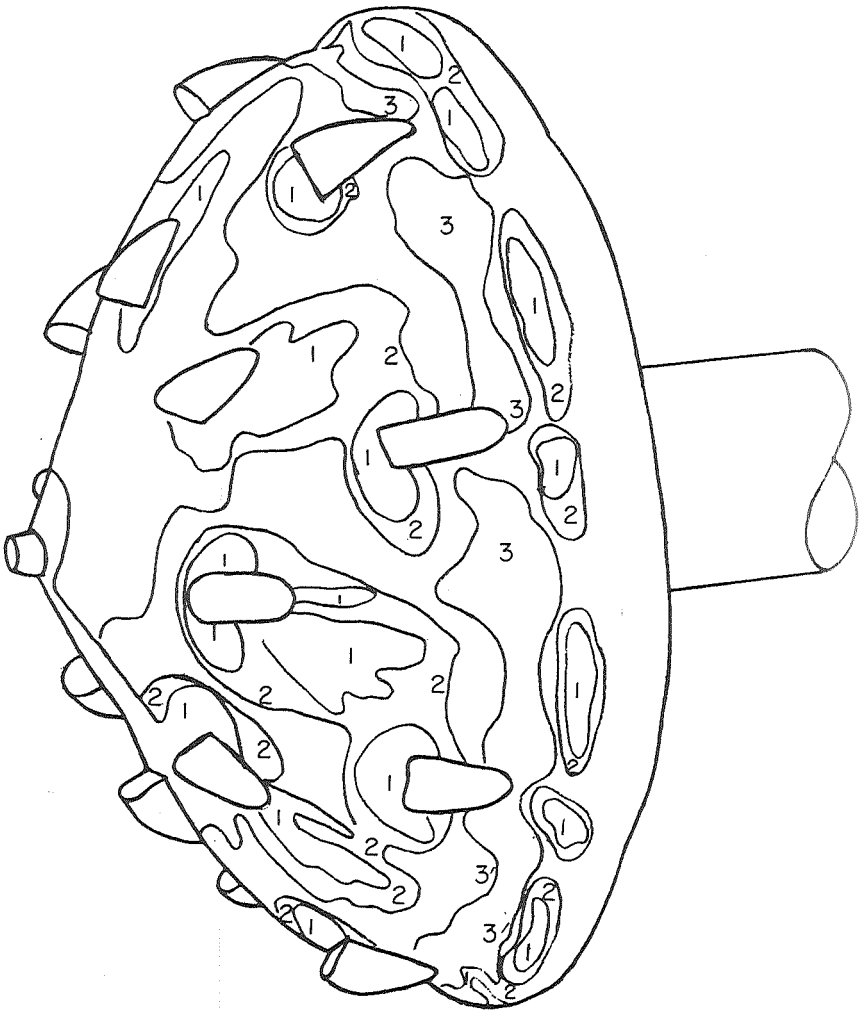

CONTOUR	T,SEC	H,WATTS/METER(SQ)-DEG-K	H/HS
1	.60	2.34103E+02	5.30287E-01
2	1.90	1.31555E+02	2.97996E-01
3	7.10	6.80541E+01	1.54155E-01

(c) $N_{Re,\infty} \approx 6.7 \times 10^5$.

Figure 33.- Continued.

ALPHA=10.000 MINF = 7.950
R/M= 9.67021E+06
HS= 5.74016E+02 WATTS/METER(SQ)-DEG-K

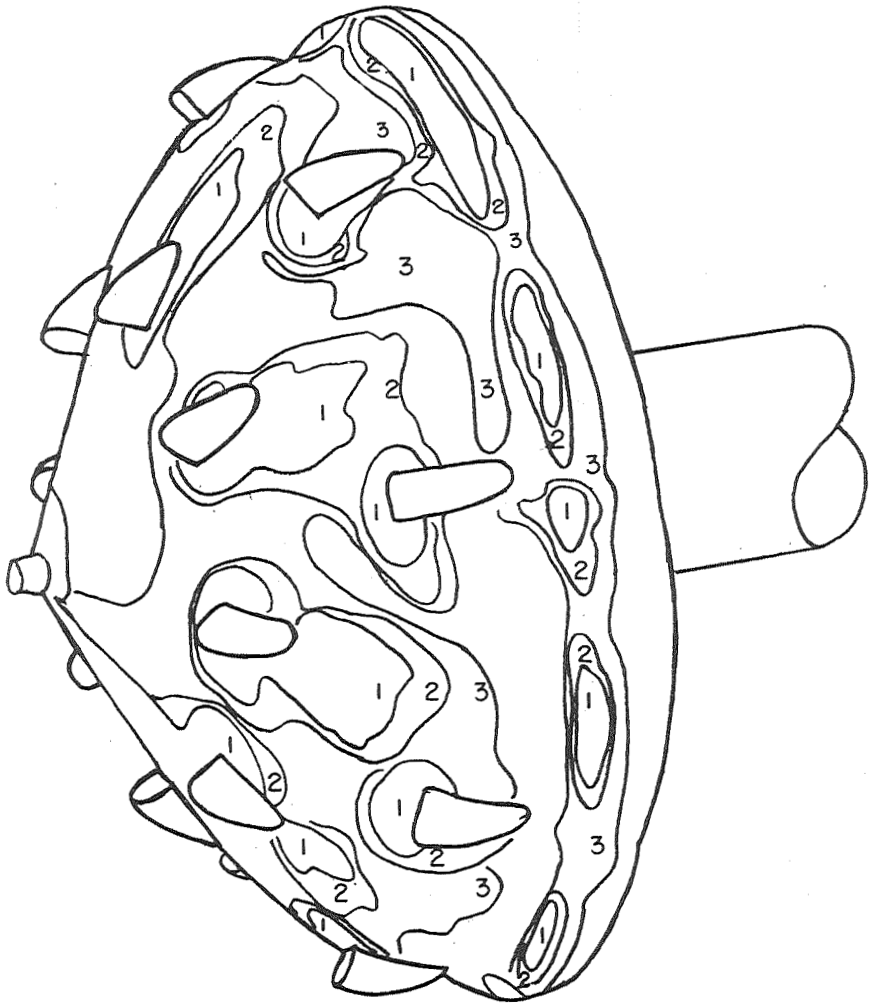

CONTOUR	T.SEC	H.WATTS/METER(SQ)-DEG-K	H/HS
1	.50	3.71797E+02	6.47713E-01
2	1.40	2.22191E+02	3.87083E-01
3	3.00	1.51786E+02	2.64428E-01

(d) $N_{Re,\infty} \approx 1.1 \times 10^6$.

Figure 33.- Concluded.

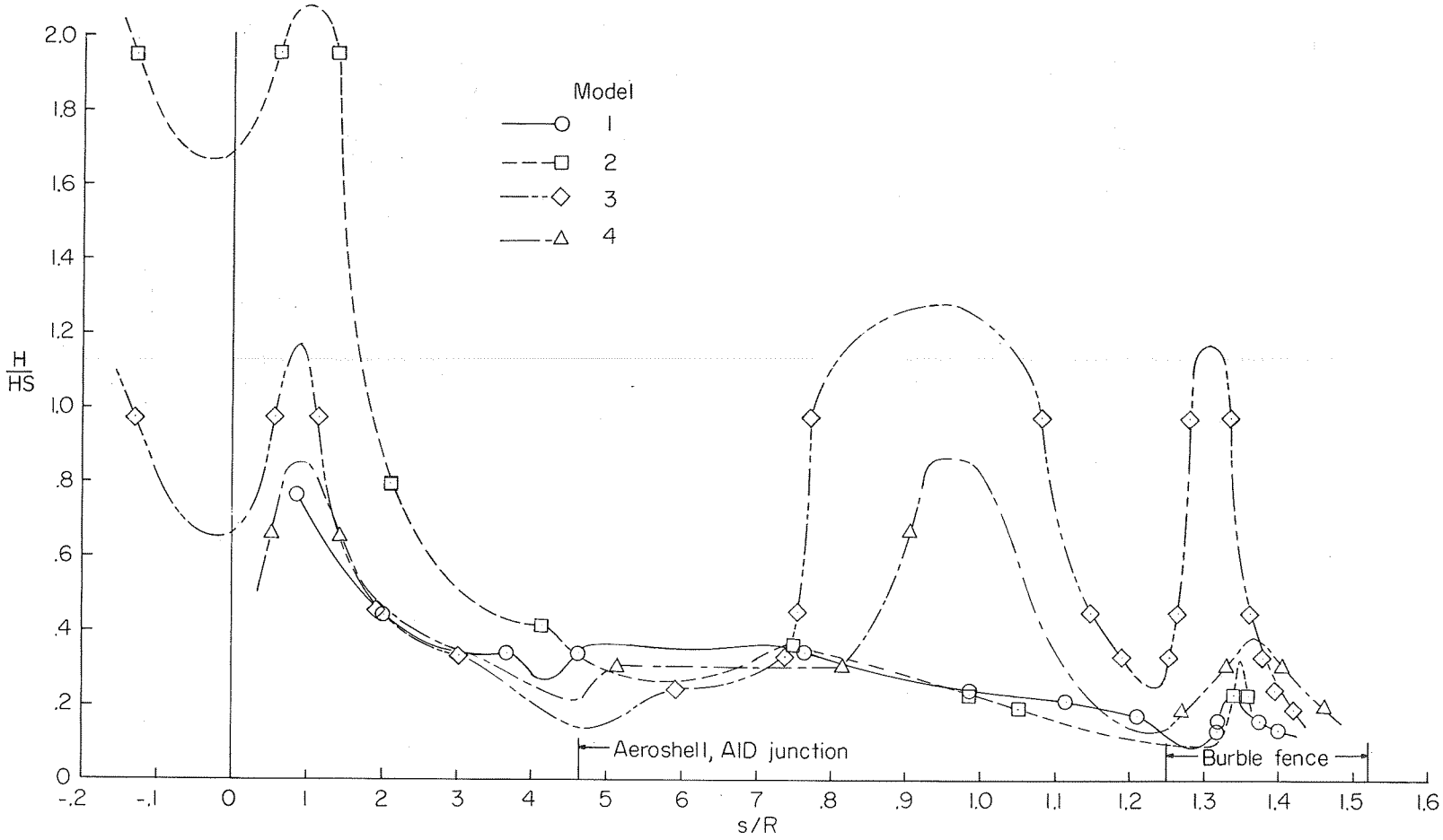

Figure 34.- Comparison of relative heat-transfer coefficients for a Reynolds number $\approx 2.2 \times 10^5$ at $\alpha = 0^o$.

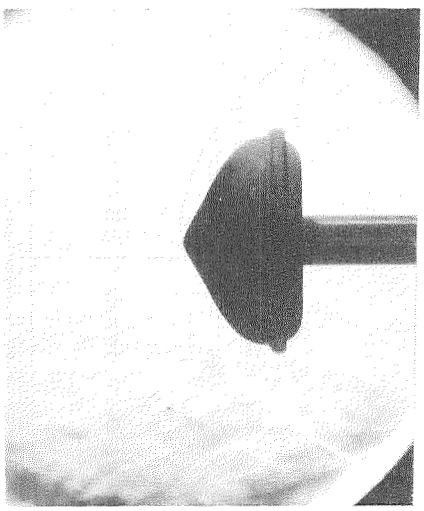

(a) Model 1.

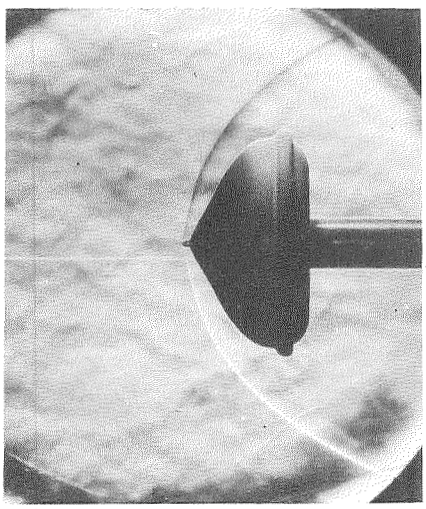

(b) Model 2.

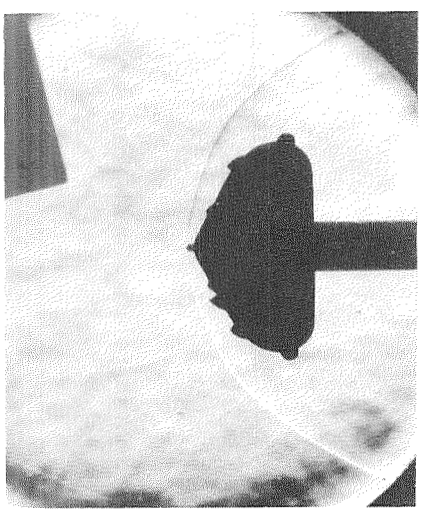

(c) Model 3.

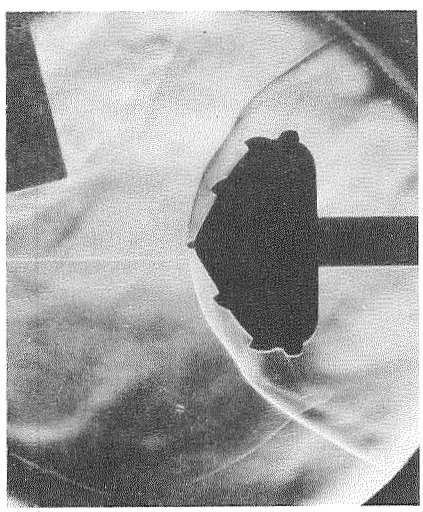

L-71-700

(d) Model 4.

Figure 35.- Typical schlieren photographs.

NASA-Langley, 1971 —— 33 L-7864

"The aeronautical and space activities of the United States shall be conducted so as to contribute . . . to the expansion of human knowledge of phenomena in the atmosphere and space. The Administration shall provide for the widest practicable and appropriate dissemination of information concerning its activities and the results thereof."

—NATIONAL AERONAUTICS AND SPACE ACT OF 1958

NASA SCIENTIFIC AND TECHNICAL PUBLICATIONS

TECHNICAL REPORTS: Scientific and technical information considered important, complete, and a lasting contribution to existing knowledge.

TECHNICAL NOTES: Information less broad in scope but nevertheless of importance as a contribution to existing knowledge.

TECHNICAL MEMORANDUMS: Information receiving limited distribution because of preliminary data, security classification, or other reasons.

CONTRACTOR REPORTS: Scientific and technical information generated under a NASA contract or grant and considered an important contribution to existing knowledge.

TECHNICAL TRANSLATIONS: Information published in a foreign language considered to merit NASA distribution in English.

SPECIAL PUBLICATIONS: Information derived from or of value to NASA activities. Publications include conference proceedings, monographs, data compilations, handbooks, sourcebooks, and special bibliographies.

TECHNOLOGY UTILIZATION PUBLICATIONS: Information on technology used by NASA that may be of particular interest in commercial and other non-aerospace applications. Publications include Tech Briefs, Technology Utilization Reports and Technology Surveys.

Details on the availability of these publications may be obtained from:

SCIENTIFIC AND TECHNICAL INFORMATION OFFICE

NATIONAL AERONAUTICS AND SPACE ADMINISTRATION

Washington, D.C. 20546